Thermal pollution in rivers due to cooling water from power plants and implications for system resilience to future change

Tianyang Du

Thesis submitted to the University of Nottingham for

the degree of Doctor of Philosophy

September 2023

Abstract

Thermal effluents discharged from power plant cooling systems can cause abrupt changes in water temperature and impose substantial thermal stress on aquatic organisms. Substantial efforts have been made to alleviate thermal stress by improving legal regulations and treating effluent using new technologies such as combined cycle gas turbine and recirculating cooling. However, riverine thermal pollution from cooling systems remains a concern due to rapid and continued expansion of thermal power plants globally. In addition, the impact of thermal effluents on rivers has been poorly studied because of limited data availability and accuracy. This thesis aimed to evaluate the impact of thermal pollution from power plants on rivers and aquatic life across different spatial and temporal scales.

Given that critical resources such as labour, material and finance are limited, it is important to locate and evaluate power plants that generate large amounts of thermal pollution, to prioritise the implementation of new technologies and regulations to reduce impacts. Therefore, a computationally simple and low data-intensive index was developed as a tool for identifying ‘hotspots’ that need particular attention. The effectiveness of the index was validated by the success in assessing and locating the power plants that potentially generate a large amount of thermal pollution. Follow-up scenario-based analyses were also performed to show that the index, in combination with background information can provide accurate assessments of thermal pollution and be not confined to the plants using once-through cooling systems.

Although the new index makes it possible to assess the impact of power plant effluent and identify rivers that are particularly vulnerable to effluent release, the interaction and cumulative impact of multiple power plants on the same river, or in the same catchment, have not been examined. We thus investigated this source of thermal pollution by simulating hypothetical power plant discharge scenarios in a conceptual water temperature model at the whole-river scale. The results indicated that the effluent discharge made a greater contribution to temperature increase than the effluent temperature, and the remaining energy advected from the effluent of upstream power plant was combined with the heat

input from the downstream power plant to cause cumulative thermal impacts. The arrangement of power plants along a river played an important role in alleviating the cumulative impacts. It was also found that water temperature change resulting from power plant discharge could be further complicated by the operation mode and climate change.

Aquatic ectotherms are dependent on the temperature of surrounding water and can be greatly influenced by elevated water temperatures due to thermal discharges and climate change. Therefore, these organisms have to make necessary physiological and behavioural adjustments (i.e. acclimation) to protect themselves from the negative consequences of elevated temperatures. However, the tolerance and survival of individuals at stressful temperatures can differ markedly, partly determined by the thermal history (i.e. habitat temperature regime) experienced by the animal. Hence, we investigated the response of aquatic ectotherms with different thermal histories to acute and chronic thermal stress via laboratory experiments with steady and variable temperatures. Organisms from thermally contrasting sites were both vulnerable to a persistently high temperature. The continuous expression of HSPs which reallocates energy from important processes like growth and respiration, possibly deteriorating animal health and increasing the difficulty in survival. When exposed to intermittently high temperatures, organisms inhabiting thermally more variable site were more tolerant to acute thermal stress than those inhabiting thermally less variable site. The improved thermal tolerance can be attributed to the wider thermal range and greater thermal variability of their habitat. By examining the impact and distribution of power plant thermal pollution, this research revealed the crucial role of thermal power plants in altering thermal regimes of streams and rivers worldwide.

Acknowledgements

Thank you to everyone who has been a part of my PhD experience. I am incredibly grateful for your support and encouragement.

To my supervisors (Matthew Johnson and Stephen Dugdale), thank you for the time you've invested in me, my research, and my career outside of the PhD. It hasn't been possible without your constant encouragement and enthusiasm.

Thanks to Simon Gosling for being my internal assessor through three years of annual reviews, and to the university for providing the funding for the PhD. Thanks also to Matthew Johnson and César Rodríguez for your assistance with fieldwork. Final thanks go to my family for your unconditional love and support.

Table of contents

List of figures

List of tables

Chapter 1: Introduction

Water temperature varies naturally both spatially and temporally in response to diurnal and seasonal (in temperate regions) cycles of solar radiation, which exerts a strong control on chemical and biological processes (e.g. metabolism, growth and reproduction) and hence affects the distribution, physiology and behaviour of aquatic life (Caissie, 2006; Calosi et al., 2008; Angilletta, 2009; Kazmi et al., 2022; Ferchichi & St-Hilaire, 2023). However, the expected, natural spatiotemporal variability in temperature can be influenced by anthropogenic activities (e.g. power generation, deforestation and flow abstraction) and climate change (Caissie, 2006; Hannah & Garner, 2015; Ficklin et al., 2023). As a consequence, an alteration to natural temperature regimes has implications for the health, performance and survival of organisms (e.g. Bellgraph et al., 2010; Dallas & Ketley, 2011; Bonacina et al., 2023a). In addition to ecological impacts, several vital socio-economic sectors, including power generation, agriculture and aquaculture are also highly susceptible to temperature changes (Pankhurst & King, 2010; Ren et al., 2014; Miara et al., 2018). Climate warming is a key driver of changes in thermal regimes over large spatial scales, particularly including extreme temperatures, altered duration of warm/cool periods, changes in the timing of seasons, and altered seasonal maximum and minimum temperatures. Past studies have shown that the Earth's atmosphere has warmed greatly since the 1970s (Kosaka & Xie, 2013; Muschinski & Katz, 2013; Nordli et al., 2014), mostly due to increased concentrations of carbon dioxide (CO_2) and other greenhouse gases (Montzka et al., 2011; Al-Ghussain, 2019), and is expected to warm further as concentrations continue to rise (Riahi et al., 2011; UNEP, 2020). Correspondingly, freshwater temperatures are also expected to warm as they are influenced by rising air temperatures resulting from climate warming, with freshwater temperatures estimated to be increasing at an average of 0.1–0.2 °C per decade (IPBES, 2017).

Anthropogenic disturbances such as fossil fuel combustion, deforestation and urbanisation, further accelerate changes in thermal regimes, causing thermal pollution (Moore et al., 2005; Maria et al., 2013; Raptis et al., 2017; Kaka et al., 2021). Among these disturbances, power plants are a major source of thermal pollution, discharging warmer effluent from their cooling systems, potentially

leading to large and abrupt changes in water temperature and imposing thermal stress on aquatic organisms (Squires et al., 1978; Worthington et al., 2015; Rossi et al., 2017). Although great efforts have been made to alleviate thermal stress (e.g. improving legal regulations and using new technologies and renewable energy), riverine thermal pollution from cooling systems remains a concern due to rapid and continued expansion of thermal power plants, globally (Dittmar, 2012; Pfister & Suh, 2015; Raptis et al., 2016; Raptis et al., 2017; Miara et al., 2018). In addition, little research has been conducted to evaluate the impact of thermal effluents and their impact on different river types and regions. As such, there is an urgent need to better understand and mitigate power plant thermal pollution in global freshwaters.

Aquatic ectotherms are vulnerable to unnatural changes in thermal regimes because of the dependence of body temperatures on the temperature of surrounding water (Brown et al., 2004; Narum et al., 2013; Akbarzadeh & Leder, 2016). In order to optimise their survival under unfavourable thermal conditions, aquatic ectotherms can acclimate to new thermal regimes, a rapid and reversible physiological adjustment that protects them from the negative consequences of temperature changes; for example, by altering respiration rates or having smaller body size (Pörtner et al., 2017; Malison et al., 2022). Where ectotherms inhabit different thermal regimes, dissimilar capacities for thermal acclimation can develop, even within a single species, governed by the experienced temperatures (Maazouzi et al., 2011; Foucreau et al., 2014). Past research has shown that warm-acclimated animals typically have lower sensitivities to thermal stress and thus higher survival rates than cold-acclimated animals (Whiteley & Faulkner, 2005; Foucreau et al., 2014; Semsar-kazerouni & Verberk, 2018). However, few studies have been focused on the influence of the thermal variability experienced over multiple generations on the tolerance to acute and chronic thermal stress in animals (e.g. Strange et al., 2002), which is critical to understanding the extent to which freshwater life will be able to adapt to future thermal regimes. Given current uncertainties in power plant discharge and the compounded impacts of climate change (e.g. magnitude, location, times of discharge), it is essential to be able to rapidly identify and evaluate power plants that might cause severe thermal pollution, and understand the potential ecological consequences of alterations to thermal regimes. This would help in developing more robust planning and management

strategies.

1.1. Thesis aims and objectives

The aim of this thesis is to evaluate the impact of thermal pollution from power plants on rivers and aquatic life across different spatial (global, regional, and local) and temporal (river: hourly temperature variations; aquatic life: survival and behavioural changes within a week to a couple of weeks) scales. To achieve this ultimate goal, the project is split into three key objectives, each representing a linked but distinct area of work, which are:

1) To map and assess the relative significance of power plants as a source of thermal pollution on a national scale and develop an impact index for thermal pollution (Chapter 3).

2) To model the whole-river scale impacts of both individual and multiple power plants to observe how far downstream thermal effluents remain distinct and/or interact along a hypothetical river system (Chapter 4).

3) To investigate how aquatic ectotherms inhabiting sites with different temperature variabilities differ in their survival and behaviours in response to acute and chronic thermal stress (Chapter 5).

1.2. Justification of aims and objectives

To mitigate thermal pollution from power plants, sustainable technologies (e.g. combined heat and power plants and combined cycle gas turbine) in combination with strict regulations, have been applied to globally phase out power plants with low thermal efficiencies. However, power plants with low thermal efficiencies are still operational in many places and, even where being phased out, are still often used to address energy demand spikes. Given that critical resources such as labour, material and finance are limited, it is important to locate and evaluate power plants that generate large amounts of thermal

pollution, to prioritise the implementation of new technologies and regulations to reduce impacts. Such prioritisation would optimise the benefits to costs, leading to better environmental and economical results. As such, Chapter 3 presents the development and initial validation of a computationally simple and low data-intensive index as a tool for identifying 'hotspots' that need particular attention (addressing Aim 1).

The new index makes it possible to assess the impact of power plant effluent and identify rivers that are particularly vulnerable to effluent release. However, most research has concentrated on the impact of power plant discharge on lakes (e.g. Kirillin et al., 2013; Råman Vinnå et al., 2017) and coastal areas (e.g. Ma et al., 2017; Yavari & Qaderi, 2020), with relatively few studies focused on the rivers at the reach (e.g. Kalinowska et al., 2012), regional (e.g. Stewart et al., 2013) or global scales (e.g. Raptis et al., 2016). This lack of work is significant because, in a river, powerplant effluents may interact in a downstream direction. The interaction and cumulative impact of multiple power plants on the same river, or in the same catchment, have not been examined despite the potential importance and complexity of this source of thermal pollution. Chapter 4 explores the impacts of individual and multiple power plants on river temperatures in a conceptual water temperature model at the whole-river scale (addressing Aim 2).

Aquatic ectotherms are dependent on the temperature of surrounding water and can be greatly influenced by elevated water temperatures due to thermal discharges. Therefore, aquatic organisms have to make necessary physiological and behavioural adjustments (i.e. acclimation) under new thermal conditions to protect themselves from the negative consequences of elevated temperatures. The capacities for thermal acclimation are partly determined by the thermal history (i.e. habitat temperature regime) experienced by the animal. As such, the tolerance and survival of individuals at stressful temperatures can differ markedly, even within a single species (Dallas & Rivers-Moore, 2012; Vehille et al., 2023). Past research has been primarily focused on the thermal tolerance and performance at steady, chronic temperatures where individuals are exposed to different thermal regimes for extended periods, and then their ability to acclimate to a new temperature is assessed (e.g. Maazouzi et al., 2011; Foucreau et al., 2014). However, the *variability* in experienced temperatures

may also dictate how organisms respond and acclimate to increased temperatures. Chapter 5 investigates the response of aquatic ectotherms with different thermal histories to acute and chronic thermal stress via laboratory experiments with steady and variable temperatures (addressing Aim 3). The three aims collectively demonstrate how thermal pollution from power plants may impose an impact on rivers across space and time, and ultimately cause significant ecological implications.

1.3. Thesis structure

This thesis is made up of six chapters. Chapter 1 provides an introduction to the topic and details the thesis aims. The literature on power plant thermal pollution and its potential impacts, are reviewed in Chapter 2. The research conducted for this thesis is presented in Chapters 3 to 5. Chapter 6 presents an overall discussion of the results from these chapters and explores the fulfilment of the aims.

Chapter 2: Power plant thermal pollution in rivers

Water temperature is a key parameter for the quality of aquatic environments as it strongly influences multiple components of aquatic ecosystems, including the rate of chemical and biological processes, the amount of dissolved oxygen, the photosynthesis rate of aquatic plants, the metabolic rates of aquatic organisms, and their susceptibility to parasites, disease, and pollution (Angilletta, 2009; de Paul Obade & Moore, 2018; Priya et al., 2023). Therefore, any deviations from natural temperature regimes can cause stress and have serious consequences for local communities and ecosystems. Besides the ecological consequences, changes in temperature regime can also pose a threat to economic and social sectors, including power generation (Miara et al., 2018), drinking water production (Ramaker et al., 2005), and recreational angling (Lynch et al., 2016). Natural temperature regimes can be altered by anthropogenic activities and climate change, widely known as thermal pollution. However, the underlying processes and mechanisms of thermal pollution are complex and largely unknown and thus not well incorporated into assessment and management, providing ample opportunities for future research. Here, we review the current knowledge of thermal pollution and its impact on river temperature regimes, which provides a solid foundation for understanding the complexities of thermal pollution and identifying research gaps.

2.1. Definition and classification of thermal pollution

Thermal pollution is broadly defined as the degradation of water quality by anthropogenic processes that results in an unnatural change in temperature of a natural water body such as ocean, river, pond and lake (Langford, 1990). Under this definition, thermal pollution can be generally divided into two categories: point source and non-point source. Point source thermal pollution is associated with the direct discharge of thermally altered water from a discrete location that can be identified as the source of the pollution. In contrast, non-point source thermal pollution is attributable to diffuse sources in connection

with a wide variety of human activities occurring over a large geographic area. Whereas diffuse thermal pollution typically leads to chronic, gradual increases in average temperatures over large areas (e.g. van Vliet et al., 2013; Wanders et al., 2019), point source thermal pollution can lead to sudden, large-scale changes to maximum, minimum and mean temperatures (Langford, 1990).

2.2. Sources of thermal pollution

The thermal regimes of rivers can be affected by five key types of non-point and point source thermal pollution: 1) climate change (Mohseni et al., 2002; Somero, 2010); 2) deforestation (Feller, 1981; Johnson & Jones, 2000; Jackson et al., 2001; Moore et al., 2005); 3) urbanisation (Kinouchi et al., 2007; Janke et al., 2013; Glose et al., 2017); 4) flow regime alterations (Stevens et al., 1997; Lessard & Hayes, 2010; Jiang et al., 2018), and; 5) industrial and domestic thermal effluents (Kenny et al., 2005; Tress, 2010; NRDC, 2014). Over the past 20 years, anthropogenic climate change has been recognised as an important non-point source of thermal regime change over large scales (Stefan et al., 2001). The Earth's atmosphere has warmed greatly since the 1970s (Kosaka & Xie, 2013), mostly due to increased concentrations of carbon dioxide (CO_2) and other greenhouse gases (Montzka et al., 2011), and is expected to warm further as concentrations continue to rise (UNEP, 2020). Given the close relationship between air and water temperatures, any change in the former will induce a corresponding change in the latter in the same direction (van Vliet et al., 2011; Higashino & Stefan, 2016; Naresh & Rehana, 2017). Although the magnitude of warming of freshwater associated with climate change is gradual (0.1–0.2 °C per decade [IPBES, 2017]) compared to other sources of thermal change, its contribution as a long-term process is significant and can exacerbate other existing stresses with substantial ecological implications, particularly for species living near their thermal thresholds (Somero, 2010). For example, Mohseni et al. (2002) studied 57 fish species in the USA and predicted changes in aquatic habitat under climate warming, which showed a decline of 36% of suitable habitats for coldwater fishes and a tendency of migration to higher elevations where coldwater habitats could still exist.

Deforestation, as a non-point source, has a significant and complex impact on the thermal regime of a stream or river, particularly in forested catchments. In a review by Moore et al. (2005), rises in summer water temperature were related to harvesting activities in almost all studied streams in rain-dominated catchments, with maximum summer temperature increases ranging up to 13 °C. Logging activities also increased daily temperature ranges in summer, which reached up to around 7–8 °C, compared to pre-logging ranges of about 1–3 °C (Feller, 1981; Johnson & Jones, 2000). These changes in thermal regime can be explained by deforestation activities which undermine the active participation of forest in the thermal energy budget (Fig. 2.1). Forest canopies play an important role in controlling the thermal and moisture environments beneath the canopy by reducing incoming solar radiation, precipitation, and wind speed near the ground surface, and enhancing longwave radiation received over the surface (Moore et al., 2005). The removal of these important controls in the riparian zone can contribute to marked changes in stream temperature. For example, given that riparian canopies moderate stream temperature by providing shading that reduces the influence of solar radiation, the loss of riparian shading can lead to warming of streams during the summer season, with typical temperature increases of 4.1 °C, and up to 13.0 °C (Hester & Doyle, 2011). The warming effect due to the reduction of riparian shading is most pronounced in lower-order streams and becomes less critical in higher-order rivers (Rivers-Moore et al., 2021).

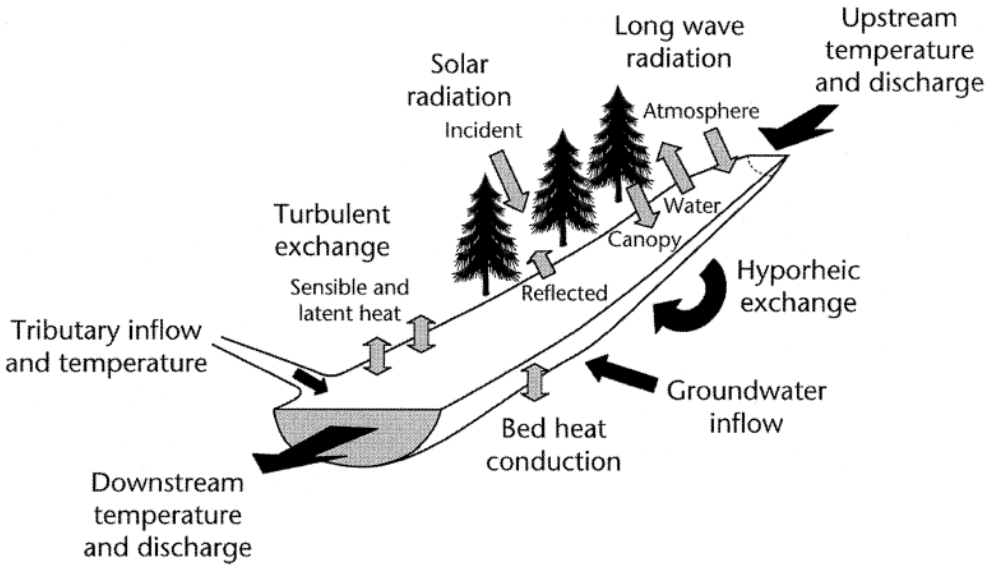

Figure 2.1. Key factors controlling stream temperature. Black arrows indicate

energy fluxes associated with water exchanges (Moore et al., 2005).

Urbanisation is the shift from agricultural-based land use to a domestic and/or industrial-based urban land use. The global population in urban areas has increased markedly from 1750 million in 1980 to 3571 million in 2010 and is estimated to reach 5058 million by 2030 (United Nation Population Division, 2018). The increasing rate of urbanisation across the world is twice as fast as population growth (Angel et al., 2011). The rapid expansion of urban areas can significantly change the physical, chemical, and biological environment in surface waters. In urban hydrological systems, water is withdrawn from nearby water sources to maintain various human activities which produce large volumes of warmer urban wastewater, which are subsequently discharged back into freshwater bodies. An investigation in central Tokyo and its suburbs showed that the stream temperature in winter and early spring increased at a rate of 0.11–0.21 °C per year from 1978 to 1998 at sites where wastewater effluent was released (Kinouchi et al., 2007). The land surfaces of urban areas are also changed from permeable to less permeable, or impermeable surfaces, such as roads, pavements and rooftops that contribute to changes in local climate and foster the development of an urban heat island (UHI; Maria et al., 2013). Materials used for these impervious surfaces are commonly concrete and asphalt, which absorb more thermal energy than most natural surfaces (Janke et al., 2013; Glose et al., 2017). Therefore, heat accumulates in these surfaces and contributes to high surface temperatures, which can reach up to 48–75 °C for a conventional pavement (Ferguson et al., 2008). The accumulated heat then propagates downward to the subsurface during the day and is released as radiative heat at night. During rainfall, the stormwater runoff receives the released heat and flows into important water bodies such as lakes, streams and rivers, which potentially raise the base temperature of surface water (Gilbert et al., 2017) and have significant ecological implications, especially for coldwater habitats (Herb et al., 2008; Herb et al., 2009).

The alteration of river flow regimes by diversion, abstraction and impoundment can be key sources of thermal stress on freshwater ecosystems via point and non-point sources. Among these flow alterations, impoundments have attracted the most attention due to their profound impacts on the downstream thermal regime. In a reservoir, thermal stratification can occur in summer because water

in the upper layer (i.e. the epilimnetic layer) is warmed by solar radiation and cold water remains underneath (i.e. the hypolimnetic layer; Weber et al., 2017). However, water in the upper layer is often cooled in the winter and thermal stratification is diminished and eventually eliminated by full vertical mixing (Ling et al., 2017). Large dams release water from deep penstocks that are mostly located in the hypolimnetic layer and hence, cold water is released to the downstream reaches, leading to significant thermal disturbances downstream, termed cold-water thermal pollution (Jiang et al., 2018). The released cold water can have significant consequences for the reproduction, growth, and distribution of organisms downstream, particularly fish (Preece & Jones, 2002) and invertebrates (Vannote & Sweeney, 1980). For example, a study in the Colorado River, USA, found almost no species of Ephemeroptera, Plecoptera and Trichoptera downstream of a major dam, suggesting the interruption of the life cycle by cold stenothermic releases (Stevens et al., 1997). Although much rarer, some relatively small dams do release water from upper layers, which can lead to warming of downstream reaches (Lessard & Hayes, 2010). Moreover, storage hydropower plants use the potential energy of water stored at high elevations to generate electricity on demand, which leads to intermittent and abrupt releases of water and thus frequent and rapid fluctuations in flow and water temperature downstream the power plant outlet, respectively referred to as hydropeaking and thermopeaking (Zolezzi et al., 2011). Recent research indicated that the thermopeaking caused by intermittent releases from hydropower plants promoted the drift and stranding of both fishes and invertebrates (Auer et al., 2022; Tonolla et al., 2022)

Finally, power plants and industrial factories are the significant contributors to point-source thermal pollution, which can lead to significant increases in water temperature. Wright et al. (1999) demonstrated that the impact of power plants on water temperatures was comparable with that by climate change. In the lower Ebro River, Spain, the thermal effluent from the Ascó nuclear power plant increased the mean annual water temperature by about 3 °C, which varied greatly as a function of river discharge (Prats et al., 2010). Wawrzyniak et al. (2012) also reported a water temperature increase of 2 °C in the French Rhône River immediately downstream of the Saint-Alban nuclear power plant, thereafter decreasing to 0.8 °C and 0.5 °C at 15 and 30 km downstream of the plant, respectively. In different seasons, the water temperature of the Danube

River showed contrasting responses to the thermal effluent from the Cernavodă nuclear power plant in Romania, which increased by 4.5 °C in summer, 5.9 °C in autumn and 13.5 °C in winter at a downstream monitoring site (Liliana, 2012). Power plants mainly draw water from nearby sources and use it for cooling before releasing the heated water back to the source or downstream. The problem of releasing heated water is particularly severe for thermoelectric power plants due to the large water withdrawal needed for cooling. It was estimated that water withdrawals for generating thermoelectric power reached approximately 761 billion litres per day in the USA, which was higher than withdrawals for any other industry in 2005 (NRDC, 2014). In the UK, total water abstraction for thermoelectric generation was 17,553 billion litres per year in 2010, with 1.1% from freshwater, 44.3% from tidal surface water and 54.6% from seawater, respectively (Byers et al., 2014). It was also reported that the amount of water drawn for thermoelectric power accounted for approximately 50% of total water withdrawals in the US and Western Europe (EEA, 2009), respectively, compared to 84% of total water withdrawals in China (Qin et al., 2015). The demand for such a large volume of water can be explained by the operating principle of thermoelectric power plants, and more specifically, the Rankine thermodynamic cycle, described below.

In most cases, water is used as the working fluid in the Rankine cycle due to its favourable properties, including its non-toxic and unreactive chemistry, high availability, and low cost, as well as its thermodynamic properties (e.g. large specific heat capacity). It is noteworthy that the water for the Rankine cycle is distinct from the water withdrawn from the nearby water source because it is required to be clean and purified and continuously circulated in a closed loop. At the start of the cycle, water is heated in a boiler until it is turned into steam by different energy sources such as nuclear fission or the combustion of fossil fuels (Fig. 2.2). The steam then drives the turbine attached to a generator to produce electricity. After the steam passes through the generator, it is sent to a condenser to be converted back into water via a cooling process using the withdrawn water and pumped back to the boiler to start another cycle (NRDC, 2014). In order to enhance the thermal efficiency and prevent turbine blades from erosion by condensed water droplets, the operating temperature is typically maintained at 500–600 °C for a typical coal-based power plant (Li & Wang, 2018), and 285–320 °C for a nuclear power plant (Vyas, 2019). These high

steam temperatures need to be reduced to below 30 °C in the condenser (BEEMS, 2011), which requires a large amount of water for this cooling process. In turn, the absorption of heat by the cooling water increases its temperature tremendously, meaning that it returns to the waterbody substantially warmer than when it was abstracted, creating thermal effluent. About 80% of the electricity in the world is generated this way (via the steam cycle; IEA, 2013), and the water withdrawals for cooling processes continue to rise with the rapid development of industry, thereby making thermal power plants a 'research hotspot' of thermal pollution.

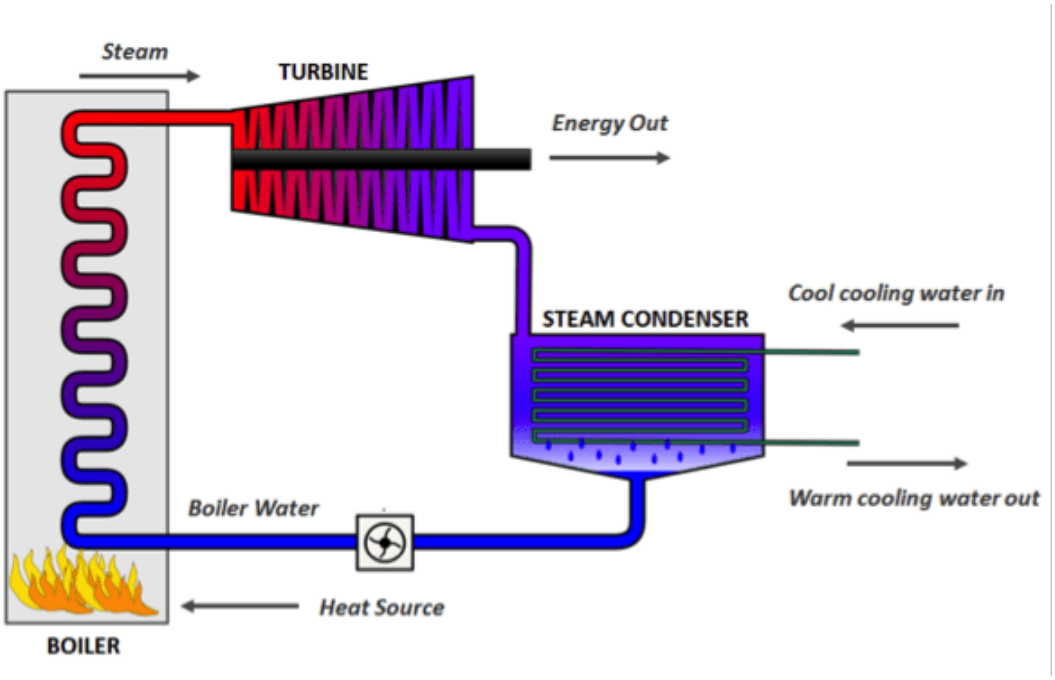

Figure 2.2. A simple ideal Rankine cycle (WATCO Group, no date).

2.3. Thermal pollution from thermal power plants

The severity of thermal pollution from power plants is mainly dependent on the applied cooling systems and power plant type, which dictate water withdrawal and consumption. Water withdrawal refers to water abstracted from the natural environment while water consumption is defined as the part of withdrawn water that is not returned to the source (Peer & Sanders, 2016). There are essentially four different types of cooling system: once-through cooling, closed-cycle cooling, dry cooling, and hybrid cooling (NRDC, 2014). In once-through cooling systems, cooling water is discharged back to its original source at very high

temperature, which imposes great thermal stress on downstream aquatic organisms. Once-through cooling systems do not recycle cooling water and thus, considerably higher volumes of daily water withdrawals are needed relative to other methods, rendering the power plant vulnerable during hot and dry weather. The water intake structures at power plants with once-through cooling systems can also be problematic. For example, in New York approximately 17 billion fish at different life stages (i.e. eggs, larvae and juvenile fish) were sucked in and killed each year by the water intake system of a once-through powerplant and another 171 million adult fish were injured or killed annually by the intake screens (Tress, 2010). Consequently, once-through cooling is currently prohibited for new power plants in many countries and regions (e.g. once-through cooling phaseout regulations in California, USA).

Wet-recirculating or closed-cycle cooling systems use cooling towers to dissipate the heat absorbed from the boiler steam through evaporation and recirculate the remaining cooling water through the condensers for a second cycle rather than immediately discharging it back to the original water source. Compared with once-through cooling systems, wet-recirculating cooling reduces water withdrawals and the corresponding ecological impacts by about 95% (Mielke et al., 2010). Wet-recirculating cooling has thus become the most favoured technology for the majority of power plants. In 2001, the USEPA issued the Phase I rule, which mandates the use of wet-recirculating cooling systems at new plants (NRDC, 2014). However, the system tends to have significantly higher water consumption because a large amount of water is lost through evaporation.

Dry cooling systems are similar to typical wet-recirculating cooling systems but use ambient air instead of water to cool the steam. The water consumption can be decreased by over 90% since virtually no water is used in dry cooling systems (Union of Concerned Scientists, 2013). The greatly reduced water withdrawals can effectively avoid the fish kills associated with water intake systems. The trade-offs for these water savings and environmental benefits are higher capital, operation and maintenance costs and lower efficiencies. Dry cooling systems are highly dependent on the ambient air temperature and humidity and therefore, their efficiency is reduced markedly in hot and dry climates. Despite these drawbacks, dry cooling systems do not require cooling

water to operate, which offers a new power plant great flexibility in selecting a location.

Finally, hybrid cooling systems are designed to exploit the benefits of both the dry cooling and wet-recirculating cooling systems by reducing water consumption relative to wet-recirculating systems and improving the performance during hot and dry weather relative to dry systems. In this case, hybrid cooling systems are used as dry cooling systems during the cooler periods, supplemented with wet cooling during the hotter periods when dry cooling systems cannot maintain their efficiency.

Based on the type and size of the plant, a thermal power plant operates at a particular optimal temperature and pressure to achieve the highest thermal power generation efficiency. Most new coal-based power plants can maintain an operating energy efficiency exceeding 40%, with state-of-the-art, coal-fired plants at 47%; whereas nuclear power plants can only achieve thermal efficiencies of about 32–36% (World Nuclear Association, 2019). The lower thermal efficiency of nuclear power plants is attributed to the limitation of plants operating at a lower temperature in order to ensure the safe operation within the facility. In that case, nuclear power plants would generally release more heat and thus have a higher demand for cooling water than fossil-fuel power plants. It has been estimated that nuclear power plants with a low thermal efficiency (approximately 33%) require 30–100% more cooling water than other types of plants with a comparable generation capacity (Levin et al., 1972; Kirillin et al., 2013).

2.4. Global to local impacts of power plant thermal effluent on rivers

Research on thermal pollution in rivers has been conducted across different spatial scales, spanning the global to the local. Within these scales, the problem of riverine thermal pollution can be viewed from distinct perspectives, which collectively provide a comprehensive understanding for further study. Raptis et al. (2017) aimed to perform a global assessment of thermal pollution from power

plants with once-through cooling systems by building on a series of papers that developed a model at smaller scales (Verones et al., 2010; Pfister & Suh, 2015; Raptis & Pfister, 2016). They used a characterisation factor to describe the impact of heat emissions on ecosystem quality. They then applied the factor in an environmental assessment model of freshwater thermal pollution from power plants to identify pollution hotspots globally, considering space, time and applied cooling technology. The characterisation factor (CF) was calculated with a fate factor and effect factor.

$$CF_{cumulative,t} = \sum_{j} CF_{j,t} = \sum_{j} FF_{j,t} \cdot EF_{j,t}$$

where $FF_{j,t}$ is the fate factor (days $\cdot m^3_{river} \cdot °C_{river}/(°C_{cw} \cdot m^3_{cw})$) and $EF_{j,t}$ the effect factor (PDF/$°C_{river}$) for river section j in time period t. PDF stands for potentially disappeared fraction of species. The inclusion of different time periods (e.g. months) reflects the variability in environmental conditions throughout the year. The partial CFs were summed along the river to arrive at a total, cumulative CF. The fate factor describes the temperature increase in the system (a volume of water) during the residence time of a heat emission; whereas the effect factor estimates the potentially disappeared fraction (PDF) of species as a function of water temperature increase, based on species sensitivity distributions (SSD) for temperature-induced mortality of aquatic species.

The research successfully identified important watersheds under pressure from thermal pollution globally, such as the Great Lakes, Mississippi, the Danube, and the Yangtze Rivers, and related this thermal pressure to the long-term application of once-through cooling systems. However, there were limitations to their research. First, the study only focused on thermoelectric power plants and did not take into account other important factors affecting river temperatures, such as urban centres (Wang et al., 2015; McGrane, 2016; Ketabchy et al., 2019) and dams (Olden & Naiman, 2010; Ling et al., 2017; Jiang et al., 2018). Ignoring these factors could introduce significant uncertainties to the final results, particularly for watersheds that were less thermally affected by power plants. In addition, only sizable power plants with large capacities, which accounted for only 58% of total cooling system units, were included in the research. Hence,

those of smaller size were not considered despite their potential cumulative significance, especially on smaller rivers. Lehner et al. (2011) argued that multiple small and medium sized dams could contribute to significant cumulative impacts on flow regulation, as demonstrated by Grill et al. (2015) who found that fragmentation (44.7% to 65.4%) and flow regulation (65.0% to 90.1%) indices increased significantly when small dams were included in the study. Therefore, it is expected that a similar effect could be true of small thermal power plants, where multiple small thermal power plants within the same catchment could have significant cumulative implications for water temperatures. Also, predictions for future thermal pollution were not included in the study and consideration of locations that are particularly vulnerable to thermal pollution, for informing effective decision-making, was not presented.

At local scales, research on riverine thermal pollution concentrates on the temporal and spatial changes in water temperatures in the proximity of the artificial structures (Langford, 1971; Langford & Aston, 1972; Langford & Daffern, 1975). At Ironbridge Power Station in the UK, a series of studies were conducted on the short- and long-term temperature changes associated with a cooling water outfall, and the impacts on macroinvertebrates (Langford, 1971; Langford & Aston, 1972; Langford & Daffern, 1975). In comparison with the base line condition (i.e. local hydrology), the authors discovered both short- and long-term effects of heated cooling water on the river hydrology. In the short term, the daily and weekly temperature range in the river increased by up to 100%, and unnatural ‘diurnal’ variations of 2–5 °C occurred in the downstream reaches during low-flow winter periods. In the longer term, total hours when water temperature exceeded 0 °C showed moderate increases in the downstream in 1965 and 1966. These early studies successfully elucidated the impacts of cooling water on thermal regimes of the river; however, the ecological implications of these changes could not be determined, largely because of limited data availability and accuracy.

Global and local data quality and availability have improved with the help of technological developments in measurement and monitoring of river temperatures (e.g. remotely sensed thermal infrared imagery). Such advances have stimulated the growth of research in new techniques of data analysis and modelling, enhancing our understanding of thermal behaviour in space and time

(Caissie, 2006; Webb et al., 2008). Essentially, there are three types of model used for water temperatures: regression, stochastic and deterministic models. Due to the strong correlation of water temperature to air temperature, water temperatures can be effectively obtained with regression models, which have been broadly applied as a predictive tool for different time scales from daily (Higashino & Stefan, 2016) to monthly (Naresh & Rehana, 2017). Daily water temperatures can also be predicted by stochastic models when autocorrelation is important in the time series (Cassie et al., 2001). However, these models cannot provide detailed explanations for the underlying processes due to their inherently conceptual framework. In that case, deterministic models, which quantify different energy components, can be particularly useful. The descriptions of physical forcing and heat exchange processes in deterministic models are helpful in understanding and explaining the changes in flow and thermal regimes caused by power plant effluents. This is particularly important for predicting future water temperature across temporal and spatial scales (e.g. the Mediterranean region with low precipitation and warm annual temperatures) because parameter values in the deterministic model can be readily modified, in comparison to regression models which require large quantities of new data to update parameters and are only effective in the region where the data is collected. Predictions under different climate change scenarios can provide useful information for planning regulation and management within the thermal limits.

2.5. Impacts of thermal effluent on river ecosystems

Freshwater environments are affected by the thermal environment generated by the interaction of climate patterns and fluvial processes, as well as other stressors, and are therefore susceptible to climate change (Durance & Ormerod, 2009). Thermal effluent has an additive impact on projected climate change and could potentially lead to significant changes in river thermal regime, as well as exerting a direct influence on a range of riverine organisms including fish, invertebrates and microorganisms (e.g. algae and protozoa). Extensive research has been carried out on the impact of changing temperature on freshwater fish (e.g. Dugdale et al., 2016; Frechette et al., 2018; Bilous &

Dunmall, 2020). Fish are ectothermic animals and therefore compensatory responses are induced to reduce the effects of thermal stress on metabolism when temperature changes (Rossi et al., 2017). For example, Mesa et al. (2002) performed laboratory tests to assess the effects of acute temperature increase on juvenile fall chinook salmon from the Hanford Reach of the Columbia River. The exposure of fish to thermal stress did not result in significant increases in direct mortality or vulnerability to predation; however, there were considerable alterations in physiological homeostasis, particularly the synthesis of heat shock protein 70 (HSP70) which increased 25 fold, to repair and protect from thermally-induced cellular damage. Oskala et al. (2014) found similar increases in levels of studied HSPs (i.e. HSP70, HSP60, HSP90, HSC70 and GRP75) in fish *Garra rufa*. Severe implications are expected when the capability of HSP70 synthesis is overwhelmed by the demand for protecting from the multiple, cumulative stressors in a river. While short-term exposure to thermal stress is often met with compensatory responses, repeated and/or chronic exposure to stress can have serious, negative implications for fish survival.

Whilst much work has been done on the thermal tolerances of aquatic animals, less has been done to specifically identify the ecological impacts of point-source thermal pollution. In the River Fiddich, a tributary of the River Spey in Scotland, water temperature was raised by 1–3 °C above ambient due to cooling water effluent discharged from whisky distilleries (Morrison, 1989), leading to higher growth rates for salmon and trout in downstream reaches and alterations in the timing of juvenile migration. Morrison (1989) attributed these changes to enhanced feeding activity, probably due to increased metabolic rates dictated by food availability (i.e. invertebrates). However, adverse consequences would be expected if food is scarce. Auer et al. (2015) demonstrated that the metabolic rate of juvenile brown trout *Salmo trutta* increased when food was abundant and decreased when the environment switched to a low food level. In this case, the energy produced from reduced metabolism could be insufficient for sustaining the necessary activities for fish survival, such as growth, feeding, reproduction, embryonic development, migration and predation.

Temperature changes due to thermal effluent can also impose significant impacts on macroinvertebrates, which can affect the survival of individuals and species by altering the community composition, as well as individual behaviour

and phenology (Langford, 1990). A study in Canada showed that a 2–3.5 °C increase in water temperature led to a decline in the density of invertebrates, particularly Chironomidae (Hogg & Williams, 1995). Hogg and Williams (1995) indicated that this decline could be the result of increased respiration to production ratios, which reduced the efficiency of using the available resources within the stream system. In small upland streams in Wales, it was predicted that the spring abundance of some macroinvertebrates might decrease by 21% for every 1 °C water temperature rise, potentially threatening predatory species by limiting food availability and hence the energy transfer through the food web (Durance & Ormerod, 2007). However, it is not adequate to interpret the impact of temperature changes on invertebrates with merely these biological metrics. Worthington et al. (2015) conducted research on the impact of thermal effluent from a power station on the macroinvertebrate community in the River Severn. They used a similar approach to Magurran and Henderson (2003) which divided the sampled invertebrates into 'core' and 'occasional' species groups, based on the number of samples a species was recorded in and its abundance. The control site showed significantly higher abundance and taxon richness than the site closest to the power station outfall (500 m downstream); however, the Shannon-Wiener diversity and the total sample richness showed no significant differences across sampling sites, and there were no negative relationships between any above metrics and the recorded water temperature. Therefore, impacts of thermal effluent may be subtle and sub-lethal and difficult to identify in measurements of the community composition. For example, Everall et al. (2014) found that the mayfly *Ephemera danica* lived for two years as an aquatic larvae in sites on the River Dove fed by groundwater with temperature of constant 9 °C, whereas they only remained in the river for one year 500 metres upstream, where temperature variability ranged from 0 to 25 °C. Although sub-lethal changes in phenology have meant the species survives at both sites, the resilience of the population in the groundwater-fed site is much higher than that in the variable site because animals emerge when larger, lay more eggs, and have an overlapping population structure (Everall et al., 2014).

At the community level, thermal effluent could trigger the rearrangement of community composition by creating unsuitable habitats for temperature-sensitive species and providing opportunities for more temperature-tolerant species (Scrine et al., 2017), as well as thermophilic non-native invasive species

(Walther et al., 2009). Orthocladiinae are considered a cold stenothermal animal and therefore are less abundant at thermally-impacted sites (Hoang et al., 2006; Worthington et al., 2015). In contrast, *Asellus aquaticus*, *Sphaerium corneum*, *Erpobdella octoculata*, *Limnius volckmari* and *Bithynia tentaculata*, are considered more thermally-generalist, and show significantly higher abundances at thermally-impacted sites (Worthington et al., 2015). The positive correlation of the abundances of some species with water temperature is explained by their tolerance to thermal pollution. For example, *Bithynia tentaculata* is capable of adapting to unfavourable conditions by undertaking metabolic depression (Hahn, 2005). *Asellus aquaticus*, can also acclimate to increased temperatures (Korhonen & Lagerspetz, 1996); however, this is achieved at the price of a reduced life cycle length (Langford, 1990). Similarly, the abundance of some pollution-sensitive Ephemeroptera, Plecoptera, and Trichoptera (EPT) species has been found to increase with temperature, possibly associated with induced changes in the egg incubation period (Brittain, 1990). Therefore, the impacts of temperature interact in complex ways with life-cycle (Clusella-Trullas et al., 2021) and other pressures, including chemical pollution (e.g. Delnat et al., 2019), which makes the direct impacts of water temperature on aquatic animals hard to identify.

Chapter 3: Development of a thermal pollution index to assess the impact of power plant effluent

3.1. Introduction

Water pollution is primarily associated with human activities which contribute to the release of domestic sewage (Huang et al., 2003; Liu & Qiu, 2007; Chen et al., 2018b) and agricultural and industrial wastewater (Panizza & Cerisola, 2001; Cobas et al., 2016; Burdon et al., 2019). The receiving water bodies can suffer from severe degradation of water quality by introduced excessive and toxic chemical substances. Despite significant global concern about degradation in freshwater quality currently and historically, thermal pollution, has received considerably less attention than many other types of water pollution. However, evidence suggests thermal pollution, here defined as the increase or decrease in water temperature caused by human activities (Langford, 1990), is likely to be highly significant (Dittmar, 2012). In addition, the impact of thermal pollution on water temperature could be further exacerbated due to climate change (Roberts et al., 2017) and the ongoing reduction in riparian shading associated with land use change (Johnson & Wilby, 2015; Dugdale et al., 2018; Jackson et al., 2021).

Thermal pollution can be attributed to various direct (e.g. dam release and power plant discharge) and indirect factors (e.g. deforestation and urbanisation), with a key direct source being cooling water from thermal power plants which utilise heat energy to generate electric power (Hester & Doyle, 2011). Thermal power plants are a particularly significant source of thermal pollution because the warmer effluent discharged from their cooling systems can cause abrupt changes in water temperature, imposing substantial thermal stress on aquatic organisms including algae, macroinvertebrates and fish (Worthington et al., 2015; Rossi et al., 2017; Muftin et al., 2020). For example, Chang et al. (2010) conducted research on a species of thornfish which had widespread vertebral deformity due to enhanced requirement of vitamin C attributed to increased water temperature associated with the thermal effluent of a nuclear power plant

in Taiwan. Similar results were also found by Shao et al. (2018) on the malformation of largescale mullet. The spinal deformity seemed to be an acute response and not lethal to the fish, and juvenile thornfish could recover after the habitat returned to regular water temperature. The finding highlights the fact that the impact of thermal pollution on aquatic organisms is not limited to changes in species abundance, richness and diversity but involves more complex sub-lethal impacts, such as deformity and phenological changes (Everall et al., 2014).

Although great efforts have been made to alleviate thermal stress by improving legal regulations (e.g. UK: Standard rules SR2010No2; USA: the Clean Water Act and National Pollution Discharge Elimination System program) and treating effluent using new technologies such as recirculating (tower) cooling (Environment Agency, 2016; McCall et al., 2016), riverine thermal pollution from cooling systems remains a concern due to rapid and continued expansion of thermal power plants globally (Dittmar, 2012; Pfister & Suh, 2015; Raptis et al., 2016; Raptis et al., 2017; Miara et al., 2018). In India, 40 coal-fired power-plant projects are currently under construction, accounting for 61 GW of capacity (Mint, 2021). Despite the ongoing transition towards renewable energy in developed countries, the USA still has plans to build 10–20 GW of new gas-fired power plants in each of four major regions (i.e. Great Lakes, Northeast, Southwest and West Coast) during 2018–2022 (Burt & Ramey, 2020). In light of continued projected rises in water temperature due to climate change (van Vliet et al., 2011) and power-plant expansion (Raptis & Pfister, 2016), it is of vital importance to understand the current status of thermal pollution in rivers and the likely impacts of the decommissioning and construction of power plants.

Raptis et al. (2017) were the first to perform a global assessment of thermal pollution from power plants with once-through cooling systems. Their work is based on a series of papers, starting with smaller-scale (individual power plants) assessments and building to a global scale assessment of power plant-related thermal pollution (Verones et al., 2010; Pfister & Suh, 2015; Raptis & Pfister, 2016). Using a characterisation factor, they described the impact of heat emissions on ecosystem quality and identified important watersheds under pressure from thermal pollution globally, including the Great Lakes, Mississippi, the Danube, and the Yangtze Rivers (see section *2.4*). The heat emissions were

calculated by solving relevant thermodynamic cycles (e.g. Rankine cycle) for power generating units with relevant data from the World Electric Power Plants Database (WEPP; Raptis & Pfister, 2016). However, the calculations were computing- and data-intensive, and the proprietary database WEPP is financially expensive to access, difficult to obtain, and contains uncertain power generating units that cannot be found in other databases (e.g. 'Aachen Works 1'; Gotzens et al., 2019). In addition, the research overlooked small-capacity power plants, which might have great cumulative significance, especially on smaller rivers. Therefore, we aimed to develop a less computing- and data-intensive index, based on more readily accessible datasets, for assessing the relative importance of much larger size range of thermal power plants on riverine thermal pollution.

This study documents the development of a thermal pollution index to explore thermal effluent pollution from power-plant discharge on a national (i.e. conterminous USA) scale. Many areas globally are data poor, so model construction and validation is taking place in the USA by *1)* compiling a national power-plant dataset with information on cooling systems by integrating different datasets and inspecting uncertain plants via Google Earth, *2)* examining the global and regional distribution of power plants in the catchment by estimating their upstream catchment areas, *3)* developing a new index to quantify thermal pollution from power plants and applying the index to investigating power plants located on rivers in the USA, and *4)* exploring potential statistical relationships between power-plant parameters and the index for estimating indices for rivers near plants where thermal impact is unknown to provide a more holistic view of vulnerable places for future planning.

3.2. Materials and Methods

3.2.1. Compilation of a USA power-plant dataset with cooling information

3.2.1.1. Selection of power plant databases for compilation

Power plant databases are diverse and built for different purposes and regions

(Table 3.1). For instance, the Carbon Monitoring for Action (CARMA, 2021) is a global database providing information on the carbon dioxide emissions of over 50,000 power plants worldwide, with significantly better coverage in generating capacities and the number of plants than most other databases. However, like the majority of power plant databases, it contains no information on the applied cooling systems or their discharges. In contrast, the World Electric Power Plants Database (WEPP), one of the most widely used power plant databases by academics (e.g. Raptis & Pfister, 2016; Raptis et al., 2017), contains detailed information on power generating units (typically composed of a power generator, boilers [for fossil fuelled power plants] and the working fluid which moves the turbine of generator [e.g. steam, gas and water]), including the type of cooling system and parameters for computing thermal emission rates by using the Rankine cycle (Raptis & Pfister, 2016). However, this proprietary database is relatively expensive, difficult to obtain and contains uncertain generating units which cannot be found in other databases.

Table 3.1. Most used power plant databases. Adapted from Gotzens et al. (2019).

Database Supplier	Abbr.	No. Units	Capacity (GW)	Scale	Version	Cooling Systems
Carbon Monitoring for Action	CARMA	50,570	4931.96	Global	2012	N
European Network of Transmission System Operators for Electricity	ENTSOE	55,064	1085.70	EU	2018	N
Open Power System Data (Conventional Power Plants)	OPSD	6,093	606.58	EU	2020	N
World Electric Power Plants Database	WEPP	127,623	5218.62	Global	2012	Y
World Resources Institute	WRI	Unknown	5572.08	Global	2018	N
Union of Concerned Scientists	UCS EW3	14,772	1041.97	US	2012	Y

As a result of the difficulty associated with obtaining databases such as WEPP and uncertainty over the content of others, two power plant databases were used for this study: the World Resources Institute Global Power Plant Database (WRI, 2019) and UCS EW3 Energy-Water Database (Union of Concerned Scientists, 2012; Table 3.1). The Global Power Plant Database is a comprehensive, global, open-source database of power plants, which covers

approximately 30,000 power plants from 164 countries, with information on plant capacity, generation, ownership, and fuel type. Despite detailed information and accurate location data, there is no information on the applied cooling systems or their emissions. The UCS EW3 Energy-Water Database provides information for the nearly 5,000 USA power plants with cooling information such as cooling technology, water source, water withdrawal and consumption, and intake and outlet peak summer temperatures. However, it suffers from inaccurate location data and the exclusion of some operating power plants (e.g. West County Energy Center, Oak Grove Power Plant & Elm Road Generating Station). Hence, the two databases were compared and merged to produce a single higher-quality dataset with accurate location and cooling system information for the USA.

3.2.1.2. Dataset compilation and power plant inspection

Before the two databases were combined, pre-processing steps were undertaken to ensure that the most relevant information was retained and matched correctly (Fig. 3.1). First, all power plants that do not use fossil or nuclear fuels (e.g. solar, wind & hydro power) were removed from both databases since our research was solely focused on thermal pollution. The UCS EW3 provides data for individual generators and so, data for each power plant was calculated by summing values for all units that contribute as part of a larger power plant. The combined information for each power plant and its cooling systems was then assigned to the appropriate plant in the UCS EW3 database as a function of its plant ID. Plant IDs in UCS EW3 were converted to the same format as those in WRI and used as the reference for subsequent comparison and matching. The comparison and matching of the two databases were undertaken by first comparing the duplicate data (e.g. coordinates, fuel types, plant names, etc.) and verifying discrepancies by performing internet searches. One single set of accurate data was kept. Additional data that was only available in one of the two datasets (e.g. cooling systems, water sources, etc.) was then added to the matched dataset to form one master dataset of relevant and verified information.

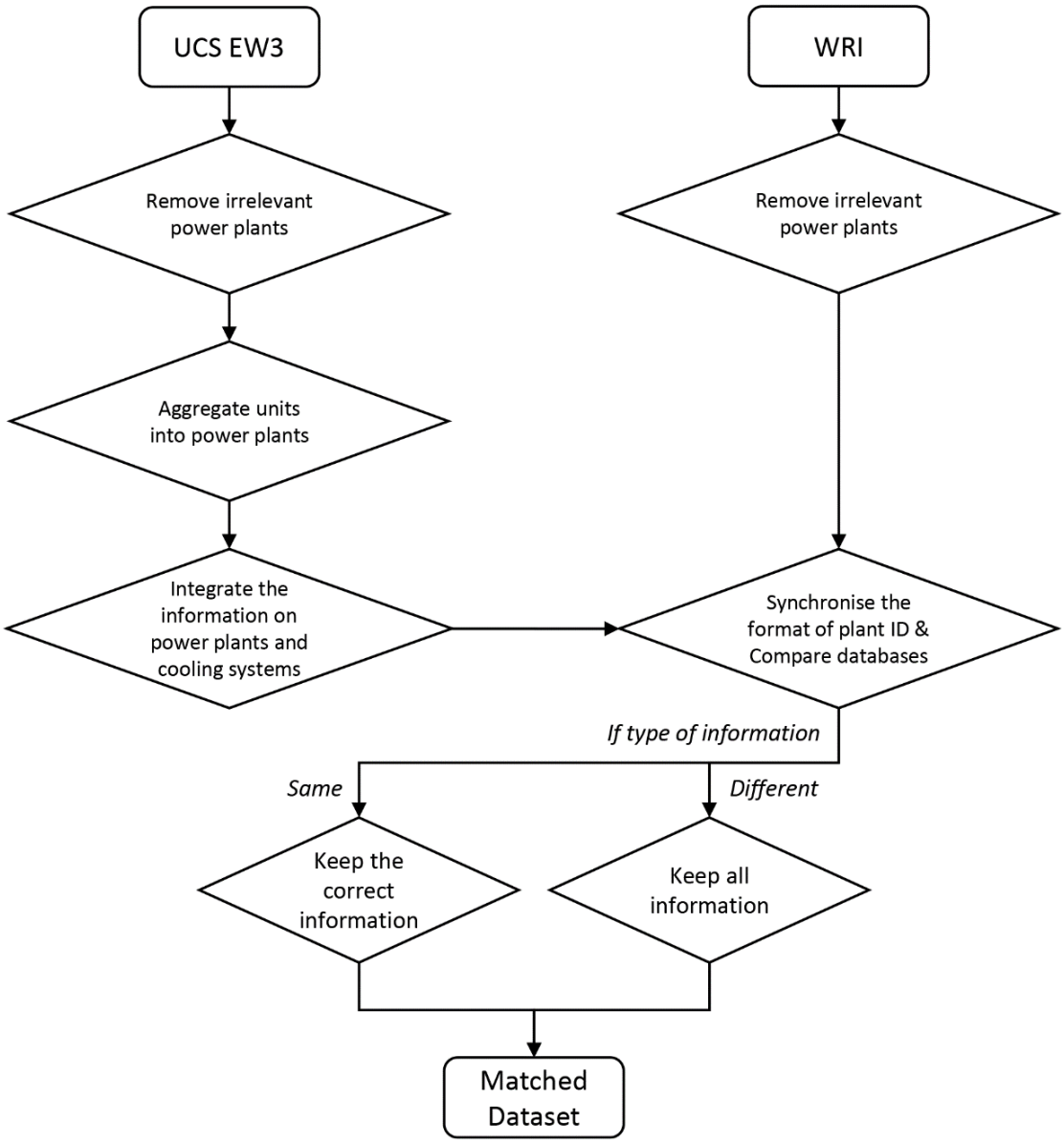

Figure 3.1. Processes of matching the two databases.

Once the combination was completed, a further validation was performed to minimise uncertainties in the dataset. Some power plants included in the Global Power Plant Database were not included in the USA national database (UCS EW3 Energy-Water Database), possibly because some decommissioned plants had not yet been removed. Therefore, the cooling systems for these plants were not known (Fig. 3.2). In addition, some power plants recorded in the USA national dataset were labelled 'no cooling necessary' but it is unclear how this is possible given some had high generating capacities (e.g. > 150 MW). In these cases, the dataset was validated by inspecting power plants and their cooling systems using Google Earth imagery, taking advantage of the fact that different

types of cooling systems can have distinct structures; for example, once-through cooling systems have an intake and outlet for cooling water while recirculating systems use cooling towers (Fig. 3.3). Further confirmation was possible using two power plant search engines: Energy Justice Network (2021) and MAPSearch (2021).

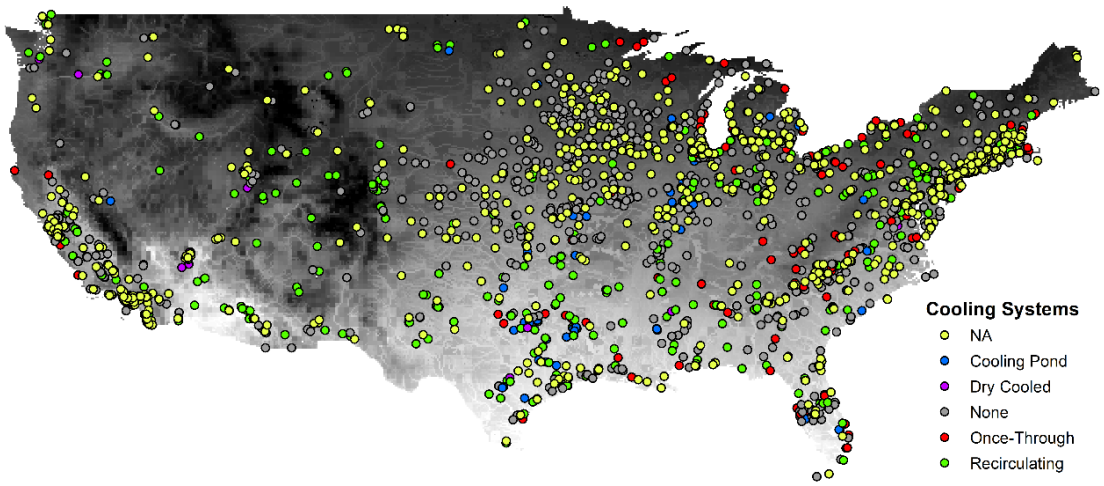

Figure 3.2. A map of power plants with different types of cooling systems in the compiled dataset. It is noteworthy that many plants (*in yellow*) still do not have cooling information after matching.

Figure 3.3. A once-through cooling system (*left*) and cooling towers in operation (*right*) identified via satellite image on Google Earth.

The resultant dataset also lacked information on the water bodies that received cooling water. In response to this uncertainty, a series of criteria were generated and applied for filtering out irrelevant power plants in the dataset. After the first general inspection, it was noticed that power plants with small capacities (≤ 5 MW) accounted for a reasonably high percentage (18.5%) of power plants in the USA and most (97.9%) had no information on water source or were in proximity to no streams or rivers. Considering the potentially minor thermal

impact from small power plants and the efficiency of filtering process, all these small-capacity plants were removed. Every plant larger than 5 MW was manually checked in Google Earth, with particular caution on those without cooling information. After manual checking, power plants where cooling technology was still uncertain and where generating capacity was no larger than 20 MW were removed. Apart from those removed due to distant location from rivers, most USA power plants within this range (≤ 20 MW) were removed because they generated electricity using reciprocating engines primarily for emergency power supply or balancing variable renewable energy (e.g. wind and solar; EIA, 2019), and would operate with low frequency, resulting in thermal impact of less significance.

Cogeneration plants, also known as combined heat and power (CHP) plants, are energy-efficient plants which utilise the high-temperature heat supplied by fuel combustion for generating electricity and remaining low-temperature waste heat for heating. The waste heat is not emitted to nearby rivers from cogeneration plants, thereby leading to uncertain thermal impacts. In that case, cogeneration plants which were discovered on Google Earth to be not withdrawing water and not discharging water, and that also did not have information about water sources, were assumed to be irrelevant with river thermal pollution and thus removed. Power plants located within 10 km from the coastline (i.e. outline of shapefile) were assumed to be near to or drawing water from the ocean. These power plants, along with those near to or drawing water from lakes or reservoirs as well as using groundwater or wastewater for cooling, were removed as the main focus of this research is the thermal impacts on rivers. Additionally, power plants using dry cooling systems were removed since they used considerably less water than other types of cooling systems and had negligible impacts on river temperature. Power plants drew water from unknown sources were also removed since it was difficult to determine the river which the cooling water was discharged into. It was noteworthy that the removal of power plants according to the water source was based on the assumption that plants returned the cooling water to the water source after cooling process. However, this will not affect the subsequent analyses of thermal impact since the excessive removal contributes to conservative results.

3.2.2. Upstream catchment areas of power plants

In addition to the type and size of the power plant, the size and characteristics of the river into which cooling water is discharged is important in determining the impact of thermal pollution. Power plant effluent is expected to have a greater thermal impact on a smaller river than a larger river because the lower discharge in the smaller river will be more readily heated and cooled by solar shortwave and thermal longwave radiation due to its smaller water volume. Upstream catchment areas of power plants can be regarded as surrogate representation of river discharge and calculated with a high degree of accuracy using Arc Hydro Tools, which enables extraction of watershed characteristics such as network, length and catchment area from a raster-based Digital Elevation Model (DEM) (Lin et al., 2008; Li, 2014). However, this method was deemed sub-optimal for this study owing to the necessity of manually locating the specific outlet of each individual power plant and given that the resolution of computed upstream catchment areas was higher than necessary for the analysis. Therefore, catchment areas upstream of each power plant were calculated from HydroBASINS, a subset of the HydroSHEDS database (Lehner & Grill, 2013), which provides 12 levels of catchment delineation globally by following the topological concept of the Pfafstetter coding system (Fig. 3.4). The upstream catchment area for the polygon where the power plant resided, using the finest resolution catchment area available, was used as an approximation of the catchment area of each power plant. Using this information, upstream catchment area was grouped into five size categories: < 500 km^2, 500–1500 km^2, 1500–3000 km^2, 3000–6000 km^2 and > 6000 km^2. These size groups were selected at increasing intervals (500, 1000, 1500 and 3000 km^2) as the number of power plants was noted to be the largest in the higher reaches and decrease in the lower reaches of their catchments. This assisted in revealing the distribution pattern of power plants within their river basins and exploring potential impacts of thermal effluent relative to river discharge. Power plants within 10 km from coastline, assumed to be affected by tidal effects, were removed from the analysis.

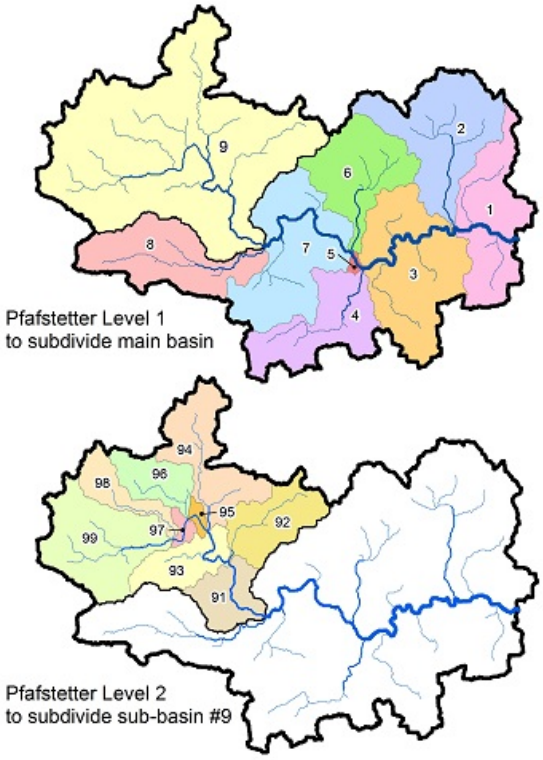

Figure 3.4. Examples of delineations by different Pfafstetter levels used in HydroBASINS (Lehner & Grill, 2013). The finer resolution (*bottom*) of a sub-basin delineation is achieved by adding one digit to the code of the previous level (*top*).

The analyses were undertaken at regional and global scales to examine the consistency of findings. In the global analyses, a map of grouped thermal power plants was created to discover the general pattern of their global distribution. Given their large number and relatively small impact, small-capacity plants (≤ 20 MW) were removed to manifest the distribution pattern of larger power plants that were more likely to cause significant thermal changes. Despite the non-negligible impact of small-capacity plants on smaller streams (particularly the cumulative impact), their removal had limited impact on the findings as the analyses intended to identify power plants with the greatest potential (i.e. generating capacity) to individually contribute to thermal impacts at a global scale. In order to further inspect these plants, regional analyses were conducted. Seven major regions or countries of the world were selected, which were USA, China, Russia, Europe, South America, Africa and Australia. The percentage of grouped catchment areas upstream of thermal power plants in these regions was individually inspected at three levels: all power plants, plants with upstream

catchment area smaller than 10,000 km^2, and plants with generating capacity larger than 20 MW and upstream catchment area smaller than 10,000 km^2. This hierarchical inspection assisted in exploring the ratio of power-plant size to upstream catchment area with the hypothesis that larger power plants in smaller catchments will have a greater thermal impact than smaller plants in larger catchments.

3.2.3. Creation and computation of a thermal pollution index

3.2.3.1. Creation of a thermal pollution index

We developed a thermal pollution index (TPI) based on the Degree of Regulation (DOR) presented by Grill et al. (2015). DOR was developed to describe the potential impact of dams on downstream flows by calculating the proportion of a river's annual discharge volume that could be withheld by a reservoir or a cluster of reservoirs upstream. Similarly, TPI describes the cumulative contributions of the heated water from one or multiple plants to the water temperature increase in the thermally-impacted river within the catchment. As the abstraction or discharge of cooling water changes not only the river discharge, but also the heat carried by the water (ultimately, the temperature), TPI compares the increased heat due to power generation carried by cooling water with the heat carried by river flow, expressed as:

$$TPI = \sum_{i=1}^{n} \frac{F_i \cdot \Delta T_i}{D \cdot T}$$

where n is the number of power plants in the upstream portion of the basin, F_i is the annual discharge of cooling water from power plant i ($m^3 \cdot s^{-1}$), ΔT_i is the difference between summer peak intake and outlet temperatures at plant i (°C), D is the annual discharge at the reach near the plant i ($m^3 \cdot s^{-1}$) and T is annual mean river temperature (°C). ΔT_i was used for computing TPI because mean intake and outlet temperatures were not available and peak temperatures indicate the maximum cooling water temperature at the intake and outflow for the 'peak load month', the month of highest electricity generation at the plant, thus describing the most severe cases of thermal pollution from the plants

(Madden et al., 2013).

3.2.3.2. Input data preparation for computation

Only four parameters are necessary to compute TPI, but the original datasets containing these inputs were required to be processed before computation (Fig. 3.5). Processing cooling system datasets (i.e. F_i and ΔT_i) were relatively simple since annual discharge of cooling water and summer peak intake and outlet temperatures respectively were included in Form EIA-923 (EIA, 2008) and UCS EW3 Energy-Water Database (Union of Concerned Scientists, 2012). However, river temperature (T) and streamflow (D) data were rarely recorded or measured at the specific location of power plants and hence preparations for these data were more complicated. In order to derive river temperature data for stream reaches corresponding to the location of power plants, we used extracted temperatures from Wanders et al. (2019) who used a 1-D dynamic water energy routing model (DynWat) to simulate monthly river temperatures at 10-km resolution globally. The model accounts for surface water abstraction, lake mixing, reservoir operations, riverine flooding, and ice formation, enabling a realistic representation of the water quantity and temperature (Wanders et al., 2019). Despite the lack of calibration, water temperatures computed from the model have been validated using the same model set-up and the ERA-40 and ERA-Interim reanalysis data as forcing, which showed a good correspondence between the modelled and observed water temperature ($R^2 = 0.861$, using observations at 358 locations), thereby providing confidence in the quality of the dataset.

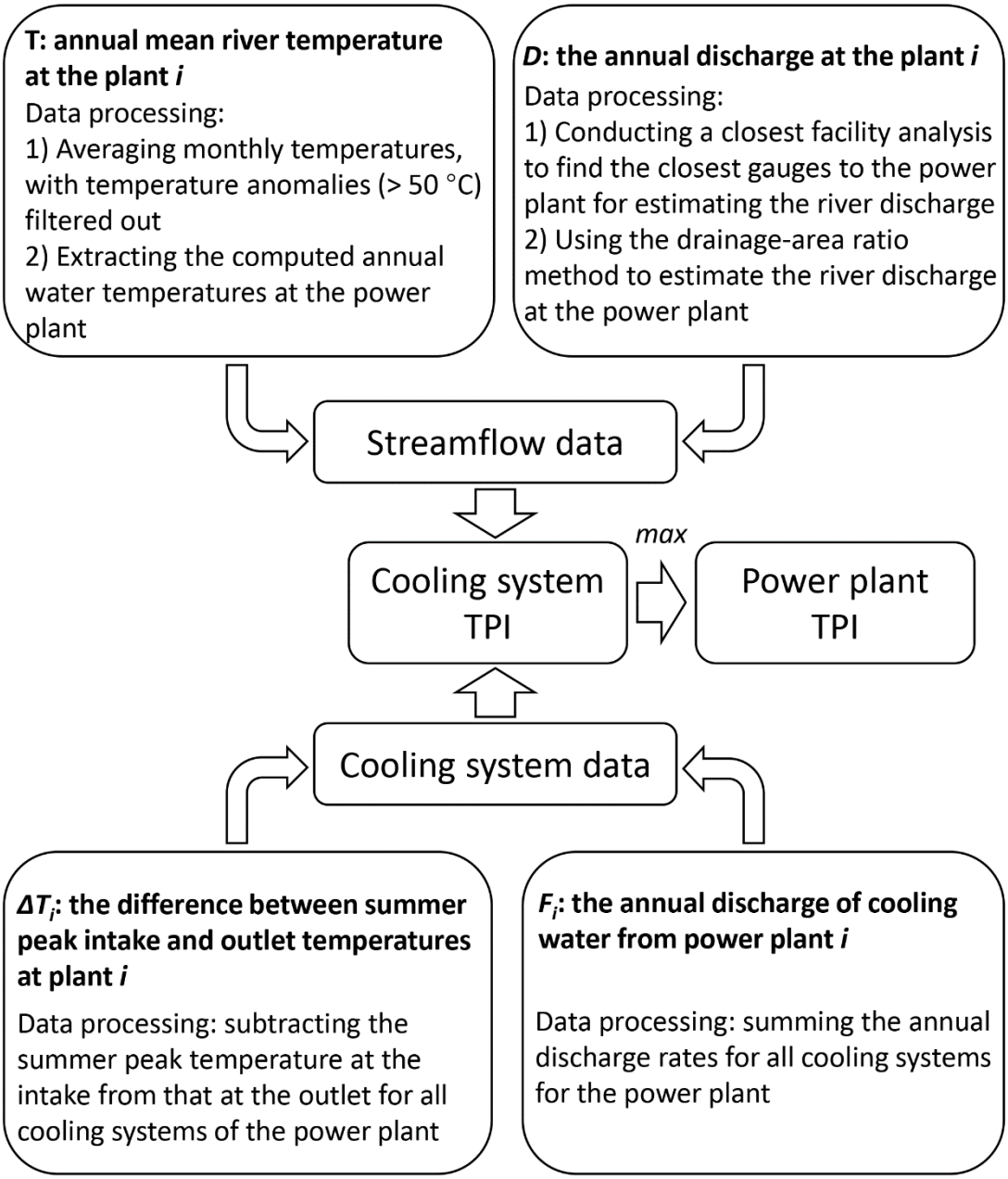

Figure 3.5. Processes of computing TPI for power plant *i.*

The modelled water temperature without calibration could be of low accuracy in smaller watersheds where heat budgets are complex and limited observations are available for validation. However, this is the only water temperature dataset available with fine resolution at a global scale and, more importantly, the TPIs for power plants in these areas were only computed in scenario analyses for examining the applicability of TPI to thermal power plants rather than providing accurate calculations of TPI. Hence, the use of water temperature data produced by the uncalibrated model has limited impacts on this study. Monthly

temperature simulations extracted from this dataset were then processed with bespoke ArcPy scripts, which filtered out temperature anomalies (> 50 °C) and computed annual mean temperatures by averaging monthly temperatures. The computed annual water temperatures were extracted by power plants that fall within the cells and used as estimations for temperatures of nearby rivers.

Although river discharge is measured and recorded by stream gauges installed across the USA river network, it is rarely available at the exact location of power plant outfalls. We therefore applied the drainage-area ratio method to obtain the estimated discharge at the cooling water outflow of each power plant:

$$Q_Y = Q_X(\frac{A_Y}{A_X})^{\varphi}$$

where Q_Y is the streamflow for the ungauged location, Q_X is the streamflow at a nearby gauging station, and A_Y and A_X are the upstream catchment areas for the ungauged location and the streamflow-gauging station, respectively. In widespread practice, the exponent φ is set to 1 (Asquith et al., 2006). Given the volume of data necessary to be downloaded and processed from the National Water Information System (NWIS), python scripts were written to achieve automated retrieval and compilation of the data. Additionally, a GIS-based stream network analysis (closest facility analysis) was conducted to find the closest gauges to each power plant (Fig. 3.6). NHDPlusV2 was used as the river network for this analysis, with small rivers (order < 3) removed to simplify the searching process. According to the inspection of some randomly selected sites, we also applied a search tolerance of 60 km to increase the rate of success in matching the gauges because of its effectiveness in both maximising the searching range and avoiding irrelevant matches (i.e. not in the same catchment). As a result, network analysis ensured that gauges and their plants were within the same catchment, ultimately improving the estimation by drainage-area ratio method.

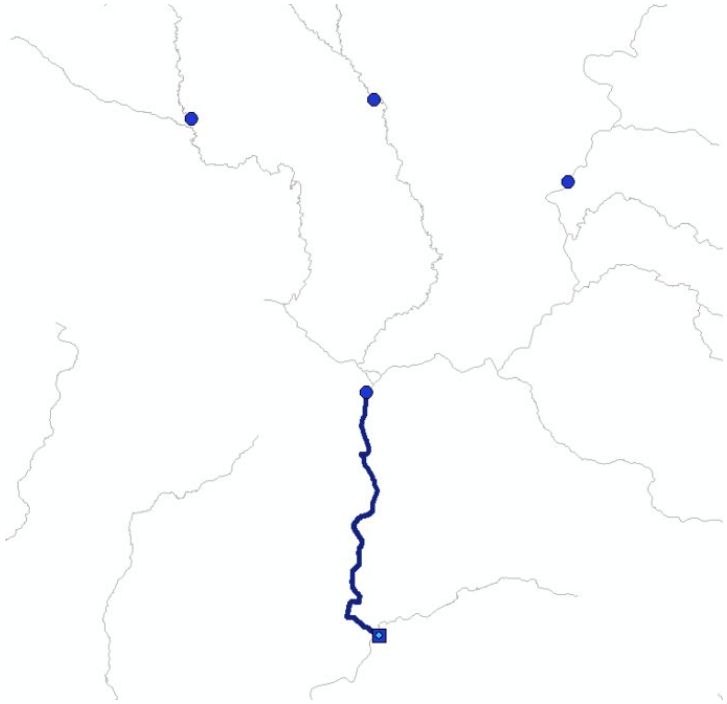

Figure 3.6. Example of closest facility analysis showing power plants (*facilities; square*) and gauges (*incidents; circle*).

After the removal of unrealistic estimated streamflow rates (> 20,000 $m^3 \cdot s^{-1}$), TPIs were initially computed for cooling systems by using the annual discharge of cooling water from power plant obtained from the summation of that from its cooling systems, and the difference between summer peak intake and outlet temperatures at the cooling system. The highest cooling system TPI for each power plant was thus selected as the TPI for the power plant to overcome the absence of summer peak intake and outlet temperatures for power plants and represent the maximal potential thermal impact. Each TPI was classified into four levels based on the cumulative distribution function (Fig. 3.7), which were severe (1.6%, TPI > 10), high (8.1%, TPI: 1–10), moderate (11.3%, TPI: 0.5–1), and weak (100%, TPI < 0.5). However, there were occasional cases where no gauges were available for power plants or only gauges with inaccurate measurements. Consequently, severe sites (TPI > 10) were individually inspected to ensure that the TPI value did not result from erroneous gauging data. Those cooling systems whose power plants were noted to be located in coastal areas (e.g. Haynes Power Plant and Yorktown Power Station; gauging potentially affected by tidal cycle) or have no gauges within the same or connected catchments (e.g. Gerald Gentleman Station) were removed from the analysis.

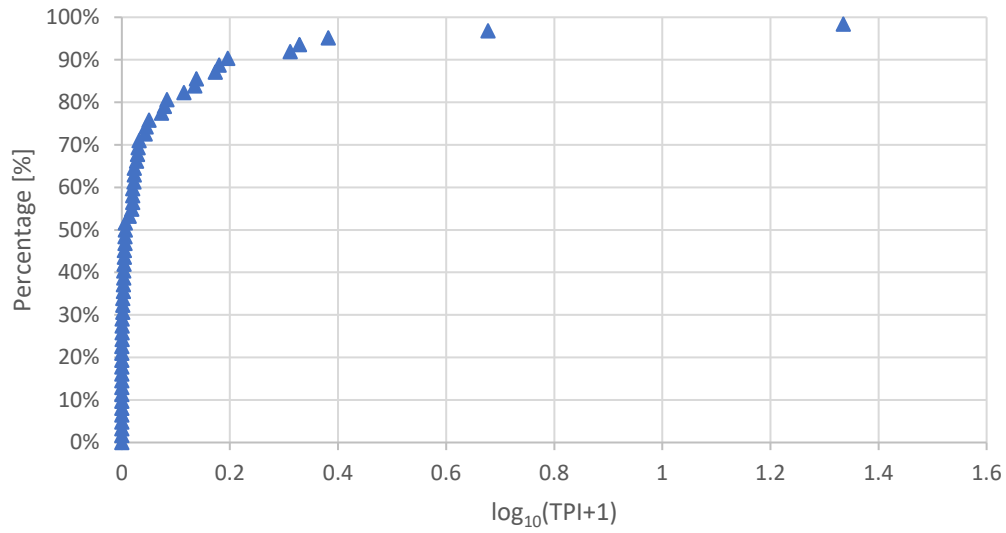

Figure 3.7. Cumulative distribution function plot for TPI. It was noteworthy that TPIs were transformed to show the distribution clearly and avoid zero values for log transformation.

3.2.4. Exploratory analysis of statistical linkages between power plant parameters and TPI

Because information on cooling systems for many power plants was incomplete and given that intake and outlet temperature and discharge of cooling water at small power plants were rarely recorded, we explored the possibility of estimating TPI as a function of other power plant parameters, with a view to providing a more complete picture of thermal pollution from power plants across the USA, even in locations where the TPI could not be calculated conventionally due to the absence of necessary input data. This can be achieved by exploring the potential relationships between power plant parameters and TPIs. Shapiro–Wilk tests were used to determine the normality of power-plant parameters. However, the majority of power-plant parameters did not follow a normal distribution. Spearman's non-parametric correlation analyses were thus undertaken in a correlation matrix between TPI and available parameters from the complied dataset including generating capacity, latitude, longitude, altitude, actual electricity output, distance from sub-basin outlet to the outlet of the main river basin along the river network, sub-catchment area, upstream total catchment area, total discharge of cooling water, mean temperature difference,

reported water withdrawal and consumption as well as mean, minimum and maximum of calculated water withdrawal and consumption.

Generating capacity is the maximum electric output that a power plant can produce and therefore related to the largest amount of heat absorbed by cooling water. In addition, fuel type and cooling system type are two important factors of thermal pollution from power plants, which dictate the thermal efficiencies and operating temperatures, and thereby the temperatures of cooling water. Other factors such as geographical factors (i.e. altitude and latitude) can also affect the cooling water via controlling the intake temperature. Therefore, the two cooling water parameters, total discharge of cooling water and mean temperature difference between inlet and outlet, were examined individually using descriptive analyses for different categorical groups, including fuel, cooling system, generating capacity, altitude and latitude. In order to reveal potential connections between the two parameters and the groups, four groups, which split power plants into each group with reasonable numbers (at least 10), were each created for generating capacity (< 400 MW, 400–800 MW, 800–1600 MW and > 1600 MW), altitude (< 120 km, 120–180 km, 180–240 km and > 240 km) and latitude (< 31°, 31°–36°, 36°–41° and > 41°). The result from above analyses would collectively assist in determining the presence of statistical linkages between TPI and power plant parameters, for subsequent application of TPI across all USA power plants.

3.2.5. Scenario analysis for examining the TPI applicability on a national scale

In order to further examine the applicability of TPI to thermal power plants and investigate the potential threat of power plants to vulnerable streams or rivers, thermal power plants from the regional analyses (in section *3.2.2*) were used to create TPI scenarios. Thermal power plants with generating capacities lower than 20 MW or in upstream catchment areas exceeding 10,000 km^2 were removed because of their lower significance and relevance to the study (1,012 power plants remained, excluding the plants for designing scenarios). Given the river discharge data is readily available (via measurement or estimation), the scenarios were created by leveraging the cooling data (i.e. cooling system type,

intake/outfall temperature difference and cooling discharge) of the power plants from TPI calculation that had the complete cooling information (see section *3.2.3.2*). The maximum, mean and minimum of their mean temperature differences and cooling discharges were individually calculated for four generating capacity groups using once-through cooling (OTC) and non-OTC (e.g. cooling pond and recirculating cooling) systems, resulting in six scenarios, which were Max-OTC, Mean-OTC, Min-OTC, Max-Non-OTC, Mean-Non-OTC, Min-Non-OTC, respectively.

As the preparation for TPI calculation, closest facility analysis was undertaken to find the closest gauges to power plants for the subsequent estimation of discharges at plants by using the drainage-area ratio method (see section *3.2.3.2*). However, some closest gauges could provide measurements for tributaries or canals near the confluence with the main rivers (e.g. the Ohio River), which led to overestimated TPIs due to much smaller discharges. Hence, power plants with severe impact (TPI > 10) in the Mean-OTC scenario (286 plants), in which the overestimation was most liable to occur, were individually inspected on Google Earth loaded in ArcMap. As a result, there were 913 power plants remaining in the following analysis, with 27 and 72 plants removed, respectively due to lack of data for water temperature and gauged streamflow within the searching radius (60 km).

The TPIs for different scenarios were first mapped with all power plants, but those plants inspected to be using cooling ponds or discharging into lakes or the ocean were subsequently removed to produce ‘filtered’ maps as they were beyond the scope of river thermal pollution. However, this does not convey the message that the TPI was inapplicable to these power plants but that the maps would be less effective if these high TPI plants benefiting from abundant water were included, interfering with the exploration of more related plants.

3.3. Results

3.3.1. Compilation of a USA power-plant dataset with cooling information

After the removal following the criteria in *3.2.1.2.*, the total number of power plants decreased from 2282 to 144 (Fig.3.8 & Table 3.2). The remaining power plants were primarily located in the states using once-through cooling (e.g. Virginia & Ohio), recirculating cooling (e.g. Wyoming, Colorado & Utah) or a mixture of the two (e.g. Pennsylvania, Tennessee & Alabama) which were highly dependent on cooling water from river. Conversely, a large proportion of removed power plants were in the states where cooling water was withdrawn from the Great Lakes (e.g. Michigan, Illinois & Wisconsin) or river sections near the coast (e.g. California, New York & Connecticut). In addition, small-capacity power plants (≤ 20 MW) accounted for over 60% removed power plants in Minnesota, Iowa, Missouri, Kansas and Nebraska. In terms of the changes in numbers for different cooling systems after removing process (Table 3.2), once-through cooling, recirculating cooling and cooling pond showed significantly lower decreases than other cooling systems, by 74.3%, 80.6% and 84.9%, respectively. Only less than 2% from groups of uncertain cooling (NA) and no cooling (None) were retained for subsequent analysis.

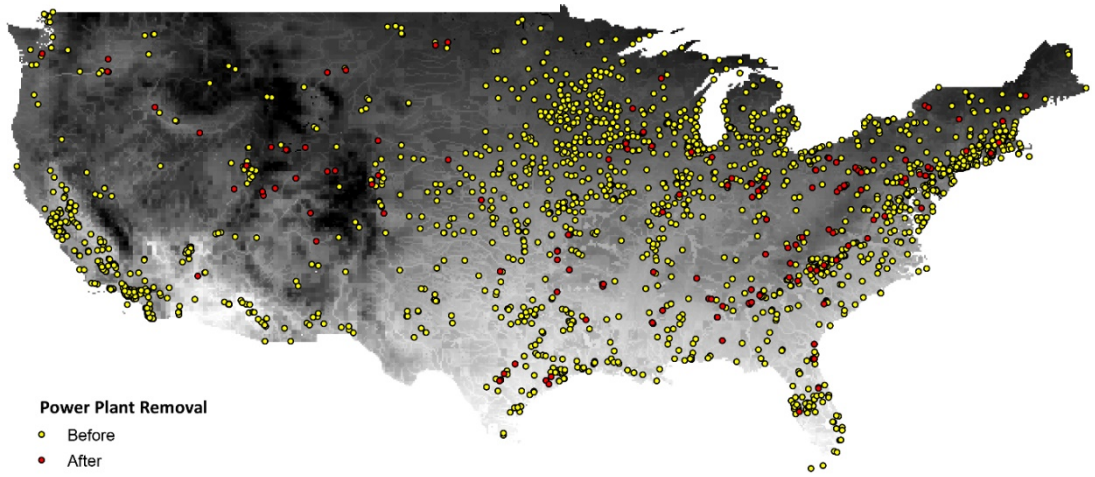

Figure 3.8. Power plants in the USA before (yellow) and after (red) the removing process.

Table 3.2. The number of different cooling systems before and after the removing process.

	NA	Cooling Pond	Dry cooled	None	Once-Through	Recirculating	Total
Before	729	53	32	942	140	386	2282
After	10	8	0	15	36	75	144

3.3.2. Upstream catchment areas of power plants

Globally, the majority of thermal power plants were located in upstream catchment area smaller than 500 km^2, followed by upstream catchment areas of 500–1,500 km^2 (Fig. 3.9). Besides, the United States, China, Europe and India had the highest numbers of power plants as well as proportions of these plants with small upstream catchment areas (< 1,500 km^2). Power plants with large catchment areas (> 6,000 km^2) were also concentrated in these regions. By contrast, there were only small densities of power plants in Canada, Africa and Australia, most of which had small upstream catchment areas.

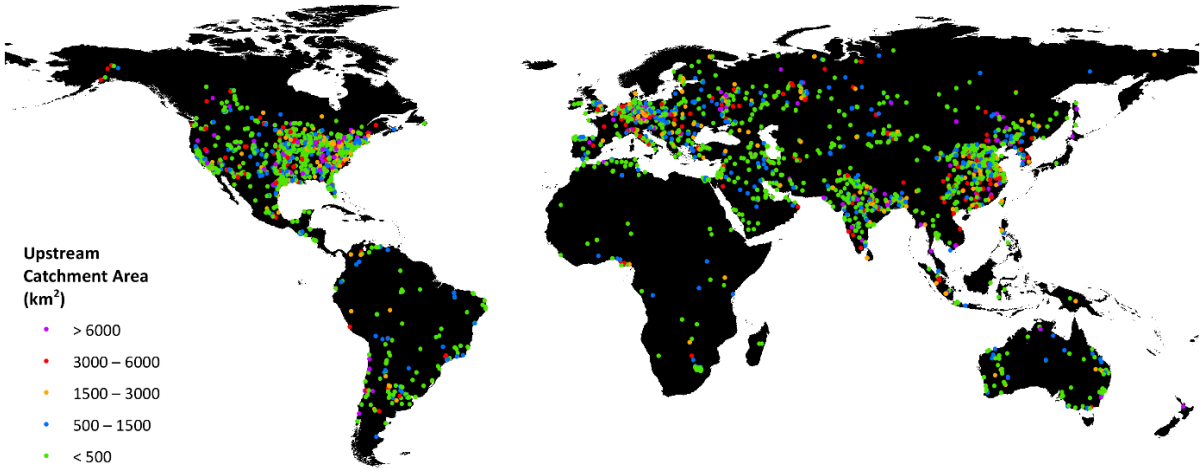

Figure 3.9. Global distribution of thermal power plants with upstream catchment areas < 500 km^2 (*green*), 500–1,000 km^2 (*blue*), 1,500–3,000 km^2 (*orange*), 3,000–6,000 km^2 (*red*), and > 6,000 km^2 (*purple*), respectively. It is noteworthy that this map shows power plants excluding those in coastal areas (within 10 km of the coastline) or with small capacities (≤ 20 MW).

Before the removing process, all study regions showed high percentages of power plants with small upstream catchment areas (< 1,500 km^2), ranging from 48.0% to 80.4% (Fig. 3.10a). Among these regions, Europe and Russia shared the lowest percentages (< 50%) for small upstream catchment areas (< 1,500 km^2) but highest percentages (> 30%) for large upstream catchment areas (> 6,000 km^2). In comparison, the USA and China both had higher percentages (> 58%) in power plants with small upstream catchment areas but lower percentages (< 30%) in those with large upstream catchment areas. On the contrary, Australia had the highest percentage (80.4%) for small upstream catchment areas but lowest percentages (8.8%) for large upstream catchment

areas, followed by South America and Africa with lower percentages (< 70%) for small upstream catchment areas and higher percentages (> 15%) for large upstream catchment areas.

After removing power plants with upstream catchment areas exceeding 10,000 km^2, there were significant changes in different groups of upstream catchment areas across regions, particularly in those regions with high proportions of plants with upstream catchment areas exceeding 10,000 km^2 (Fig. 3.10b). Europe and Russia, the two regions which had the highest percentages for large upstream catchment areas, both showed sharp declines (by 24.0% and 28.1%) in this group (> 6,000 km^2) after the removal, followed by the USA, China and Africa with slightly smaller decreases (by 21.1%, 19.3% and 18.6%). By contrast, there were only marginal decreases in percentages of power plants with large upstream catchment areas for Australia (by 6.6%) and South America (by 13.0%).

With all small-capacity power plants (≤ 20 MW) removed, the percentages of different upstream catchment area groups showed no significant changes in general (Fig. 3.10c). Most regions showed minor changes in groups of small upstream catchment areas (< 500 km^2 & 500–1,500 km^2), with small decreases by less than 3%. However, there was a moderate decrease of 5.3% in groups of small upstream catchment areas for Africa. As a result of the two-step removing process, Europe and Russia continued to have the lowest percentages of power plants with small upstream catchment areas, immediately followed by the USA and China. South America shared a similar pattern in percentages for small and medium-sized upstream catchment areas (< 1,500 km^2 & 1,500–6,000 km^2) with the USA and China but had a lower percentage for large upstream catchment areas. Despite the highest percentages for small upstream catchment areas, Africa and Australia both had small total numbers of power plants remaining, 88 and 101, respectively. Besides, compared to Australia in terms of small upstream catchment areas, Africa showed a higher percentage for upstream catchment areas smaller than 500 km^2 but a lower percentage for those within 500–1,500 km^2.

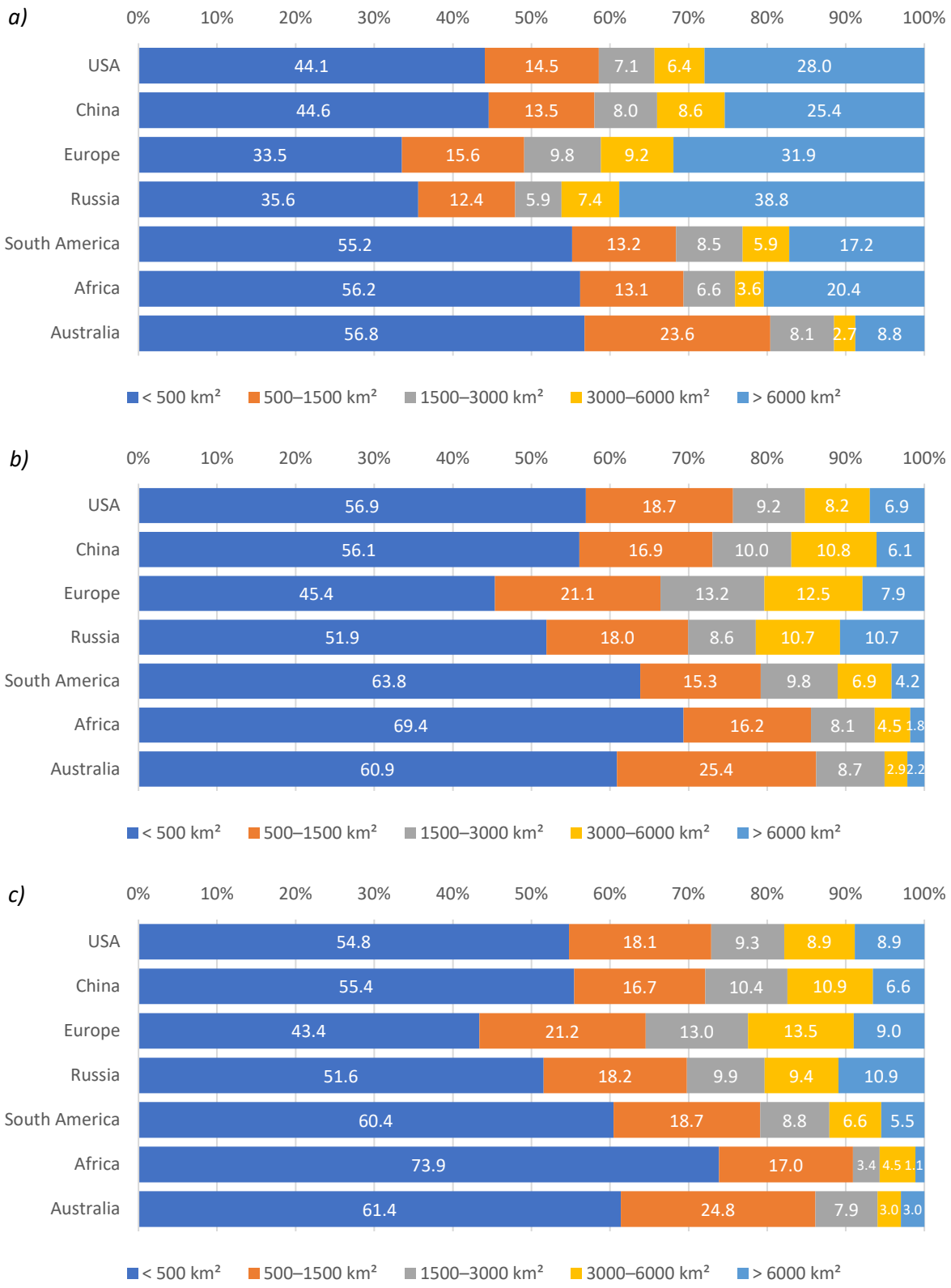

Figure 3.10. Percentages of power plants within different ranges of upstream catchment area for the United States (USA), China, Europe, Russia, South America, Africa and Australia. The bar charts respectively show hierarchical inspections of *a)* all power plants, *b)* plants with upstream catchment areas

smaller than 10,000 km^2, and *c)* plants with generating capacities larger than 20 MW and upstream catchment areas smaller than 10,000 km^2.

3.3.3. Creation and computation of a thermal pollution index

Calculation of TPI associated with power plants considered in this study indicated distinct variability in the distribution of thermal pollution within rivers. According to the initial TPI computation (Fig. 3.11), most rivers near power plants were not vulnerable to thermal effluent release (i.e. 'weak' impact); however, some rivers were severely (Colbert power plant) and highly vulnerable (Allen Fossil Plant, Ernest C. Gaston Electric Generating Plant, Joliet 9 & 29 Generating Station) to thermal stress. Their high TPIs were attributed to large discharges of cooling water relative to streamflow.

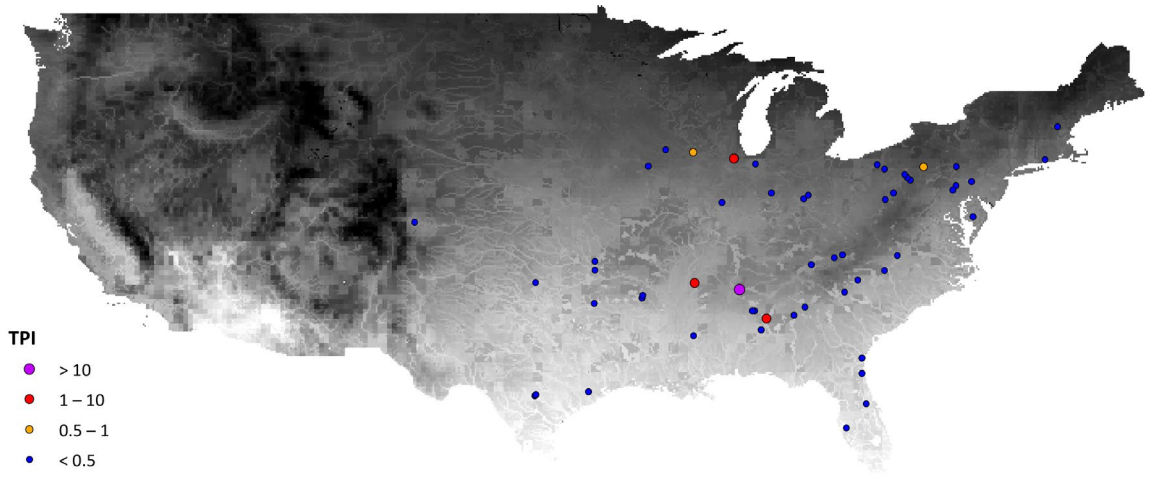

Figure 3.11. TPIs for thermal power plants in the USA in 2008. The points show the potential vulnerability of power plants to thermal stress, classified into severe (*purple*), high (*red*), moderate (*orange*), and weak (*blue*) impacts with sizes scaled according to classifications.

3.3.4. Statistical linkages between power-plant parameters and TPI

The correlation matrix shows the results of exploratory analysis between power-plant parameters and TPI (see section *3.6*). In general, there were no significant correlations between parameters and TPI ($r < .210$, $n = 62$), except the weak non-linear correlation for the total generating capacity ($r = .304$, $p < .05$). Strong

correlations were found for the mean temperature difference ($r = .453$, $p < .001$) and the total discharge ($r = .747$, $p < .001$) which are inputs to TPI and are thus colinear, and water withdrawals ($r > .510$, $p < .001$) which directly determines the amount of available water for cooling (i.e. reported water withdrawal, and mean, minimum and maximum of calculated water withdrawal) and is thus strongly correlated ($r > .480$, $p < .001$) with the total discharge. The two parameters of cooling water also showed weak correlations with other power plant parameters ($r < .390$), excluding the correlations of total discharge with parameters related to water withdrawals which directly determined the amount of available water for cooling (i.e. reported water withdrawal, and mean, minimum and maximum of calculated water withdrawal).

For different fuel types (Fig. 3.12 & Table 3.3), gas- and coal-fired plants showed higher mean and median total discharges but lower mean temperature differences than oil-fired plants. The minimum total discharges were consistently low across three fuel types; however, the Interquartile Range (IQR) and maximum of oil-fired plants were significantly smaller than the other two types. Besides, oil-fired plants had higher IQR and maximum of mean temperature difference than the other two types.

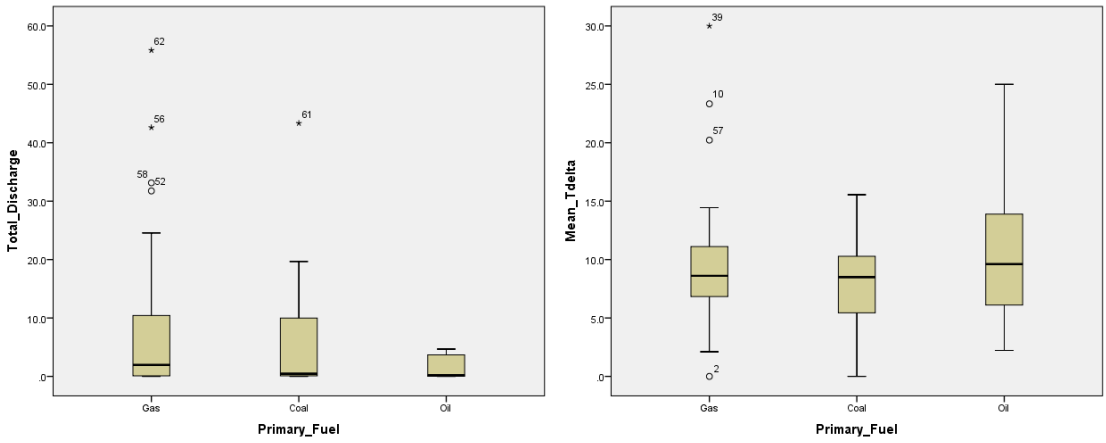

Figure 3.12. Boxplots of total cooling discharge and mean temperature difference for different *primary fuel types*.

Table 3.3. Means and medians of total cooling discharge and mean temperature difference for different *primary fuel types.*

	Total Cooling Discharge (m^3/s)			Mean Temperature Difference (°C)		
Fuel type	Gas	Coal	Oil	Gas	Coal	Oil
Mean	8.55	5.80	1.47	9.75	7.49	11.07
Median	1.96	0.45	0.22	8.61	8.50	9.61

For different cooling systems (Fig. 3.13 & Table 3.4), once-through cooling showed significantly higher mean, median, maximum total discharges as well as greater IQR than the other cooling systems. The mean and median of mean temperature differences were also the highest for once-through cooling. Recirculating cooling and cooling pond both had extremely small cooling discharges; however, the maximum, range and IQR for mean temperature differences of recirculating cooling were considerably larger than cooling pond. Power plants with no cooling system also showed relatively high mean and median total discharges with broad range of mean temperature difference.

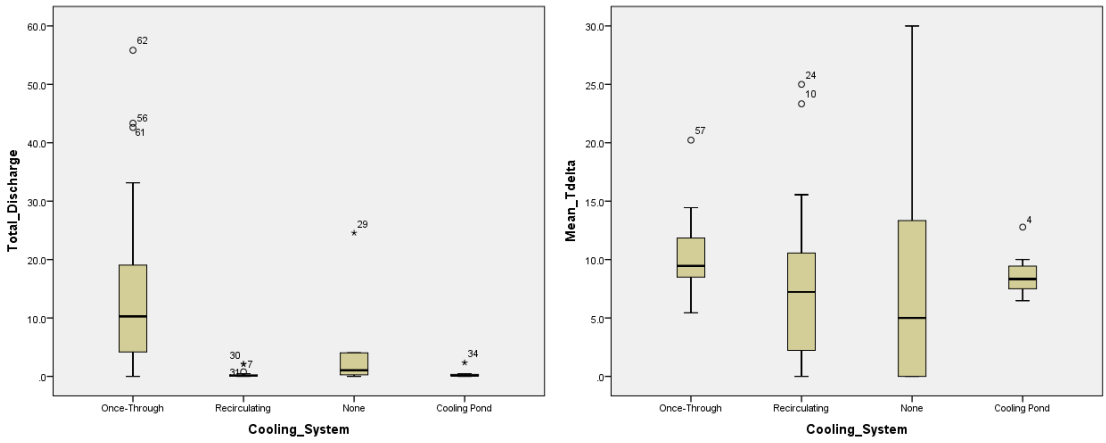

Figure 3.13. Boxplots of total cooling discharge and mean temperature difference for different *cooling systems*.

Table 3.4. Means and medians of total cooling discharge and mean temperature difference for different *cooling systems*.

	Total Cooling Discharge (m^3/s)				Mean Temperature Difference (°C)			
Cooling Type	Once-Through	Recirculating	None	Cooling Pond	Once-Through	Recirculating	None	Cooling Pond
Mean	15.58	0.32	5.16	0.48	10.23	7.73	8.89	8.78
Median	10.26	0.09	1.04	0.14	9.46	7.22	5.00	8.33

In terms of generating capacity (Fig. 3.14 & Table 3.5), large-capacity (> 1600 MW) power plants showed significantly lower mean and median cooling discharges than the other plants (except median for 400–800 MW), with a small

IQR. The mean and median of mean temperature differences were also significantly lower in large-capacity group than the other groups, but the IQR was comparatively large. By comparing means and medians, small-capacity power plants (< 400 MW) had higher mean temperature difference than medium-capacity plants (400–800 MW & 800–1600 MW) but similar cooling discharges with medium-capacity plants. The 400–800 MW group showed relatively large IQR and maximum with respect to both total discharge and mean temperature difference while the 800–1600 MW group had only similarly large IQR and maximum for total discharge but significantly smaller IQR and maximum for mean temperature difference.

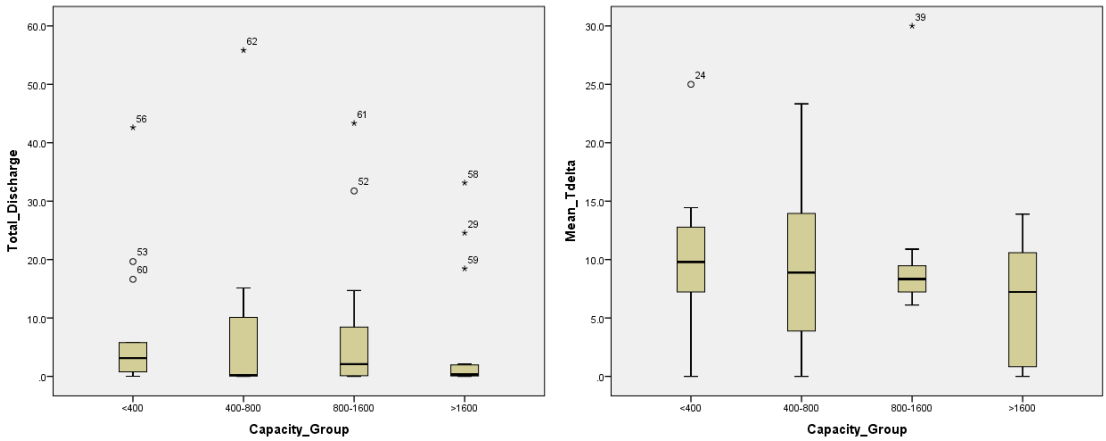

Figure 3.14. Boxplots of total cooling discharge and mean temperature difference for different *capacity* groups.

Table 3.5. Means and medians of total cooling discharge and mean temperature difference for different *capacity* groups.

	Total Cooling Discharge (m^3/s)				Mean Temperature Difference (°C)			
Capacity (MW)	<400	400-800	800-1600	>1600	<400	400-800	800-1600	>1600
Mean	7.58	6.59	7.75	5.12	10.41	9.27	9.70	6.55
Median	3.14	0.22	2.10	0.33	9.79	8.89	8.33	7.22

For the two geographic factors, there were no significant trends or patterns in mean temperature differences (Fig. 3.15 & Table 3.6), with lowest mean and median values in 120–180 km and 31°–36° and highest mean values in 180–240 km and 36°–41°, respectively. In contrast, cooling discharges were higher in groups of lower altitudes (< 120 km & 120–180 km) than groups of higher

altitudes (180–240 km & > 240 km), particularly for means, maximums and IQRs. In addition, cooling discharges showed a clear general trend of an increase with latitudes. By comparing means, medians, maximum and IQRs, the high-latitude group (> 41°) showed the highest cooling discharges, followed by medium-latitude group (31°–36° & 36°–41°). The low-latitude group only had small cooling discharges, which were significantly lower than the other groups.

a)

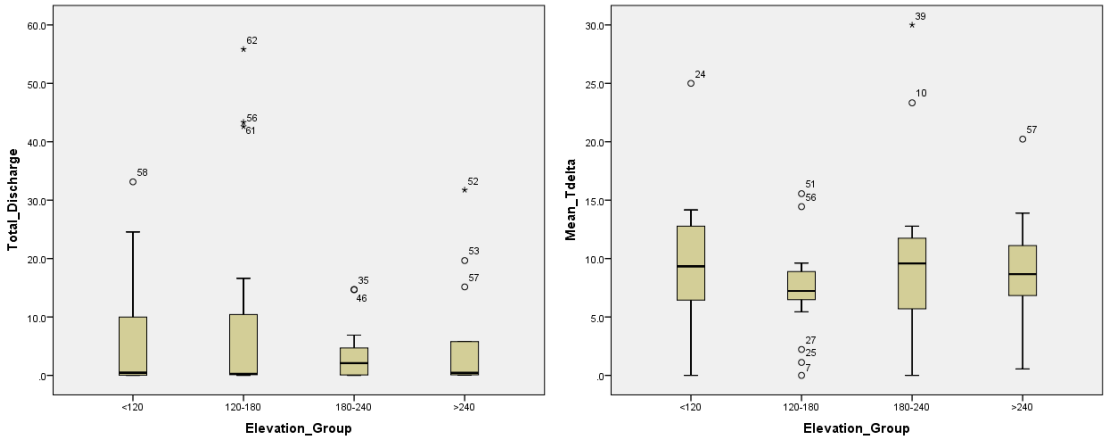

b)

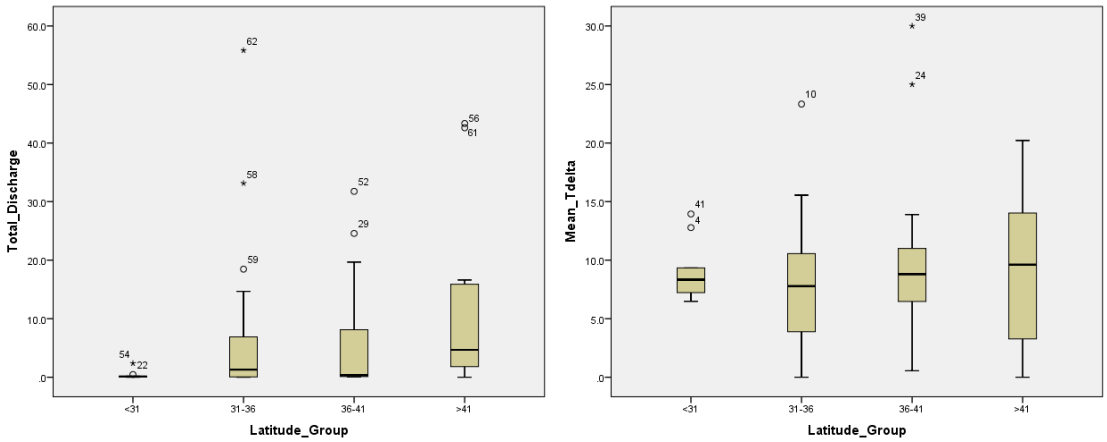

Figure 3.15. Boxplots of total cooling discharge and mean temperature difference for different a) *elevation* and b) *latitude* groups.

Table 3.6. Means and medians of total cooling discharge and mean temperature difference for different a) *elevation* and b) *latitude* groups.

a)

Elevation (km)	Total Cooling Discharge (m^3/s)				Mean Temperature Difference (°C)			
	<120	120-180	180-240	>240	<120	120-180	180-240	>240
Mean	6.28	10.09	3.84	6.17	9.52	7.47	9.71	9.16
Median	0.46	0.26	2.10	0.43	9.33	7.22	9.58	8.67

b)

Latitude (degree)	Total Cooling Discharge (m^3/s)				Mean Temperature Difference (°C)			
	<31	31-36	36-41	>41	<31	31-36	36-41	>41
Mean	0.38	7.03	5.91	12.72	9.11	7.93	9.96	8.92
Median	0.11	1.30	0.35	4.68	8.33	7.78	8.81	9.61

3.3.5. Scenario analysis for examining the TPI applicability on a national scale

In general, power plants in once-through cooling (OTC) scenarios (Fig. 3.16) showed higher TPIs than in non-OTC scenarios (Fig. 3.17), with 85 and 61 plants from OTC scenarios consistently showing weak/medium and severe impacts compared to 467 and 0 plants from non-OTC scenarios. High and severe impacts of Min-, Mean- and Max-OTC scenarios accounted for 25.9%, 72.2% and 89.8% of the total number of power plants, whereas high and severe impacts took up 0%, 12.4% and 44.0% of the total in Min-, Mean- and Max-Non-OTC scenarios, respectively. The discrepancies between OTC and non-OTC scenarios were expected as there was no substantial discharge and/or temperature difference of thermal effluent from non-OTC cooling systems, compared to a large amount of thermal effluent discharged by OTC systems.

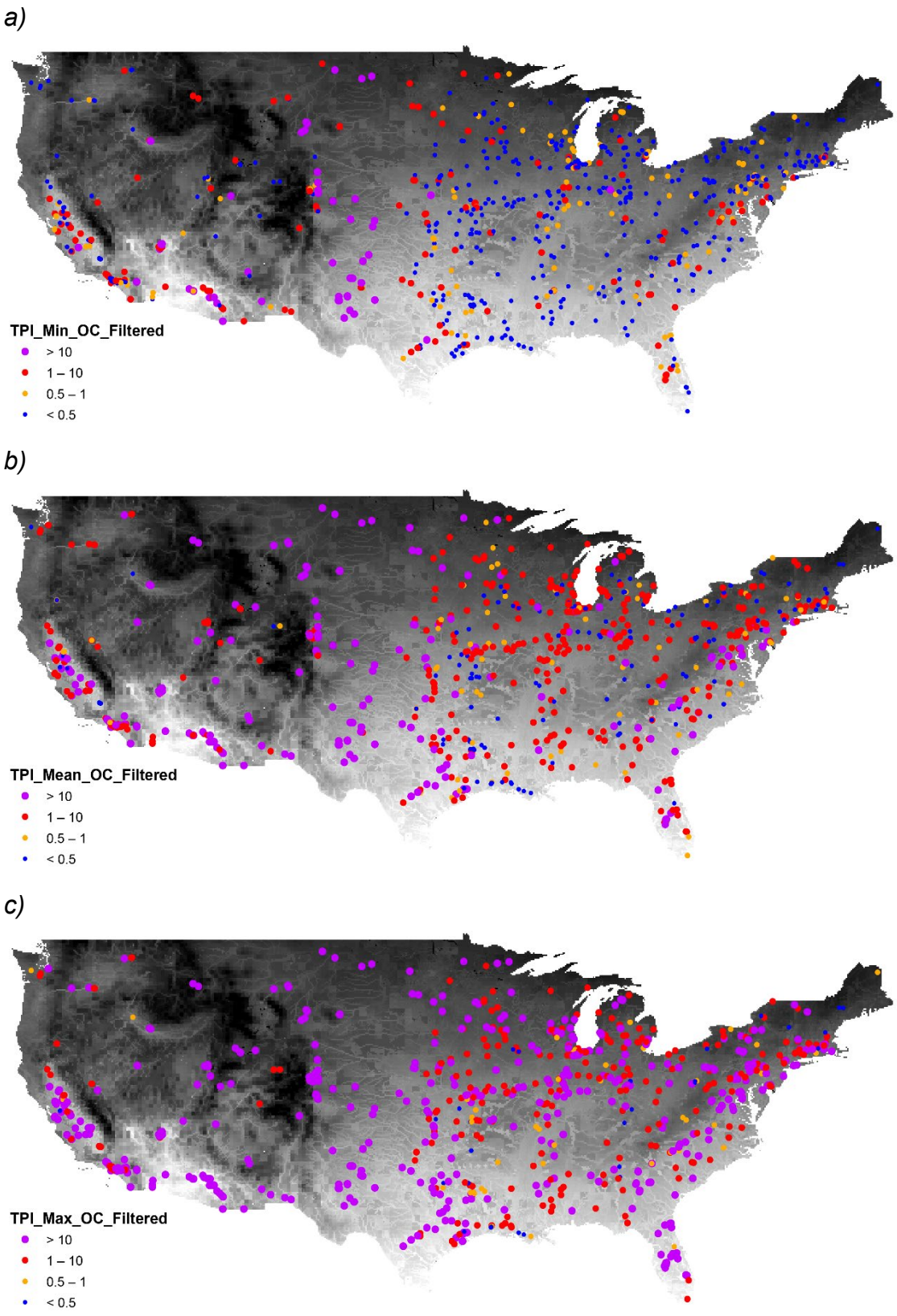

Figure 3.16. TPIs for a) *minimum*, b) *mean* and c) *maximum* scenarios of thermal power plants using once-through cooling (OC) systems in the USA. The points show the potential vulnerability of power plants to thermal stress, classified into severe (*purple*), high (*red*), moderate (*orange*), and weak (*blue*)

impacts with sizes scaled according to classifications.

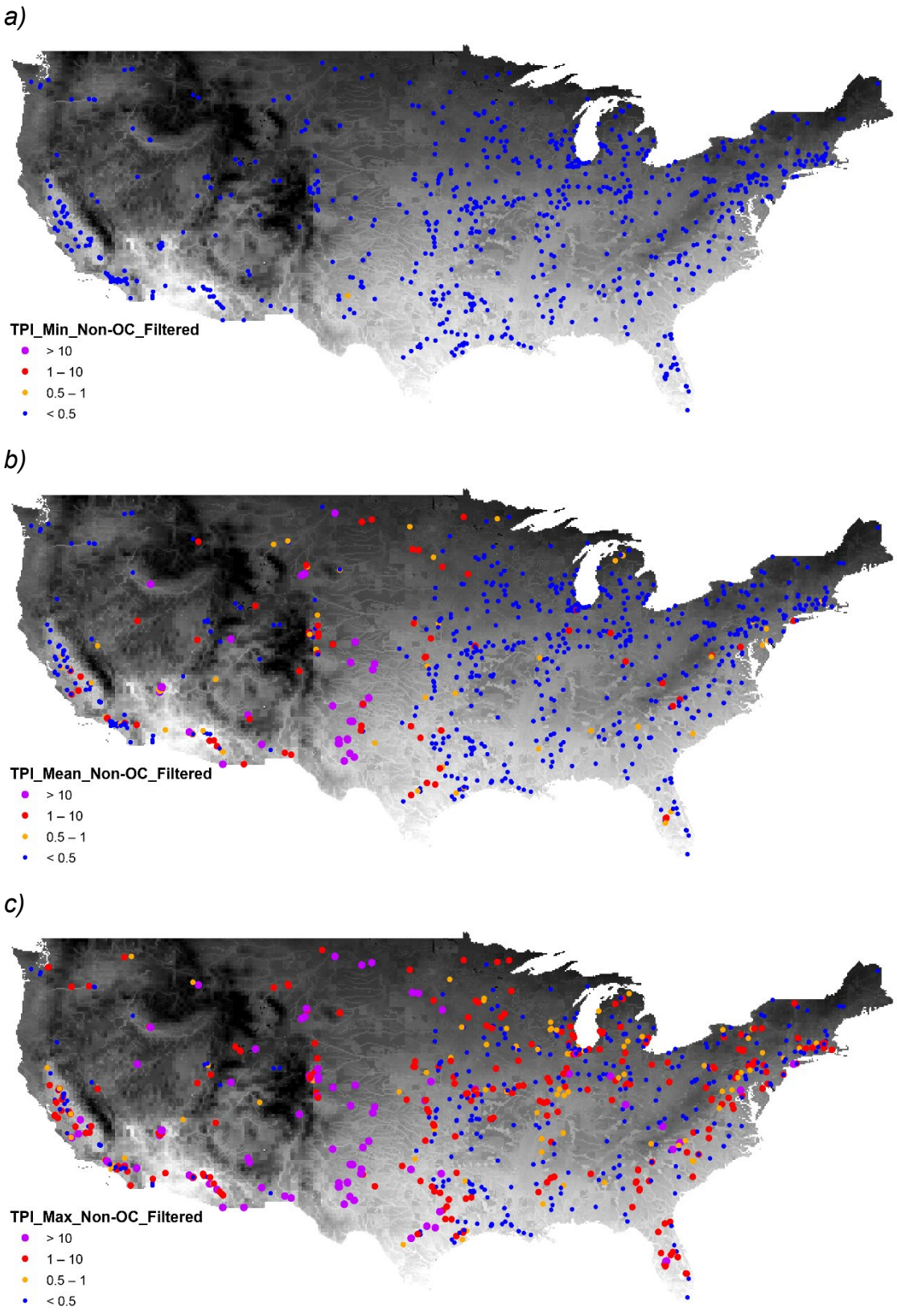

Figure 3.17. TPIs for a) *minimum*, b) *mean* and c) *maximum* scenarios of thermal power plants not using once-through cooling (Non-OC) systems in the

USA. The points show the potential vulnerability of power plants to thermal stress, classified into severe (*purple*), high (*red*), moderate (*orange*), and weak (*blue*) impacts with sizes scaled according to classifications.

3.4. Discussion

3.4.1. Compilation of a USA power-plant dataset with cooling information

The ultimate goal of dataset compilation and power-plant inspection was to create a dataset which contained key information on power plants and their cooling systems from both databases with low uncertainties. In general, the inspection process succeeded in identifying the number of power plants with no cooling water information and also highlighting those with unknown cooling systems. However, only 6.3% of power plants were retained after the process, with some having unknown linkages between cooling systems and their water sources (i.e. NA: 10; None: 15). This could be partly attributed to the uncertainties in the process of identification. Although the identification of recirculating systems was achievable by searching for presence of cooling towers or steam emerging from these in aerial imagery (Fig. 3.3), identifying once-through cooling systems by their intake and outlet systems as well as proximity to water bodies was much more challenging. Typical once-through cooling systems are theoretically located close to rivers and have clear intake systems; however, it was difficult to identify some intake systems because they were not clear from remote sensing imagery and could easily be confused with intake systems for hydropower at combined thermal-hydro power plants. Additionally, under the assumption that power plants returned the cooling water to the water source after cooling process, a number of power plants in the global dataset were removed due to being listed as using municipal water, groundwater and lake water as the source of cooling water, but it was uncertain whether these power plants discharged cooling water into river and were thus mistakenly removed. Water source was the key information for determining where the cooling water was discharged, and various freshwater sources excluding rivers increased the difficulty of determination.

The patchy and poor-quality data surrounding power plants raise important questions about the past work in this area. For example, Raptis and Pfister (2016) used the World Electric Power Plants database and identified cooling systems using Google Earth imagery, completing cooling system information for over 3,800 additional generating units. The improvement was dependent on the identification via satellite imagery and hence likely involved similar uncertainties to those mentioned above. The uncertainties surrounding cooling water discharge also indicate the need for a power-plant database with accurate information on their locations and cooling systems. A new python-based toolset, called 'powerplantmatching' (PPM) which cleans, standardises and combines multiple power plant databases (Gotzens et al., 2019), could be a possible solution to obtaining a high-quality dataset. However, the focus of this study is developing an index of thermal pollution rather than creating a high-quality power-plant data. Therefore, PPM was not applied in this study.

3.4.2. Upstream catchment areas of power plants

The global analysis revealed a consistent pattern that most thermal power plants were in the upper section of the catchment. However, there were significant discrepancies in power plants with larger upstream catchment areas (> 1,500 km^2) among regions or countries, with high concentration of these plants in large countries or regions which were heavily based on manufacturing factory, including United States, China, Europe and India. This is likely due to the existence of power plants with high generating capacities that are more capable of meeting the high electricity demand in these areas, and also the paucity of renewable energy resources in comparison to other regions (e.g. Canada and South America). These high-capacity power plants have higher water withdrawals for cooling purposes and thus tend to be located in lower reaches where water is more readily available.

In the regional study, the removal of power plants with upstream catchment areas exceeding 10,000 km^2 aimed to filter out plants in closer proximity to coastal areas which were likely to be affected by tidal effects, whereas removing small-capacity power plants of lower significance was for examining the distribution of power plants of higher capacity, particularly those with small

upstream catchment areas. The USA and China shared a similar pattern that power plants were mainly located in the upper section of the catchment, with over 72% with small upstream catchment areas (< 1,500 km^2). In comparison, Europe and Russia both showed lower percentages (< 70%) for the same groups of upstream catchment areas. Such differences might be due to the better environment protection policy in European countries which forces new power plants to be installed in lower reaches where abundant water is sufficient for cooling and renders the thermal impact of cooling discharges less pronounced. South America had similar percentages with the USA and China for power plants with medium-sized upstream catchment areas (1,500–6,000 km^2) but lower percentages for plants with large upstream catchment areas (> 6,000 km^2). This might reflect not only the dominance of small rivers in the region (except some rivers in the Amazon and Paraná basin) which are unable to supply large amount of cooling water to high-capacity power plants, but also the fact that the electricity generation is mainly achieved by utilisation of hydropower (> 900 hydroelectric power plant) and hence does not require large-sized high-capacity power plants that withdraw large quantities of water more often.

In contrast to non-significant changes of percentages in most regions after filtering out the small-capacity power plants (≤ 20 MW), South America and Africa respectively showed a decrease from 63.8% to 60.4% and an increase from 69.4% to 73.9% for plants with upstream catchment areas less than 500 km^2. The decrease in South America indicated high percentages of small-capacity power plants, most likely resulting from the dominance of small rivers as well as the broad utilisation of hydropower in the region. The increase in Africa was, however, attributed to the small total number of power plants which manifested the high coverage of medium-capacity plants (20–500 MW) in the region. Besides, Africa shared similar percentages for small upstream catchment areas with Australia but showed higher percentages in power plants with upstream catchment areas smaller than 500 km^2 as well as lower percentages in plants with upstream catchment areas within 500–1,500 km^2. However, these differences in percentages only represented less than 20 power plants, which could be considered of low significance or non-significant. Instead, the patterns of two regions could be more dictated by the existence of the Sahara and Australian desert which limited the availability of water source and

thereby the site selection for power plants.

Despite the different distribution patterns of power plants around the world, the high percentage of power plants with upstream catchment areas smaller than 500 km^2 was consistent throughout the hierarchical analysis, irrespective of policy, economic and geographical factors. More importantly, the high percentages of these plants only changed by a small amount after filtering out smaller plants with generating capacities no larger than 20 MW, which strongly highlighted a prevailing pattern of larger capacity power plants in relatively small sub-catchment areas, which are likely discharging high volumes of warm cooling water into small rivers. Compared to a large river, the thermal regime for a small stream or river is more complex and determined by mixed factors such as shading, groundwater inflow, hyporheic exchange and bed conduction (Moore et al., 2005; Hester & Doyle, 2011; Garner et al., 2017; Lewandowski et al., 2019). This is because smaller rivers in the upper reaches are generally shallower and narrower and hence more susceptible to changes caused by interactions of the water column with air, riparian vegetation and sediments. In a study of a karstic region in the Spring Creek watershed in central Pennsylvania, USA, a groundwater-fed stream was compared to a stream with negligible groundwater inputs, which showed increased longwave, latent and sensible heat losses in winter as a result of larger temperature and vapour pressure gradients between the stream and the air (O'Driscoll & DeWalle, 2006). Consequently, more complex and greater thermal impacts could be expected to occur in small streams or rivers if cooling water as an external disturbance is introduced, especially from a large power plant producing a consistent and large power output.

Such thermal impacts could be further exacerbated by cumulative discharges from closely installed power plants. Miara et al. (2018) conducted research on thermal pollution impacts and plant-to-plant interferences in the Mississippi River watershed using the coupled Water Balance Model and Thermoelectric Power and Thermal Pollution Model (WBM-TP2M). The comparison between simulations with and without plant-to-plant interferences indicated that thermal effluent from upstream power plants with once-through cooling system increased river temperatures, leading to elevated water temperature for condenser inlet of downstream plants and accordingly decreased thermal

efficiencies. In order to meet the demand for electricity, power plants in the downstream would operate for a longer time and discharge additional thermal effluents, which further reduces the thermal efficiency of downstream plants. As a result, the increased thermal effluents together with thermal effluents from upstream power plants would extend the area impacted by thermal pollution and elevate the average temperature of rivers within the catchment. However, both possible impacts have not been thoroughly studied and understood, with unavailable monitoring (particularly on the cooling water) and incomplete information on these power plants, potentially concealing related ecological impacts such as phenological shifts (Scranton & Amarasekare, 2017) and species invasion (Stachowicz et al., 2002). Hence, more rigorous legislation on monitoring and publicising pollution data, followed by more research efforts focused on this area, should be encouraged.

3.4.3. Creation and computation of a thermal pollution index

The first computed TPI indicated that five coal-fired power plants applying once-through cooling system in the USA were severely or highly vulnerable to thermal stress. All these power plants were commissioned before 1970s, and therefore might use outdated generating units with deteriorating condition and low thermal efficiencies, resulting in large discharges of substantially warmed cooling water. Although these plants have been decommissioned or run as peaking plants (which only operate when there is a high demand) for environmental issues (fine particle pollution & groundwater contamination; Global Energy Monitor, 2022a & 2022b) other than thermal pollution, their potential thermal impacts are still non-negligible since coal plants withdraw higher volumes of water than plants using other energy (e.g. Natural gas combined-cycle plants) as compensation for low efficiencies (Averyt et al., 2011).

Apart from the large water withdrawal, thermoelectric power plants, particularly coal-fired baseload power plants, have been gradually replaced by more sustainable plants with increased thermal efficiencies and reduced water demand for cooling (e.g. combined cycle gas turbine, and combined heat and power plants) and thus operate more often as peaking power plants to fulfil occasionally high energy demands (e.g. Ratcliffe-on-Soar power station, UK).

The intermittent operations result in discontinuous releases of warm cooling water that can cause additional short-term temperature fluctuations (i.e. thermopeaking) and have severe ecological implications, particularly on temperature-sensitive aquatic organisms (Kern et al., 2015; Salinas et al., 2019; Verheyen & Stoks, 2019). Despite the ecological importance, this impact cannot be assessed with the TPI as the index is calculated as a function of cooling system and streamflow data for a particular year to broadly show the potential vulnerability of power plants to thermal stress and thus cannot cope with temperature changes and associated impacts that occur at finer time scales (i.e. on an hourly scale). In other words, power plants that were assessed to have weak impacts can still contribute to substantial disturbance to the thermal regime within a shorter time interval. This highlights that TPI should be only used as a tool to identify power plants that need particular attention rather than as an absolute measure of the actual thermal impact.

More importantly, TPIs were originally expected to be computed at a catchment scale but here only calculated at power plants because of incomplete information on power plants and their cooling systems. If the dataset for power plants is improved, possibly using the PPM tool set, power plants of similar importance to aforementioned five coal-fired power plants could be discovered and catchment-scale TPIs computed by summing all TPIs at power plants within the same catchments. This would provide an overview of vulnerabilities to thermal pollution in different parts of the USA, which could be an important piece of information for decision-makers.

3.4.4. Statistical linkages between power-plant parameters and TPI

In the correlation matrix, no useful correlations between parameters and TPI were discovered for expected TPI estimation of power plants lacking of cooling information. Despite the significant correlation between the total generating capacity and TPI, the total generating capacity cannot be used for TPI estimation as the correlation was weak. Therefore, descriptive analyses were undertaken to explore the major factors which dictate the two cooling-water parameters, total discharge of cooling water and mean temperature difference between inlet and outlet. Fuel type and cooling systems are two key descriptive

parameters determining the characteristic of a power plant, thereby the discharge of thermal effluent. Compared to oil-fired plants, gas- and coal-fired plants discharged more cooling water with lower temperature increases after cooling process. This could be associated with higher generating capacity of those two types of power plants which draw and discharge more water for cooling purposes, and hence allow the heat to be absorbed by plenty of water with lower mean temperature differences. Among different cooling systems, once-through cooling contributed to the highest cooling discharges with largest mean temperature elevations. Once-through cooling systems discharge warmed cooling water directly to the receiving water body and therefore have higher cooling discharges and mean temperature differences than systems with recycling and settling processes. Both recirculating cooling and cooling pond discharge only a small amount of cooling water to remove impurities and prevent the system (e.g. pipes and condensers) from fouling, corrosion and biological growth (also known as ‘blowdown’; Pan et al., 2018). However, recirculating cooling could discharge this water immediately after cooling process with high temperature while cooling pond would discharge after settling process, leading to more stable and lower mean temperature differences. In spite of the relatively high values of both parameters for power plants with no cooling system, there is no possible explanation for these values due to unclear operating mechanism of power plants without cooling systems and thereby the usage of the water.

Generating capacity, as an important parameter closely linked to power-plant size, showed significantly lower cooling discharges and mean temperature differences in the large-capacity group. This might be because small- and medium-capacity power plants are sufficient for the required electric power and thus operate more often than large-capacity plants, leading to higher thermal discharges. The small IQR for cooling discharges and large IQR for mean temperature differences also confirmed the intermittent operation as well as variable electricity generation for meeting the demand accordingly. With similar cooling discharges, the higher mean temperature differences for small-capacity power plants relative to medium-capacity plants could be an indication that small-capacity power plants tend to be installed in less urbanised areas with relatively low demand for electricity and nearby rivers are relatively small which warm more quickly with higher temperature when receiving similar amount of thermal discharge. Within the medium-capacity groups, the smaller IQR and

maximum for mean temperature difference in the 800–1600 MW group is likely the result of the higher proportion of once-through cooling which discharge cooling water with consistently high temperatures.

With respect to geographic factors, the result showed no clear connections with mean temperature differences, which is contrary to the conventional expectation that river temperature should decrease as latitude or altitude increases and decreased intake water temperatures would result in lower water withdrawals, ultimately lower cooling discharges and higher mean temperature differences. This can be attributed to the fact that the temperature limit for cooling water is generally set at a temperature threshold of 32 °C to protect aquatic organisms (e.g. the Clean Water Act, 1972) but allowed to be exceeded by different temperatures varying from state to state (Madden et al., 2013). For example, Pennsylvania has a limit of 30.5 °C while Wisconsin has a smaller limit of 28.9 °C which is permitted to be exceeded by 2.8 °C (Madden et al., 2013). In that case, power plants in the state with higher temperature limit would discharge warmer cooling water and therefore tend to have higher mean temperature differences. However, the temperature limits by state showed no distribution pattern across latitudes, thereby leading to no significant pattern in mean temperature differences. One possible explanation for the increasing trend of cooling discharge with latitudes is that power plants in low-latitude regions (e.g. Texas) achieve cooling process predominantly by cooling ponds which recycle and reuse most cooling water after evaporation (EIA, 2014) and discharge only a small amount of cooling water for ‘blowdown’ (Pan et al., 2018). In comparison, cooling discharges tended to be higher in groups of lower altitudes than groups of higher altitudes. This is because reaches in lower altitudes are generally lower sections of river with readily available water which can provide more sufficient cooling water and greater thermal tolerance to large volumes of warmed cooling water. Besides, power plants in high- and medium-latitude region (e.g. Ohio and Tennessee) had more extensive applications of once-through cooling systems which return heated cooling water from condenser to water sources, thus contributing to high cooling discharges.

The results of correlation matrix indicated no strong correlations between TPI and power-plant parameters; however, this was unexpected for some potentially strong correlations such as mean temperature difference with latitude and actual

electricity output which were both closely related to temperature of cooling water. Therefore, five mostly related factors were examined in detail by comparing the two parameters of cooling water, cooling discharge and temperature difference. The comparisons indicated that cooling discharge and mean temperature difference could be primarily determined by types of fuel and cooling system and partly affected by policy, economic and geographical factors, which was consistent with the results of correlation matrix. However, the sample size of statistical analyses was rather small (62 in total) and there were no available data accounting for the operation of power plants using particular fuels and their cooling systems, which could be essential for exploring the correlation with cooling discharge and mean temperature difference. In that case, it is highly expected that the monitoring and accessibility of data for cooling systems or/and their operations can be significantly improved.

3.4.5. Scenario analysis for examining the TPI applicability on a national scale

During inspection, it was noted that overestimated TPIs occurred less frequently as TPI decreased, indicating a lower probability of overestimation for smaller impacts (TPI < 10). Besides, these power plants as well as their cooling systems were noted and counted, which included 79 plants using cooling ponds or discharging into lakes or the ocean (27.6%) and 68 plants using unknown cooling systems in arid areas (23.8%), particularly in the western USA (here defined as the west section of the USA separated by the eastern boundary of the Great Plains). The high percentage of these power plants not utilising river water (51.4% in total) confirmed that power plants which were not connected to or in close proximity to rivers could be effectively detected and explained by high TPIs as well, showing great potential of applying TPI to plants with all types of cooling systems. This is because the calculation of TPI was based on the estimated discharge at the power plant which was not necessarily associated with an actual gauge or river and could be viewed as an indication of local or regional water availability. The fact that the site selection for power plants is dependent on water availability also supports this idea. Besides, there were respectively 246 and 61 power plants in OTC and non-OTC scenarios having undergone progressive changes of thermal impacts from weak or medium-high-

severe as the scenario was switched from minimum-mean-maximum. The variable impacts subject to the input value of cooling water parameters underline that the thermal impact of power plant can be only determined if the cooling water data is provided, regardless of the type of applied cooling system.

Although minimum (Fig. 3.16a & 3.17a) and maximum scenarios (Fig. 3.16c & 3.17c) are extreme cases that would rarely occur in reality, they provide some useful prospects and orientation for the future thermal pollution as a function of whether policies are effectively implemented (or violated) and whether the technologies or management reduce (or aggravate) the impacts. For the Min-OTC scenario, power plants with high or severe impacts are more likely to apply sustainable non-OTC systems or operate as peaking plants, otherwise the receiving water body would suffer from serious thermal pollution that results in irreversible damages to local ecology. Conversely, the Min-Non-OTC scenario is an ideal future for power plant thermal pollution, where 99.9% of the power plants have shown weak impacts. In recent years, there has been a gradual transition from traditional coal-fired power plants to more sustainable thermal power plants employing technologies such as CCGT and CHP, which was mainly promoted in developed countries to reduce the discharge of thermal effluent as well as the carbon footprint by utilising the hot exhaust gases for power generation at connected smaller gas-fired plant and/or the waste heat for water heating in local buildings. However, the energy demand is high and continues to grow, which exceeds the power supply by these new plants and is thus partly fulfilled by coal-fired plants in intermittent operation, especially during the peak periods (e.g. Ratcliffe in the UK).

Mean scenarios (Fig. 3.16b & 3.17b) are a better representation for real situations as the mean of cooling system parameters, unlike minimum and maximum, were calculated by taking account all values, rather than extreme values only. These scenarios cannot fully reflect the reality but could indicate the disparities in water availability across catchments and regions. Power plants with severe impacts from both mean scenarios were all located in the western USA, mainly in southern section (eastern New Mexico and western Texas) and then in central section (eastern Colorado and western Kansas) of the Great Plains. The majority of power plants in the west showed a significant increase in TPI from non-OTC to OTC scenario. In contrast, most TPIs in the east

increased only to high impacts and some even remained at low impacts. Given the distinct values of cooling water parameters between the two mean scenarios, the impacts exacerbated from non-OTC to OTC scenario were mainly determined by river discharge, thereby indicating local water availability. Consequently, the overall less elevated impact was attributed to a higher water availability in the east than in the west.

Such comparison also applies to the TPIs within a smaller region such as state or city. In the eastern USA, those TPIs increased significantly from non-OTC to OTC scenario were mostly close to community structure and residential districts in urban area where no streams or rivers were available for cooling water (e.g. East Texas: San Antonio, Houston and Dallas). These urban thermal power plants were less likely to be using OTC systems as they were peaking plants using diesel or gas turbine for emergent power supply which do not require large amount of cooling water. This can be further confirmed by the fact that a coal-fired power plant using OTC system occupies a sizable space with low cost and causes air pollution by exhausting ash, dust, and smoke to the ambient environment, which are both undesirable inside a city.

However, the water availability cannot be reflected by the TPI in regions where lakes and reservoirs are used as the major water source of cooling water (e.g. East Texas). In these regions, power plants with weak impacts (TPI < 0.5) were the result of connected rivers with gauges showing high flow rates (e.g. Lavon Lake & Lake Ray Hubbard), whereas plants with high and severe impacts (TPI > 1) showed proximity to connected small creeks with low discharges (e.g. Lake Arlington, Mountain Creek Lake, Twin Oak Reservoir and Smithers Lake). The TPI was calculated with the estimated discharge from known discharge of a stream or river using drainage-area ratio method; however, lakes can be fed and drained by multiple small streams or larger rivers and only one or some of these rivers are gauged, contributing to seriously underestimated water availability with the consideration of a limited number of inflows and outflows. In that case, the interpretation of TPIs for power plants in vicinity of lakes should be treated cautiously.

Despite the lack of cooling data for accurate assessments, the scenarios exemplified one of the major applications of TPI by providing a broad overview

of power plants with different ranges of the vulnerability to thermal pollution on a national scale, and a preliminary assessment of power plants in the USA by incorporating relevant information obtained via Google Earth inspection (e.g. the distance to the city, cooling systems, water sources, etc.). These scenarios prioritise the power plants or the regions containing the plants that require immediate investigation and confirmation on cooling system and/or operation mode to assess the severity of the actual impact, as opposed to other plants which are consistently less prone to thermal pollution across scenarios. However, the assessment using the TPI should abide by the precautionary principle as there is not necessarily any linkage between cooling system type and water availability. For example, Luminant Forney Station (1894 MW) and Moselle Power Station (512 MW) showed weak impacts (TPI < 0.5) in OTC scenario owing to the proximity to abundant water resources (East Fork Trinity River and Leaf River); however, in reality, the two plants use cooling tower instead of heavily water-dependent OTC system and thus contribute to even smaller impacts as a result of lower discharge of cooling water. Power plants of similar kind, employing more sustainable recirculating cooling systems as well as advanced technologies like combined heat and power plants (CHP) and combined cycle gas turbine (CCGT), will become increasingly common in the future, particularly under the further tightened environmental protection policy and growing trend of phasing out the application of OTC systems.

As a result, the TPI assessment is a rudimentary approach to thermal pollution from power plant, which compares the temperature and discharge of cooling water with that of the receiving river, irrespective of whether the river really exists, and therefore relies on complete information of the cooling system and its discharge for determining the actual impact. This coincided with our purpose of designing the TPI that the index was intended to show the potential vulnerability of power plants to thermal pollution rather than the actual thermal pollution. In that case, TPI, in combination with background information (e.g. technology used, lake or cooling pond nearby, and power plants used as peaking or base load power plants), can provide more accurate assessments of thermal pollution and not be confined to plants using OTC systems only. This is particularly important as power plants using OTC systems are being gradually eliminated and replaced by more sustainable plants (e.g. CHP and CCGT). Our scenario analysis is also a useful demonstration of how to process and leverage cooling

system data (intake/outfall temperature difference and the total discharge of cooling water) to calculate and apply TPI to a wider geographic area in response to the current challenging situation of data deficiency. However, the reliability of results can be substantially undermined when insufficient data is provided for each categorical group (i.e. OTC and non-OTC systems). Therefore, it is hoped that the quality and availability of cooling system data will be further improved so that cooling system data can be standardised according to a range of power plant variables (e.g. the type and size of power plant) to achieve broader application of TPI (e.g. in other countries and globally).

3.5. Conclusions

This study concentrates on developing a thermal pollution index (TPI) to explore the vulnerability of rivers to discharged cooling water from thermal power plants in the USA. As preparation, readily-accessible databases relating to power plants were examined to determine the relevant parameters for computing the index. As a result, a USA national power-plant database with cooling information was matched and combined with a global power-plant database with detailed information and accurate location data to create a high-quality dataset. The newly complied dataset was further improved by inspection on Google Earth and removal following designed filtering criteria, providing the most complete and relevant data for development and computation of the index. However, the uncertainties from inspection, together with unclear and missing cooling information, increased the difficulty of the filtering process and decreased the number of power plants dramatically from 2282 to 144. A significantly improved dataset is thus expected to become available for the completeness of the research.

In addition to the cooling information, upstream catchment areas for thermal power plants were also examined. The global analyses demonstrated that most thermal power plants were located in upstream catchment areas smaller than 500 km^2, whereas the regional analyses showed consistent results both before and after removing small-capacity power plants (≤ 20 MW) across study regions. These findings could be a strong indication that thermal power plants were

mostly located in higher reaches of streams or rivers where more severe thermal impacts relative to lower reaches could be expected due to smaller sizes of the channel. Besides, the impacts could be further concealed by the lack of cooling information on these plants.

Owing to the paucity of data with which to calculate TPI, we hoped to develop statistical functions linking TPI to other (available) power plant properties to estimate TPI for locations without information on cooling systems. However, the correlation and descriptive analyses were based on a small sample size, showing a consistent result that the index was most associated with the type of fuel and cooling system, which dictate the operation of power plants. As the data accounting for the operation was unavailable, we decided to exploit the potential of available data rather than pursue the collection of a new data, which would be difficult to obtain. Therefore, a series of scenarios of thermal discharges from power plants were created to examine the TPI applicability on a national scale. The scenario analysis demonstrated that there is great potential and a broad prospect for the application of TPI in assessing power plant thermal pollution. With the gradual improvement of data quality and availability, we are confident that the applicability can be extended to other countries or geographic regions via standardising cooling system data according to most relevant power plant variables.

3.6. Supplementary materials

Table 3.S1. Results showing no strong correlations between TPI and power-plant parameters.

Spearman's rank correlations (n = 62)																			
		2.	3.	4.	5.	6.	7.	8.	9.	10.	11.	12.	13.	14.	15.	16.	17.	18.	TPI
1. Total capacity (MW)	Correlation Coefficient	-.243	-.006	.067	.133	-.098	-.192	.180	.036	.005	.035	.247	.258*	.237	-.234	.699**	.048	-.197	-.304*
	Sig. (2-tailed)	.057	.964	.607	.303	.449	.136	.161	.782	.972	.788	.053	.043	.064	.068	.000	.713	.125	.016
2. Latitude	Correlation Coefficient		.415**	.483**	-.192	-.007	.359**	-.089	.036	.094	.034	-.065	-.113	-.043	.069	.097	.388**	.350**	.204
	Sig. (2-tailed)		.001	.000	.136	.959	.004	.490	.783	.466	.794	.615	.383	.739	.592	.451	.002	.005	.113
3. Longitude	Correlation Coefficient			-.099	-.234	.135	.112	-.090	-.047	.002	-.041	-.195	-.230	-.181	.201	.037	.052	.200	.050
	Sig. (2-tailed)			.443	.068	.297	.388	.489	.717	.987	.754	.130	.072	.160	.117	.777	.690	.119	.702
4. Dist to the outlet of the main river basin (km)	Correlation Coefficient				-.096	.197	.268*	.123	.149	.203	.149	.216	.185	.228	-.044	.304*	.728**	.150	.000
	Sig. (2-tailed)				.456	.125	.035	.339	.247	.114	.248	.092	.149	.074	.734	.016	.000	.244	.998
5. Area of the subbasin (km^2)	Correlation Coefficient					-.273*	-.160	.022	-.075	-.178	-.074	-.020	-.002	-.020	-.381**	-.001	-.193	-.206	-.055
	Sig. (2-tailed)					.032	.214	.865	.562	.167	.566	.877	.988	.875	.002	.994	.132	.108	.669
6. Total_Up_Area (km^2)	Correlation Coefficient						.088	.002	.010	.074	.009	-.114	-.111	-.106	.161	-.114	.303*	.125	-.043
	Sig. (2-tailed)						.497	.990	.938	.570	.943	.377	.392	.411	.212	.379	.017	.332	.739
7. Reported_Withdrawal (L/yr)	Correlation Coefficient							.383**	.793**	.815**	.793**	.427**	.350**	.425**	.194	.196	.158	.738**	.654**
	Sig. (2-tailed)							.002	.000	.000	.000	.001	.005	.001	.131	.127	.220	.000	.000
8. Reported_Consumption (L/yr)	Correlation Coefficient								.319*	.301*	.320*	.483**	.481**	.490**	-.133	.254*	.094	-.029	-.070
	Sig. (2-tailed)								.012	.018	.011	.000	.000	.000	.302	.047	.469	.824	.588
9. Calculated_Withdrawal (L/yr)	Correlation Coefficient									.956**	.999**	.727**	.668**	.708**	.244	.343**	.033	.480**	.558**
	Sig. (2-tailed)									.000	.000	.000	.000	.000	.056	.006	.797	.000	.000
10. Calculated_Withdrawal_MIN (L/yr)	Correlation Coefficient										.952**	.685**	.637**	.667**	.251*	.304*	.068	.511**	.514**
	Sig. (2-tailed)										.000	.000	.000	.000	.049	.016	.602	.000	.000
11. Calculated_Withdrawal_MAX (L/yr)	Correlation Coefficient											.720**	.660**	.701**	.245	.340**	.032	.483**	.559**
	Sig. (2-tailed)											.000	.000	.000	.055	.007	.805	.000	.000
12. Calculated_Consumption (L/yr)	Correlation Coefficient												.992**	.997**	.030	.551**	.072	-.014	.094
	Sig. (2-tailed)												.000	.000	.817	.000	.579	.913	.467
13. Calculated_Consumption_MIN (L/yr)	Correlation Coefficient													.988**	.001	.532**	.050	-.085	.028
	Sig. (2-tailed)													.000	.995	.000	.701	.511	.832
14. Calculated_Consumption_MAX	Correlation Coefficient														.020	.551**	.076	-.014	.090
	Sig. (2-tailed)														.879	.000	.557	.915	.488
15. Mean_Tdelta (°C)	Correlation Coefficient															-.050	-.031	.236	.453**
	Sig. (2-tailed)															.699	.812	.064	.000
16. Actual_Electricity_Output (MWh)	Correlation Coefficient																.228	.133	.058
	Sig. (2-tailed)																.074	.302	.652
17. Elevation (km)	Correlation Coefficient																	.122	-.008
	Sig. (2-tailed)																	.344	.951
18. Total discharge (m^3/s)	Correlation Coefficient																		.747**
	Sig. (2-tailed)																		.000

*. Correlation is significant at the 0.05 level (2-tailed).

**. Correlation is significant at the 0.01 level (2-tailed).

Chapter 4: Modelling water temperature changes due to thermal effluents from power plants

4.1. Introduction

River temperature is an important physical parameter of water quality that influences and regulates many physical, chemical, and biological processes (Caissie, 2006; Hannah & Garner, 2015; Ouellet et al., 2020). Therefore, unnatural changes in river temperature can cause serious ecological impacts as most aquatic organisms are ectotherms and their growth, migration, and survival are strongly dependent on water temperature (Seebacher et al., 2015; Andrews et al., 2021; Auer et al., 2022; Tonolla et al., 2022; Kanno et al., 2023). An increase in water temperature exerts an impact on aquatic organisms by reducing oxygen availability (Ficke et al., 2007), altering metabolic rates (Claireaux et al., 2000), increasing susceptibility to disease (Marcos-López et al., 2010), disrupting natural phenological patterns (Bonacina et al., 2023b) and favouring high-temperature tolerant and invasive species (Rahel & Olden, 2008). In addition, water temperature change can also have profound socio-economic consequences. Thermoelectric power plants, particularly nuclear and coal-fired plants (and to a lesser extent gas-fired plants), withdraw large quantities of water from nearby water sources for cooling processes, and hence their thermal efficiency and power output is highly dependent on water temperature (Ibrahim et al., 2014; Attia, 2015; Cook et al., 2015; Miara et al., 2018; Henry & Pratson, 2019).

Thermal impacts on rivers are primarily associated with climate change and anthropogenic activities such as deforestation, urbanisation, and flow abstraction (Caissie, 2006; Hannah & Garner, 2015; Ficklin et al., 2023). While climate change is widely recognised as a major cause of large-scale and long-term thermal impacts (van Vliet et al., 2013; Rajesh & Rehana, 2022; Michel et al., 2022), heated effluents from thermoelectric power plants and other point sources cause immediate and profound alterations to river thermal regimes

(Kinouchi, 2007; Madden et al., 2013; Adams et al., 2023). In the lower Ebro River, Spain, the thermal effluent from the Ascó nuclear power plant resulted in an increase of approximately 3 °C in the mean annual water temperature, which varied greatly as a function of river discharge (Prats et al., 2010). A water temperature increase of 2 °C was also noted in the French Rhône River immediately downstream of the Saint-Alban nuclear power plant, thereafter decreasing to 0.8 °C and 0.5 °C at 15 and 30 km downstream of the plant, respectively (Wawrzyniak et al., 2012). In different seasons, the water temperature of the Danube River showed contrasting responses to the thermal effluent from the Cernavodă nuclear power plant in Romania, which increased by 4.5 °C in summer, 5.9 °C in autumn and 13.5 °C in winter at a downstream monitoring site (Liliana, 2012). Moreover, multiple power plants that are deployed on the same river or in the same catchment can trigger plant-to-plant interferences and cumulative thermal impacts (Miara et al., 2018; Johnson et al., 2019). Despite a scarcity of relevant research, similar impacts can be speculated from 'run of river' hydropower plants within a cascade system, which can lead to abrupt local warming by diverting river flow and shift the thermal regime from a continuous to a disrupted pattern (Bonacina et al., 2023b). Owing to the larger heat input from power plants, the magnitude of impact is expected to be even greater than for run-of-river hydropower schemes.

River temperature models are an effective approach for simulating river temperature and can be generally categorised into statistical and process-based models (Caissie, 2006; Benyahya et al., 2007; Dugdale et al., 2017). Statistical models, including regression and stochastic models, are established on the basis of statistical linkages between water temperature and related covariates such as air temperature. In their most basic sense, they can be relatively simple and require minimal data inputs (Benyahya et al., 2007; Dugdale et al., 2017). Regression models can provide accurate river temperature estimations at coarser temporal scales (e.g. weekly, monthly and annual) based on the strong correlation between air and water temperature (e.g. Mohseni et al., 1998; Rosencranz et al., 2021). Because of the autocorrelation within the water temperature time-series, stochastic models, which account for the autocorrelation, are often used instead for finer scales (e.g. hourly and daily; Jeong et al., 2013; Zhu et al., 2018; Graf & Aghelpour, 2021). However,

statistical models are incapable of explaining fundamental energy transfer mechanisms or interactions and are limited in their transferability to different locations and times. In contrast, process-based or deterministic water temperature models simulate the spatio-temporal variations of river temperature by calculating the heat fluxes exchanged at air-water and streambed-water interfaces (Hebert et al., 2011). Due to their intrinsic complexity, the implementation of these models tends to be data-intensive and time-consuming (Benyahya et al., 2007; Jackson et al., 2021). However, they are particularly suitable for exploring thermal impacts associated with anthropogenic activities (Caissie et al., 2007; Dugdale et al., 2017). In view of the scarcity of high-quality fine-resolution water temperature time series, it is of vital importance to fully leverage the best data and approaches available to explore the impacts of thermal effluents from power plants on river temperature.

Despite the aforementioned importance of power plant impacts on river thermal regimes, most research has been focused on the impacts on lakes (e.g. Kirillin et al., 2013; Råman Vinnå et al., 2017) and coastal areas (e.g. Ma et al., 2017; Yavari & Qaderi, 2020; Issakhov & Zhandaulet, 2021; Nie et al., 2021), with the remaining relevant research primarily conducted at reach (e.g. Kalinowska et al., 2012), regional (e.g. Stewart et al., 2013) and global scales (e.g. Raptis et al., 2016), or kept largely within the grey literature. Furthermore, although thermoelectric power plants are still dominant for supplying base load power globally and responsible for serious thermal pollution in rivers (Chmelová et al., 2021; Guo et al., 2022; Kabengele et al., 2022), the relevant research on their interactions and cumulative impact along the river has been scarce and mainly based in the densely plant-populated Northeastern United States (e.g. Stewart et al., 2013; Miara et al., 2013 & 2018). In order to better understand riverine thermal pollution caused by thermoelectric power plants, we therefore aim to model the whole-river scale impacts of both individual and multiple power plants to observe how far downstream thermal effluents remain distinct and/or interact along a hypothetic river system. To achieve such goal, this investigation is structured around three key objectives:

1) Establish a conceptual water temperature model of a large, UK-typical river, which is capable of simulating stream temperature at hourly time scales using

a mix of real and simulated streamflow and water temperature data for boundary conditions.

2) Generate scenarios of thermal effluent from power plants by using different combinations of typical discharges and temperatures, operation mode (i.e. operate as peak or base load power plants) and distances between power plants in order to discover the spatial and temporal patterns in thermal effluent along receiving rivers.

3) Explore how predicted future climate-induced thermal warming will exacerbate the impacts of power plants by applying the latest IPCC climate scenarios on the 'two power plants' scenarios resulting in the smallest and the largest thermal disturbances.

4.2. Methods

4.2.1. Model Description

Heat Source is a distributed process-based model which consists of multiple modules that simulate open channel hydraulics, flow routing, stream heat and mass transfers, effective shade and the resulting stream temperature (Boyd & Kasper, 2003). It has been widely used by regulatory agencies to study stream temperature and total maximum daily load (TMDL) for temperature by considering the solar heat load as a non-point source pollutant (Cox & Bolte, 2007; NCRWQCB, 2014; ODEQ, 2008; ODEQ, 2012). Heat Source describes the net heat energy flux exchanged with the water body (all terms in units of W m^{-2}) as follows:

$$H_{total} = H_{sw} + H_{lw} + H_e + H_a + H_b \quad \text{(Eq.1)}$$

where H_{total} describes the total energy gain (or loss) at a certain river channel node, H_{sw} is solar shortwave radiation flux received by the water column, H_{lw} is longwave radiation flux between the water column and the atmosphere (or nearby terrain/vegetation), H_e and H_a are the latent (evaporation) and sensible

(convection) heat fluxes exchanged between the atmosphere and the water column, and H_b is the conduction heat flux between the water column and the underlying river bed. The resulting stream temperature is then calculated at each river channel node and timestep as a function of H_{total} and the volume, density, velocity, and specific heat capacity of water passing each river channel node at each timestep. The model operation requires continuous data including meteorology, riparian vegetation, channel cross-sectional morphology, and discharge and temperature at the upstream boundary. Further details about Heat Source and the equations used to estimate the various heat fluxes are described in Boyd and Kasper (2003).

A conceptual model of a low-gradient, moderately-sized (~150 km long) UK river was developed to run power plant discharge scenarios and indicate expected magnitudes and directions of change due to power plant discharge of relevance to similar-sized rivers, globally (Table 4.1). However, the model setup requires essential data including channel geometry and boundary conditions to characterise the channel and flow conditions. Therefore, a segment of approximately 150 km of the River Trent, UK, which was located in the lower half of its catchment (between Cavendish Bridge [Derbyshire] and the Humber), including four major tributaries, was selected as the basis of modelling to provide these data. Although our model uses the River Trent as a template, the model should *not* be considered a model of the River Trent because we intend solely that the model acts as a conceptual means to quantify the impacts of power plants on similar-sized rivers.

Table 4.1. Physical attributes of the modelled river for the study period.

	Units	Median	Mean	SD	Min	Max
Water temperature	°C	18.1	18.3	0.94	15.9	21.1
Discharge	m^3/s	36.5	36.0	2.53	20.4	39.9
Velocity	m/s	0.38	0.40	0.16	0.11	0.97
Width	m	75.5	91.6	64.1	33.3	615.5
Depth	m	1.2	1.2	0.4	0.4	2.7
Slope	m/m	0.000093	0.00018	0.00028	0.00001	0.0023
Elevation (ASL)	m	-	-	-	1.1	21.3

4.2.2. Data source and processing

A variety of input data were required by Heat Source to function correctly (Table 4.2). Meteorological data including cloudiness, wind speed, relative humidity and air temperature were extracted from the Met Office Integrated Data Archive System (MIDAS) for land surface data at four selected stations covering the modelled River Trent (Met Office, 2019). Data conversions (e.g. converting cloud cover in oktas to decimals) were undertaken to comply with the required units/formats for Heat Source. Linear interpolation was also applied to fill in small data gaps (< 3 hours). River channel and land cover geospatial data were sampled and assembled by running TTools, a collection of Python scripts that support Heat Source model implementation (in conjunction with ArcMap). The relevant data, including digital elevation model (DEM) and shapefiles for stream centreline, left and right bank, were extracted from UK Ordnance Survey data products (Ordnance Survey, 2021a & 2021b), and tailored to the desired size for the study area. Land cover data, including land cover height, canopy cover and overhang, are usually required to run Heat Source to account for the riparian vegetation present along the river. Riparian vegetation provides shading that plays a key role in inhibiting river warming, mainly via reducing incoming solar radiation. However, given that riparian shading is most effective at distances 5–20 km downstream from the source of the river (Johnson & Wilby, 2015), it has a largely negligible effect on a relatively wide river (> 100 km downstream from the source) which has a very limited area covered by tree canopy. Furthermore, it is also our desire to keep the model outputs generic and without site-specific complexities that limit its broader relevance. Therefore, variables characterising the riparian land cover were assigned zero.

Table 4.2. Detailed information about model inputs.

Model input	Description
Boundary condition	Gauged flow rate at Trent at Shardlow station; water temperature time-series extrapolated based on the low-resolution monthly samples using sine function and Fourier series stochastic models
Tributary inflow data	Gauged flow rates of four stations of the tributaries at 151 km, 147 km, 143 km, 134 km to the river mouth, Derwent at Church Wilne, Erewash at Sandiacre, Leen at Triumph Road Nottingham and Soar at Kegworth; water temperature time-series extrapolated based on the low-resolution monthly samples using sine function and Fourier series stochastic models
Meteorological data	Extracted from the Met Office Integrated Data Archive System (MIDAS) for land surface data at four selected stations, Scampton, Waddington, Cranwell and Watnall
Morphology data	Produced by running TTools using digital elevation model (DEM) and shapefiles for stream centreline, left and right bank that were tailored to the desired size for the study area
Land cover data	Assuming that riparian shading has negligible effects on river temperature as the modelled river is very wide

Hourly discharge data for the upper boundary and major tributaries of our conceptual model were converted from 15-minute flow data provided by the England's Environment Agency (NRFA, 2022). However, hourly temperature data were not available and the only accessible UK river temperature data has a monthly temporal resolution, with unstandardised times of collection (Environment Agency, 2022). Therefore, we developed a statistical function to estimate hourly water temperature as a function of these monthly measurements and generate temperature boundary conditions for the conceptual model. Stream water temperatures can be decomposed via a stochastic approach into two different components, the long-term periodic component and the short-term non-periodic component or residual (Eq. 2; Cassie et al., 1998).

$$T_w(t) = TP(t) + R_w(t) \quad \text{(Eq.2)}$$

where *t* represents the day of the year or the hour of the day, T_w is the stream water temperature, *TP* is the periodic component and R_w is the non-periodic residuals. The water temperature time-series, here as an input for a semi-conceptual model, was only required to show the major seasonal and diurnal

variations. Hence, the short-term residuals as minor variations were not considered in generating water temperature data.

Sine function (Eq. 3–5) and Fourier series (Eq. 6–8) stochastic models, were applied to extrapolate a water temperature time-series based on the low-resolution monthly samples and generate the periodic component (*TP*) of Eq 2. In order to decide the optimal model combination, modelled water temperatures were compared to measured monthly temperatures by examining the differences in development from a broad perspective (i.e. magnitude, frequency, troughs, peaks and root-mean-squared errors). The result showed that the sine function outperformed Fourier series in capturing the high temperatures throughout the year but were more susceptible to abrupt variations that were very likely to be erroneous (see Fig. 4.S1 & S3). Therefore, a sine function was used for generating daily temperatures and Fourier series for hourly temperatures.

$$TP(t) = a + b \cdot sin\left[\frac{2\pi}{365}(t + t_0)\right] \quad \text{(Eq.3)}$$

where *a, b*, and t_0 are estimated coefficients. *a* (vertical shift) can be computed from the mean annual temperatures; *b* (amplitude) and t_0 (phase shift) can be calculated by:

$$b = \frac{(T_{max} - T_{min})}{2} \quad \text{(Eq. 4)}$$

and when *TP* is at its maximum,

$$t_0 = \frac{\pi}{2} \cdot \frac{365}{2\pi} - t_{max} \quad \text{(Eq.5)}$$

where T_{max} and T_{min} are the maximum and minimum temperatures of the samples; t_{max} is the day when the maximum temperature occurs.

$$TP(t) = \frac{A_0}{2} + \sum_{n=1}^{\infty}\left\{A_n \cdot cos\left[(t - j - 1)\frac{2n\pi}{N}\right] + B_n \cdot sin\left[(t - j - 1)\frac{2n\pi}{N}\right]\right\}$$

(Eq.6)

where *TP(t)* is the periodic component for stream temperature at time t in hours (1:00 = 1 and 23:00 = 23); *N* is the number of observations (hours) for a given period T (i.e. 24); *n* is the number of harmonics used; *j* is the first hour of observation within the period *T* (i.e. 0); $A_0/2$ represents the average of the function *f(t)* for the period *N* (i.e. daily mean temperature);

$$A_n = \frac{2}{N}\sum_{t=1}^{N} f(t) \cdot cos\left(\frac{2\pi nt}{N}\right)$$

(Eq.7)

and

$$B_n = \frac{2}{N}\sum_{t=1}^{N} f(t) \cdot sin\left(\frac{2\pi nt}{N}\right)$$

(Eq.8)

where *f(t)* is the stream water temperature series.

For sine function, the coefficients were calculated for each year by using sporadic water temperature data between 1988 and 2007 and averaged to represent the general pattern of daily temperatures in a year. For Fourier series, only the first harmonic (*n* = 1) was applied to compute hourly temperatures as it explains most of the total variation in river temperature (Cassie et al., 1998). By using the highest-quality time series data available (15 min resolution; only one measurement missing throughout the year; see Fig. 4.S4), the coefficients in Fourier series were calculated for each day in a month and averaged for that particular month. Finally, the Fourier series with these monthly coefficients were superimposed on the daily temperatures generated from sine functions to produce hourly temperature data in a year. The above calculation was repeated for the upper boundary and tributaries.

Using the mean summer evaporation flux for open grassland (35.9 $W \cdot m^{-2}$ in June, July and August) in Dugdale et al. (2018) as reference, the mean evaporation flux for the conceptual model was manually calibrated to be within reasonable limits (36.9 $W \cdot m^{-2}$) by adjusting the wind function coefficients of Heat Source's Dalton-style evaporation routines (e.g. Dugdale et al., 2017).

4.2.3. Power plant discharge scenarios

Heat Source was implemented using meteorological data recorded in the first week of July 2020 (1st – 7th July) characterised by relatively high air temperatures (15.1 ± 2.3 °C) and low flows (7.2 m^3 s^{-1}). The specific period was selected to investigate temperature changes in response to a range of power plant discharge conditions during periods of warm weather and low-flow conditions with power generation at its peak when thermal effluent has its greatest impact on river temperature. Hence, we created and ran a series of model scenarios with different combinations of parameters including *a)* the temperature and discharge of effluent, *b)* the number of power plants discharging to the river and *c)* the distance between power plants (Fig. 4.1 & Table 4.3). In total, the parameter combinations contributed to 252 scenarios (excluding baseline, thermopeaking and climate scenarios). Due to the large number of scenarios to be run in Heat Source, Python scripts were written to automatically generate all designed scenarios and run multiple models simultaneously using multiprocessing functions that reduced the run time from 6 to 3 hours.

a) Single power plant

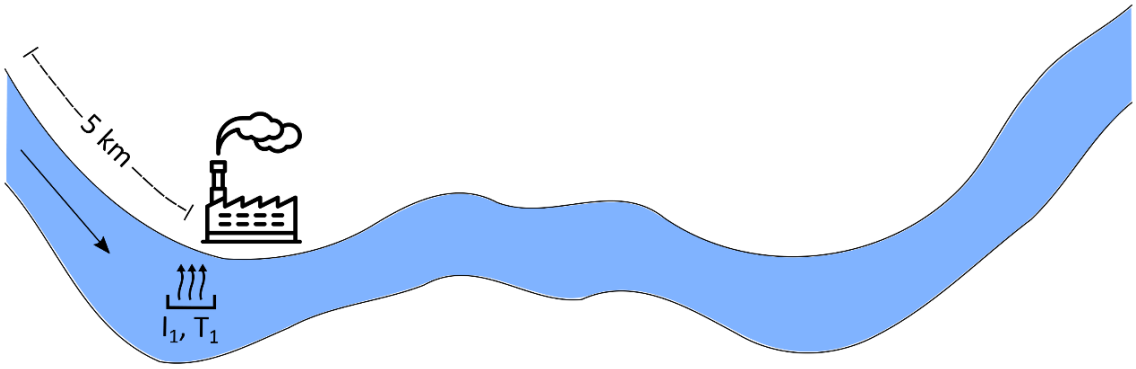

b) Two power plants

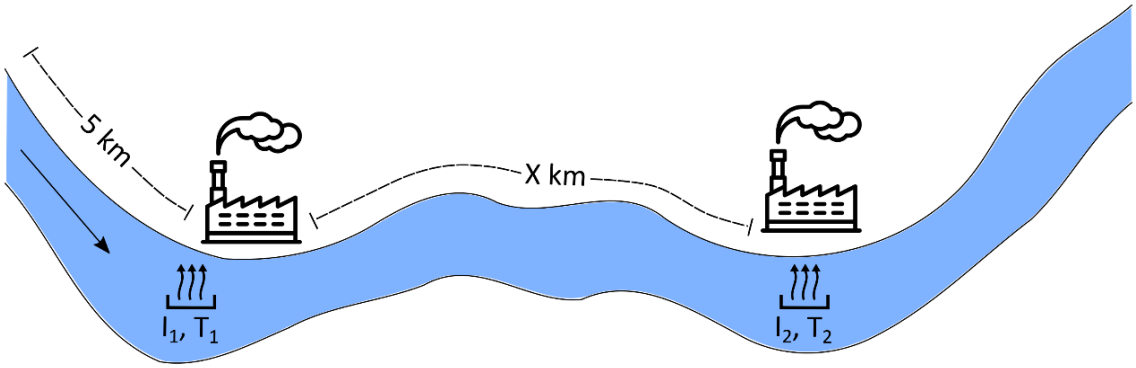

Figure 4.1. Schematic plots for thermal effluent discharged from a) single and b) two power plants into the modelled river.

Table 4.3. Parameters for creating scenarios of powerplant discharge.

Number of power plants	One	Two
Discharge (I_1 & I_2)	Q × 2%, 10%, 20%	
Temperature (T_1 & T_2, °C)	25 + 0, 5, 10	
Distance between plants (X km)	(Null)	15, 25, 40

4.2.3.1 Thermal effluent discharge

With the assumption that the discharge from a power plant is proportional to that of the water source (Q), the effluent discharges were estimated based on publicly-available data on typical power plant discharges (e.g. USC EW3 database and EIA Form 923; EIA, 2008, Union of Concerned Scientists, 2012). Here, the effluent discharge was introduced to the model as a positive inflow, with the corresponding discharge abstracted 1 km upstream to offset the additional water in the system and reproduce the abstraction process associated with power plant cooling water withdrawals.

In order to decide the effluent discharges to be used in our scenarios, we calculated the cumulative distribution function of the percentage of the total river flow that is returned to a specific river by a power plant from the USC EW3 database. As a result, the 0.2% (20th percentile), 2% (50th percentile), 10% (90th percentile) and 20% (95th percentile) discharges were selected (Fig. 4.2). However, given that the 0.2% contributed to negligible changes to the river temperature, the related results were not included in scenario comparisons.

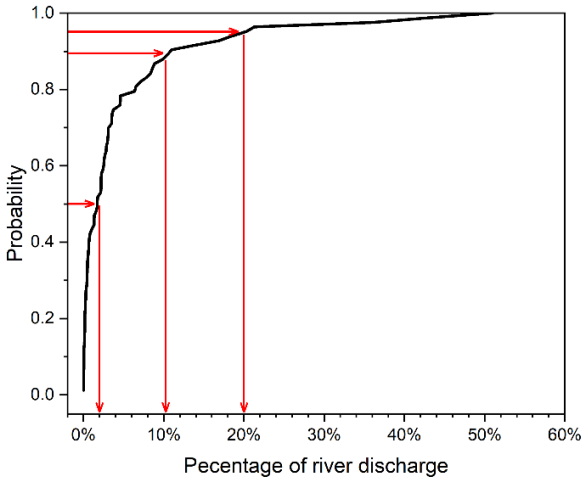

Figure 4.2. Cumulative distribution function of the percentage that the effluent discharge from typical thermoelectric power plants using once-through cooling systems accounts for the river discharge (USC EW3 database; EIA Form 923).

4.2.3.2 Thermal effluent temperature

In the absence of clarity regarding regulations on power plant discharge temperatures in the UK and EU, the temperature of thermal effluent was also based on available data from the USA which dictates a cooling water temperature limit of 32 °C (for most states) but permitted to be exceeded by 2–3 °C under certain circumstances. Similar regulations are present in other countries, but we chose to base our scenario on USA-defined limits as a) the USA encompasses a broad range of river types and sizes and b) water temperature standards are more proscriptive and clearly-defined than in other jurisdictions (e.g. UK, EU). As a result, effluent temperatures were chosen at an interval of 5 °C between 25 °C and 35 °C to represent typical temperatures, not exceeding the maximum allowed limit (Table 4.2).

4.2.3.3 Number of power plants

In single power plant scenarios, a power plant was set to discharge thermal effluent 5 km downstream from the upper boundary of the model (Fig. 4.1a & Table 4.3). For scenarios with two power plants, a second power plant was positioned 15 km, 25 km and 40 km downstream from the first plant in single

power plant scenarios (Fig. 4.1b & Table 4.3). The selected spacing distances are representative of the real-world spacings between power plants, with examples at these spacings present on similar-sized rivers (WRI Global Power Plant Database).

4.2.4. Thermopeaking scenarios

Thermoelectric power plants, particularly coal-fired baseload power plants, have been gradually phased out by more sustainable plants with improved thermal efficiencies and thus operate more often as peaking power plants to fulfil occasionally high energy demands (e.g. Ratcliffe-on-Soar power station, UK). Therefore, further scenarios were performed where power plants were set to operate as peaking power plants to examine how thermal effluents resulting from multiple single-day operations would develop, interact and affect river temperature. Thermopeaking, which usually refers to the abrupt and intermittent alterations of river thermal regime due to discontinuous releases from hydropower plants (Zolezzi et al., 2011; Feng et al., 2018; Mameri et al., 2023), was here used to describe the river temperature changes in response to periodic operations of a peaking power plant. In this study, thermopeaking scenarios were created by setting the power plant in single power plant scenarios to operate between 8 am–12 am when the average UK household electricity demand exceeded 0.4 kW in a day, which was approximately half of the maximum (Pimm et al., 2018).

4.2.5. Future climate change scenarios

The smallest and the largest thermal disturbances generated by the ‘two power plants’ scenarios (see section *2.3.3*) were individually studied with respect to the further deterioration due to global warming. This ultimately provides a general prediction of the upper and lower limit of thermal pollution from multiple power plants in the near foreseeable future. Our model is conceptual and designed to simulate power plant impacts on similar-sized rivers rather than provide an accurate estimation of the thermal impact of a particular power plant

on a particular river. Hence, without taking into account the changes in variability of air temperature (particularly the changes in the extreme events), global warming factors were introduced by uniformly (i.e. spatially and temporally) increasing air temperatures according to the estimated mean temperature increases from the most realistic combinations of Shared Socioeconomic Pathways and Representative Concentration Pathways scenarios (SSP-RCP; Table 4.4) in IPCC sixth assessment report (AR6; Irfan, 2021). SSP1-1.9 and SSP5-8.5 are less plausible and hence not considered. An increase of 1.2 °C in the global mean temperature has already been reported from the pre-industrial period (1850-1900) to 2020 (World Meteorological Organization, 2021) and was therefore deducted before generating the climate scenarios.

Table 4.4. Increases of ambient temperature (°C) for SSP-RCP climate scenarios by 2100.

Scenario	SSP1-2.6	SSP2-4.5	SSP3-7.0
Mean	1.8	2.7	3.6
Range	1.3–2.4	2.1–3.5	2.8–4.6

4.2.6. Analyses of spatial and temporal impacts

The river temperature rise in response to different power plant scenarios can vary considerably across space and time because of the contrasting combinations of parameters. However, it is *not* our intention to accurately estimate the water temperature change in response to power plant discharge at a particular time or location. We therefore used some key 'check points' to explore the thermal impact of power plants by examining how far it persists along the river against the cooling efficiency and capacity that the river preserves (i.e. latent heat losses as it flows downstream) in a generalised manner (Table 4.5). For our various scenarios, the spatial impacts of power plant effluent on river temperature were examined by calculating the 7-day mean temperatures at the upstream power plant T_{week_PP1}, the downstream power plant T_{week_PP2} and the river mouth T_{week_mouth} as well as the corresponding temperature increments relative to the baseline 'no inflow'

scenario ΔT_{week}. T_{week_PP1} and T_{week_PP2} were used to investigate the immediate response of the river to thermal effluent at the cooling water outfall, showing the maximum impact that the power plant can have on the river. T_{week_mouth} accounts for the remaining thermal impact at the end of the river and thus reflects the persistence of power plant impact on river temperature.

Due to the consistent increases in hourly mean temperature over the modelled river ($\Delta \overline{T}_{hour}$) throughout the 7-day period, a new parameter M_{7d}, which calculates the 7-day mean of $\Delta \overline{T}_{hour}$, was introduced to account for the temporal as well as the overall impact, expressed as:

$$M_{7d} = \frac{\sum_{h=1}^{N} \Delta \overline{T}_{hour}}{N} \quad \text{(Eq.8)}$$

where h is the timestep of the model and N is the number of hours in 7 days. For a given scenario, a greater M_{7d} indicates a larger overall impact on the entire river.

Table 4.5. Metrics for examining impacts of power plant effluent on river temperature.

Metric	Description
T_{week_PP1}	7-day mean temperatures at the upstream power plant
T_{week_PP2}	7-day mean temperatures at the downstream power plant
T_{week_mouth}	7-day mean temperatures at the river mouth (the end of the modelled reach)
ΔT_{week}	Increment of 7-day mean temperature relative to the baseline 'no inflow' scenario
$\Delta \overline{T}_{hour}$	Hourly mean temperature over the modelled river
M_{7d}	7-day mean of $\Delta \overline{T}_{hour}$

4.3. Results

4.3.1. Baseline 'no inflow' scenario

The baseline 'no inflow' scenario has no power plant discharge into the river and therefore was used to illustrate the temperature changes in response to

thermal effluents via comparison with power plant scenarios. In the modelled river, the longitudinal mean water temperature showed a general decrease as the flow propagated downstream (Fig. 4.3). Although the asymptotic warming paradigm dictates that instantaneous (daytime) river temperature generally increases as a function of distance downstream (Fullerton et al., 2015), our results constitute the time-averaged mean river temperature for examining how far the thermal impact remains distinct against the cooling efficiency and capacity of the river. Given the very wide channel in the lower reaches of our conceptual model, which increased the surface area for greater evaporative cooling (particularly during nighttime), our simulated streamwise mean temperature decrease is a function of increased latent heat losses in the downstream sections and during nighttime periods.

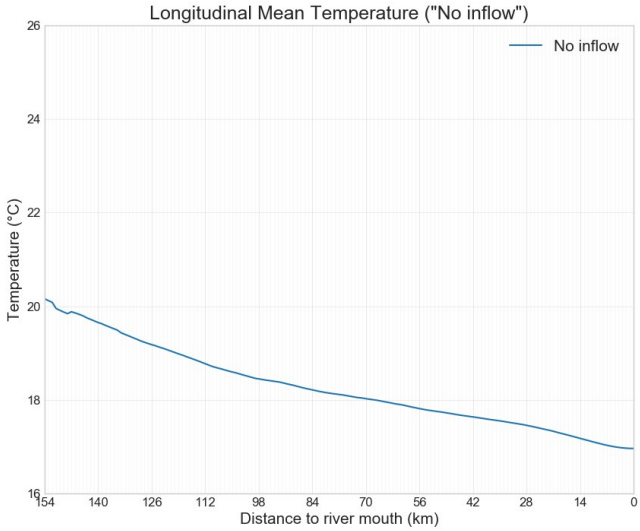

Figure 4.3. Longitudinal variations of water temperatures for baseline '*no inflow*' scenario with no power plants in conceptual river model.

4.3.2. Single power plant

In our single power plant scenarios, a temperature increase was observed immediately when thermal effluent was introduced to the river, followed by a gradual decline in temperature towards the river mouth (Fig. 4.4). The river temperature rise occurred both spatially and temporally in response to the increase in the discharge and/or temperature of effluent, leading to the highest T_{week_PP1} of 23.1 °C and the greatest M_{7d} of 1.8 °C in the largest heat input scenario (i.e. 20% discharge at 35 °C). In order to determine the relative

importance of effluent discharge and temperature in thermal impact, temperature increases from the smallest heat input scenario (i.e. 2% discharge at 25 °C) to highest discharge and temperature (i.e. 20% and 35 °C) scenarios were compared. The result showed that effluent discharge (i.e. mass) contributed to greater increases than temperature (i.e. energy) in both T_{week_PP1} and M_{7d}. From a general perspective, the differences in T_{week_PP1} between scenarios were larger immediately at the power plant outfall but progressively minimised as the flow approached the mouth. It was also noteworthy that in the scenario with the smallest heat input, T_{week_mouth} still did not return to the same temperature as the baseline, remaining 0.03 °C higher than the baseline 'no inflow' scenario.

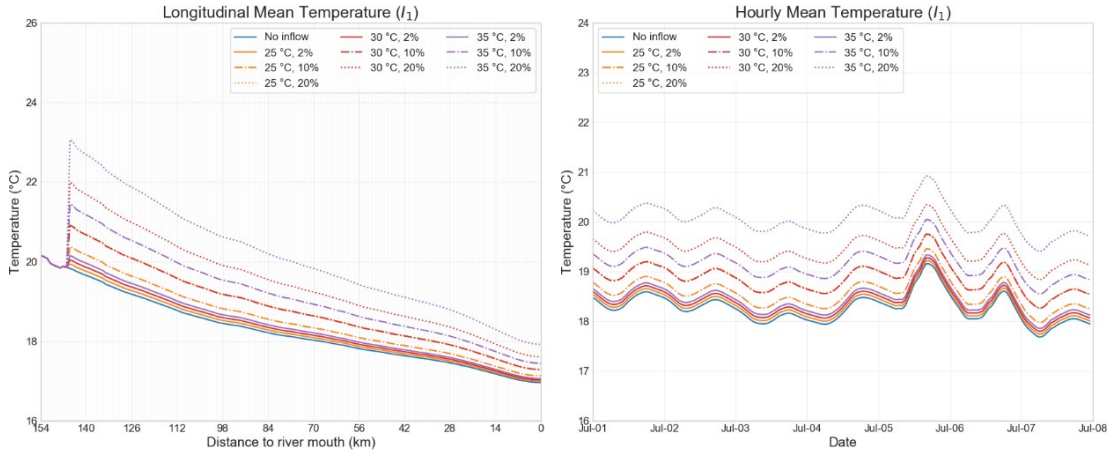

Figure 4.4. Longitudinal and hourly variations of water temperatures for single power plant scenarios in conceptual river model.

4.3.3. Two power plants

4.3.3.1 Same effluent discharge and temperature

By introducing a second power plant with the same discharge and temperature of effluent downstream of the initial (primary) power plant, the river temperature trend was interrupted by a second peak from which the thermal effluent-driven temperature increase (relative to the baseline model) was further extended (Fig. 4.5). However, whether this second peak (T_{week_PP2}) exceeds the first peak (T_{week_PP1}) is determined by the discharge and temperature of thermal effluent from the two power plants. In scenarios of lower discharges (2%), T_{week_PP2}

were all lower than T_{week_PP1}, with a smallest difference of 0.3 °C, whereas in scenarios of higher discharges (10% & 20%), T_{week_PP2} exceeded T_{week_PP1} only when effluent temperatures were rather high (30 °C & 35 °C). Furthermore, the temperature rise relative to the baseline scenario (ΔT_{week}) at T_{week_PP2} was larger than that at T_{week_PP1} across all scenarios (by 0.1–2.2 °C). The scenario of the largest thermal disturbances that was associated with the nearest distance between power plants and the highest heat inputs (15 km, 20% discharge at 35 °C) reached a maximum of 24.7 °C in longitudinal temperature. In contrast, the scenario of the smallest thermal disturbances had the furthest two power plants with the lowest heat inputs (40 km, 2% discharge at 25 °C), reaching a maximum temperature of 18.8 °C.

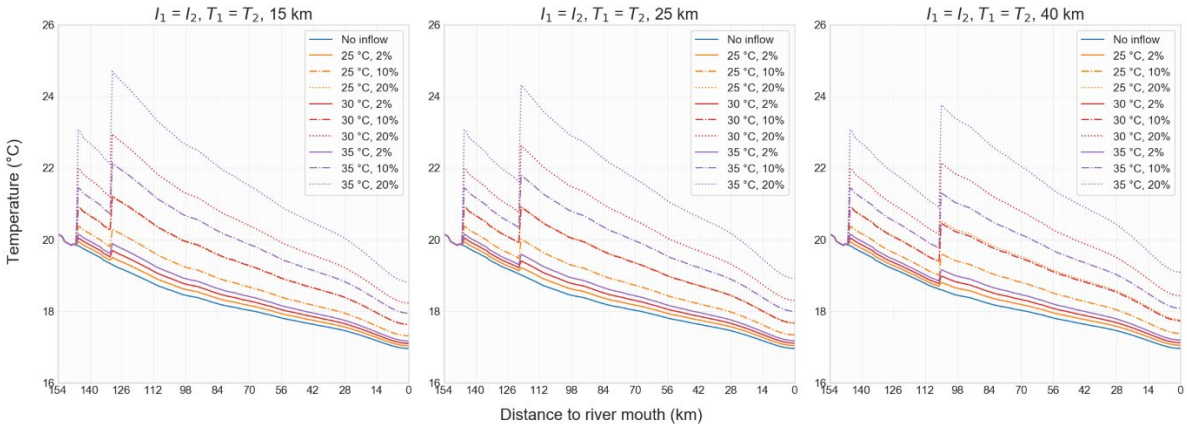

Figure 4.5. Longitudinal variations of water temperatures for scenarios of two same thermal effluents from power plants in conceptual river model.

4.3.3.2 Different effluent discharges or temperatures

If the discharge or temperature of effluent from two power plants differed (as opposed to being the same as in section *4.3.3.1*), the resulting river temperature exhibited more complex responses. When the upstream power plant had higher effluent discharge or temperature than the downstream power plant (Fig. 4.6), the majority of scenarios showed consistently lower T_{week_PP2} than T_{week_PP1} (as might be expected). Exceptions occurred in scenarios with relatively large heat inputs in close proximity (the 20%/10% discharge at 30 °C or 35 °C & the 20% or the 10% discharge at 35 °C/30 °C, 15 km apart), which only showed a lower T_{week_PP2} as a function of increasing distance between the

upstream and downstream power plants. The smallest heat input (i.e. thermal effluent of 2% discharge or 25 °C) had limited impact compared to other scenarios, extending the impacted reach (where ΔT_{week} > 0) at least 3 km downstream (the 10%/2% discharge at 25 °C & the 2% discharge at 30 °C/25 °C, 15 km apart). Conversely, when the downstream power plant had higher effluent temperature or discharge than the upstream power plant (Fig. 4.7), most scenarios exhibited a lower maximum longitudinal temperature, except for the scenarios of two plants with higher discharges and temperatures in close proximity (e.g. the 10%/20% discharge at 30 °C or 35 °C & the 20% discharge at 30 °C/35 °C, 15 km apart) which showed increased maximum temperatures.

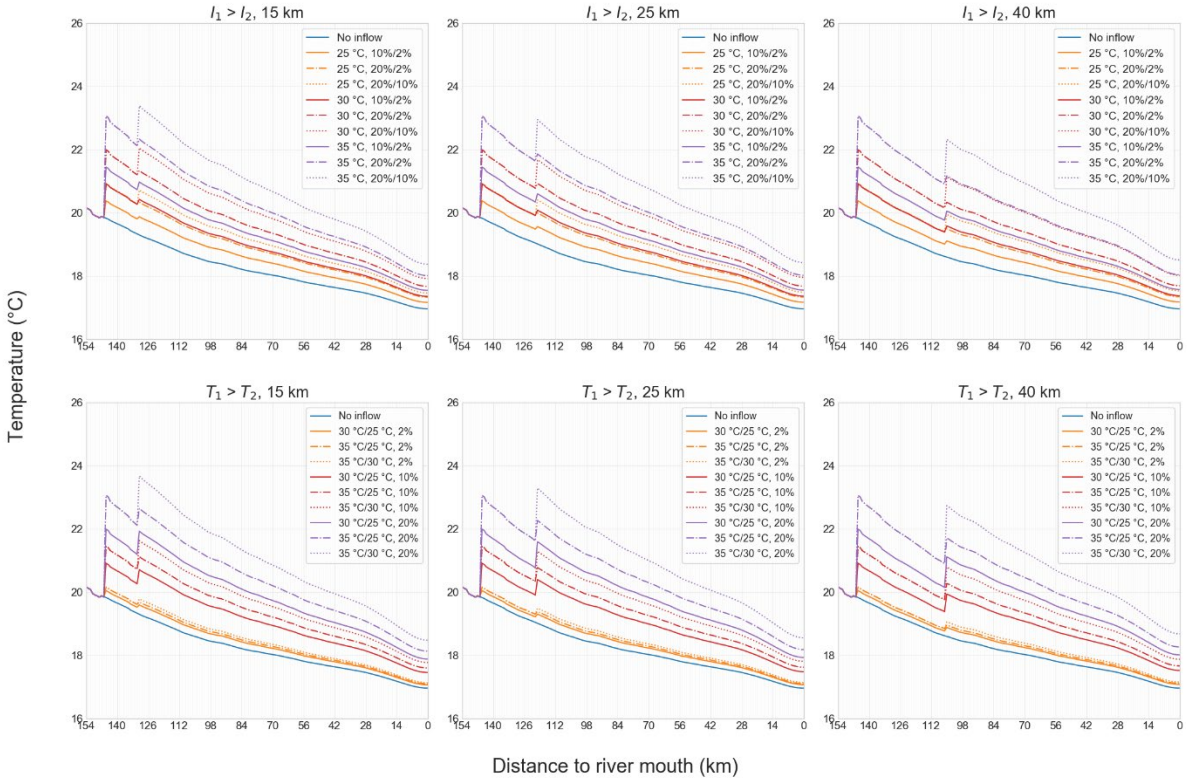

Figure 4.6. Longitudinal variations of water temperatures for scenarios of the upstream effluent with higher discharge (*top*) or temperature (*bottom*) in conceptual river model.

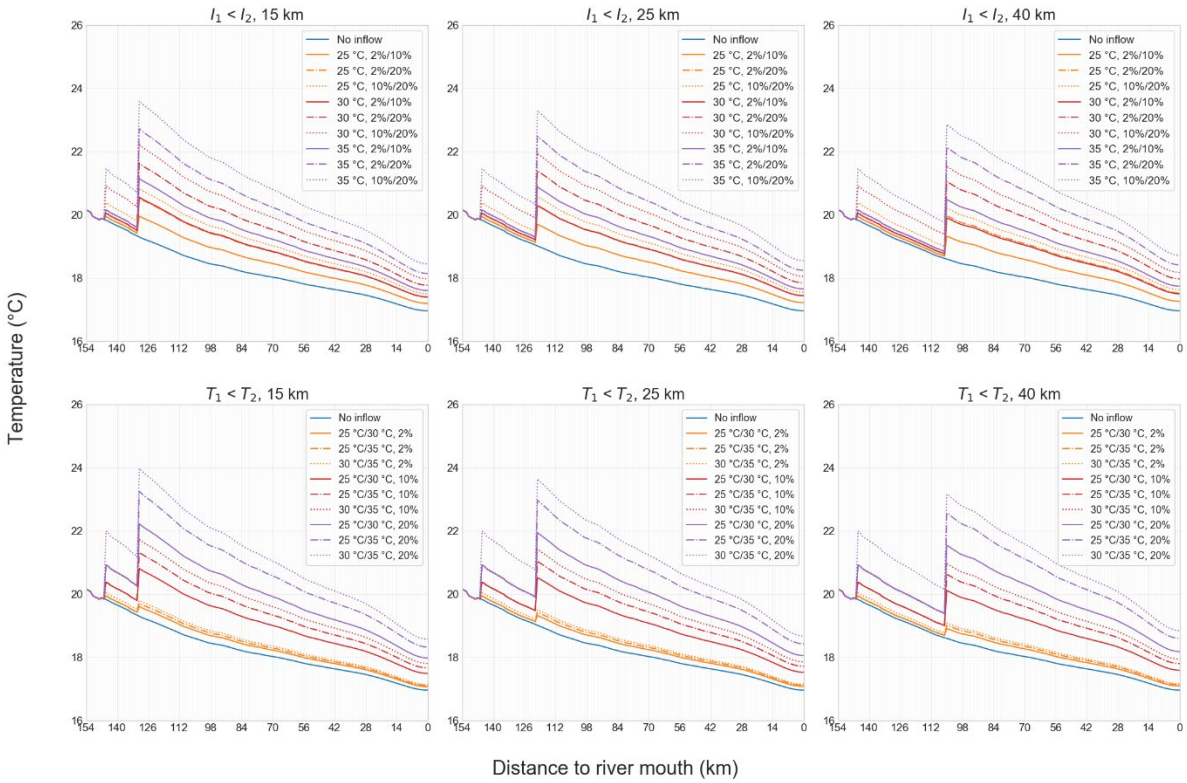

Figure 4.7. Longitudinal variations of water temperatures for the scenarios of the upstream effluent with lower discharge (*top*) or temperature (*bottom*) in conceptual river model.

4.3.3.3. The effects of increasing spacing distance on thermal impacts

In scenarios of two power plants, the increase in the distance between power plants exerted a consistent attenuating effect on temperature increase in terms of the longitudinal maximum. However, it had dissimilar impacts on the T_{week_PP2}, T_{week_mouth} and M_{7d} metrics, which were dictated primarily by the effluent discharge and temperature (Table 4.6 & Fig. 4.8). The two longitudinal temperature metrics, T_{week_PP2} and T_{week_mouth} showed completely opposite responses to the increased distance. T_{week_PP2} decreased across all scenarios as the distance between power plants increased, and the decrease was more pronounced in scenarios with higher effluent discharge (I_1) or temperature (T_1) at the upstream site (Table 4.6 & Fig. 4.8a). In contrast, T_{week_mouth} rose as the distance between power plants increased, which was enhanced when the discharge (I_2) or temperature (T_2) of downstream effluent was increased (Table 4.6 & Fig. 4.8b).

For hourly temperatures, the changes of M_{7d} in response to the increased distance between power plants were slightly more complicated (Table 4.6 & Fig. 4.8c). When the effluent temperature was relatively high at the downstream site (30 °C & 35 °C), the attenuation, namely the decrease in M_{7d} as a function of increased distance, was observed across all scenarios and was more effective for those scenarios with higher effluent discharge or temperature at the up- or downstream sites. On the contrary, the increased distance led to a higher M_{7d} when the downstream effluent was at the lowest temperature (25 °C). These rises in M_{7d} were further enhanced by increased effluent discharge or temperature at the upstream site.

Table 4.6. Summarised impacts of increasing effluent discharges (I) or temperatures (T) on the attenuation (-) or exacerbation (+) of thermal pollution by increasing distance between power plants. The attenuating or exacerbating effect on T_{week_PP2}, T_{week_mouth}, and M_{7d} when the downstream effluent temperature is low (T_2L) or high (T_2H) can be enhanced (---/+++), reduced (--/++) or unaffected (-/+) by increased heat inputs.

Effluent parameter	I_1	T_1	I_2	T_2
T_{week_PP2}	---	---	--	-
T_{week_mouth}	+	+	+++	+++
$M_{7d}\_T_2L$	+++	+++	---/+++	Null
$M_{7d}\_T_2H$	---	---	---	---

a)

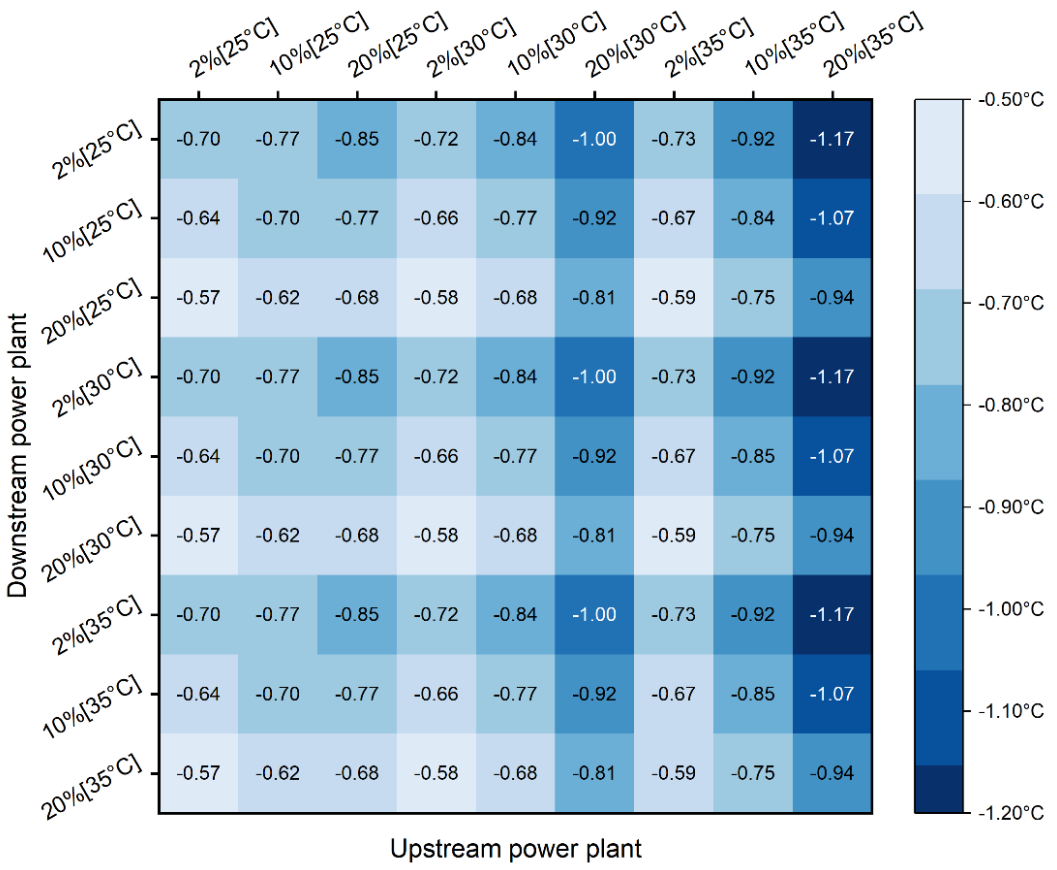
2%[25°C]
10%[25°C]
20%[25°C]
2%[30°C]
10%[30°C]
20%[30°C]
2%[35°C]
10%[35°C]
20%[35°C]
Downstream power plant
-0.70 -0.77 -0.85 -0.72 -0.84 -1.00 -0.73 -0.92 -1.17
-0.64 -0.70 -0.77 -0.66 -0.77 -0.92 -0.67 -0.84 -1.07
-0.57 -0.62 -0.68 -0.58 -0.68 -0.81 -0.59 -0.75 -0.94
-0.70 -0.77 -0.85 -0.72 -0.84 -1.00 -0.73 -0.92 -1.17
-0.64 -0.70 -0.77 -0.66 -0.77 -0.92 -0.67 -0.85 -1.07
-0.57 -0.62 -0.68 -0.58 -0.68 -0.81 -0.59 -0.75 -0.94
-0.70 -0.77 -0.85 -0.72 -0.84 -1.00 -0.73 -0.92 -1.17
-0.64 -0.70 -0.77 -0.66 -0.77 -0.92 -0.67 -0.85 -1.07
-0.57 -0.62 -0.68 -0.58 -0.68 -0.81 -0.59 -0.75 -0.94
-0.50°C
-0.60°C
-0.70°C
-0.80°C
-0.90°C
-1.00°C
-1.10°C
-1.20°C
Upstream power plant

b)

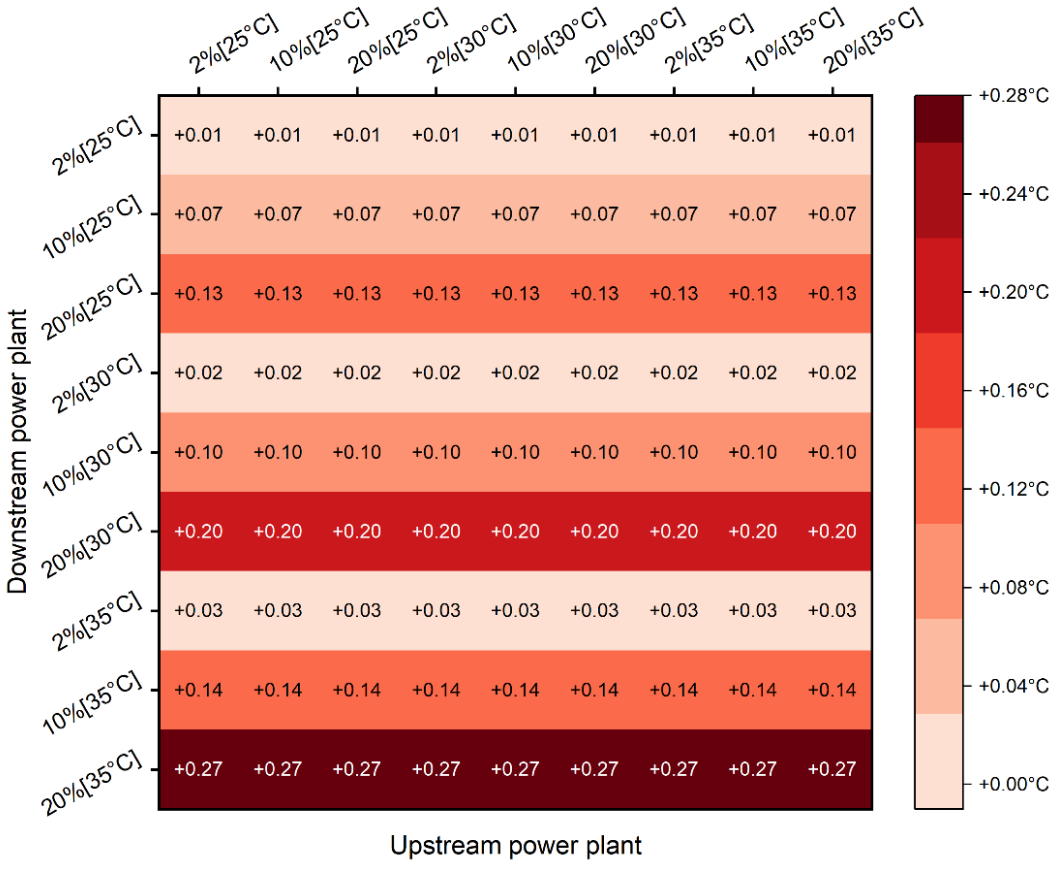
2%[25°C]
10%[25°C]
20%[25°C]
2%[30°C]
10%[30°C]
20%[30°C]
2%[35°C]
10%[35°C]
20%[35°C]
Downstream power plant
+0.01 +0.01 +0.01 +0.01 +0.01 +0.01 +0.01 +0.01 +0.01
+0.07 +0.07 +0.07 +0.07 +0.07 +0.07 +0.07 +0.07 +0.07
+0.13 +0.13 +0.13 +0.13 +0.13 +0.13 +0.13 +0.13 +0.13
+0.02 +0.02 +0.02 +0.02 +0.02 +0.02 +0.02 +0.02 +0.02
+0.10 +0.10 +0.10 +0.10 +0.10 +0.10 +0.10 +0.10 +0.10
+0.20 +0.20 +0.20 +0.20 +0.20 +0.20 +0.20 +0.20 +0.20
+0.03 +0.03 +0.03 +0.03 +0.03 +0.03 +0.03 +0.03 +0.03
+0.14 +0.14 +0.14 +0.14 +0.14 +0.14 +0.14 +0.14 +0.14
+0.27 +0.27 +0.27 +0.27 +0.27 +0.27 +0.27 +0.27 +0.27
+0.28°C
+0.24°C
+0.20°C
+0.16°C
+0.12°C
+0.08°C
+0.04°C
+0.00°C
Upstream power plant

c)

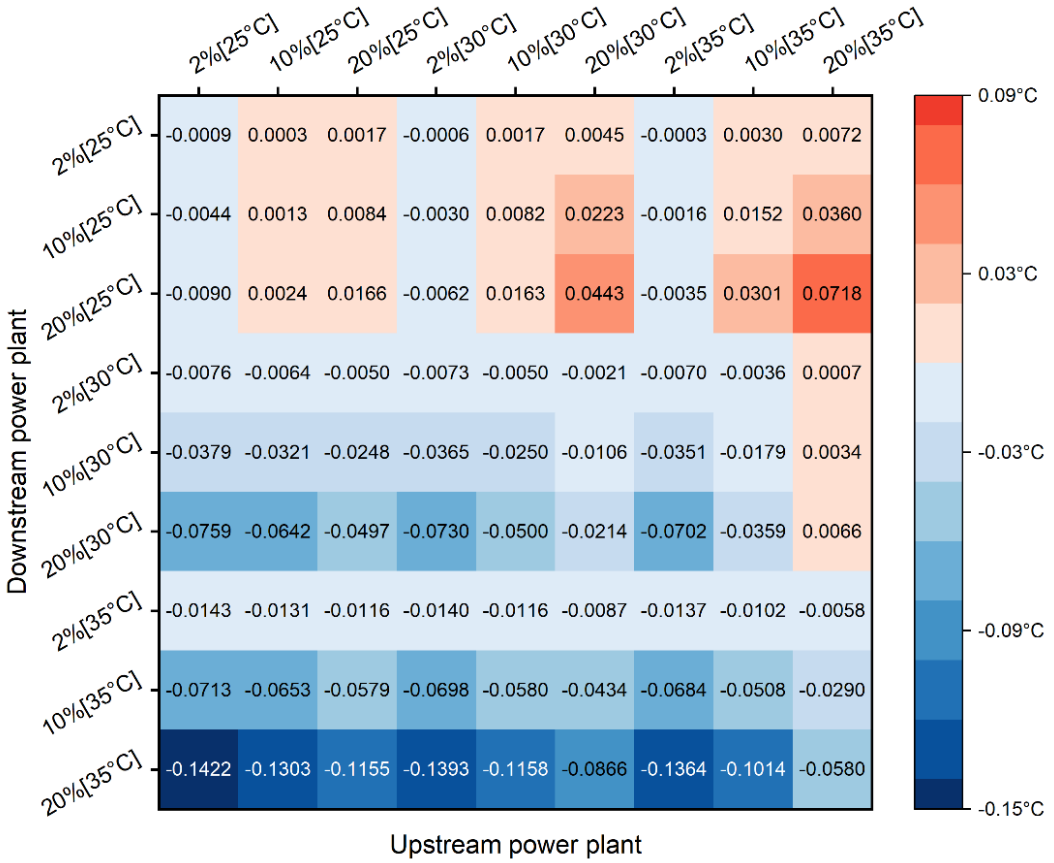

Figure 4.8. Temperature changes in a) T_{week_PP2}, b) T_{week_mouth} and c) M_{7d} as a result of the distance between two power plants increasing from 15 km to 40 km for different combinations of effluent discharge and temperature.

4.3.4. Thermopeaking scenarios

In the thermopeaking scenarios, the power plant from the single power plant scenarios operated as a peaking power plant during the busiest time of day in the UK (i.e. 8 am–12 am). The development and interaction of daily thermal effluents from the power plant and the resulting change in river temperature over the course of a week (i.e. the model runtime) were examined simultaneously from spatial and temporal perspectives (Figs. 4.9–4.11). Despite differences in the effluent discharge and temperature, all thermopeaking scenarios exhibited a similar pattern but different extents of thermal impact. Thermal impacts resulting from single-day operation persisted in the following days, and thus accumulated and extended downstream towards the mouth. When effluent discharge was low (2%), river temperatures never

exceeded 20 °C and the maximum temperature increase was only 0.4 °C. By contrast, river temperatures reached up to 23.1 °C with a maximum temperature increase of 3.7 °C in the scenario of largest heat input (20% discharge at 35 °C). In this extreme scenario, temperature increments exceeding 1.5 °C were only associated with separate single-day operations and observed in the next day at 90 km to the mouth, while temperature increments of 1–1.5 °C were noticed between the intervals of two single-day operations from 120–50 km to the mouth. Increments of over 0.5 °C were detectable throughout the length and period of the model, indicating a minimum increase of 0.5 °C in the modelled river if the power plant continued to operate on same schedule.

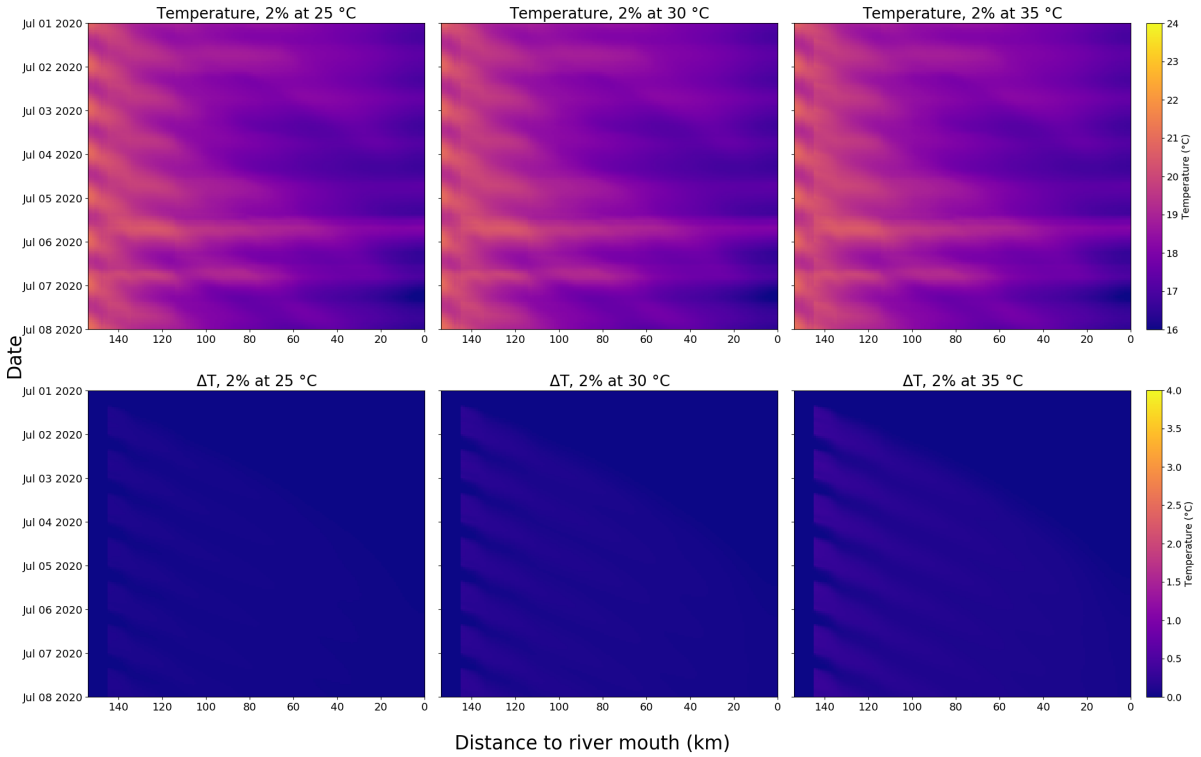

Figure 4.9. Temperatures and temperature increments as a result of the 2% discharge from a peaking power plant.

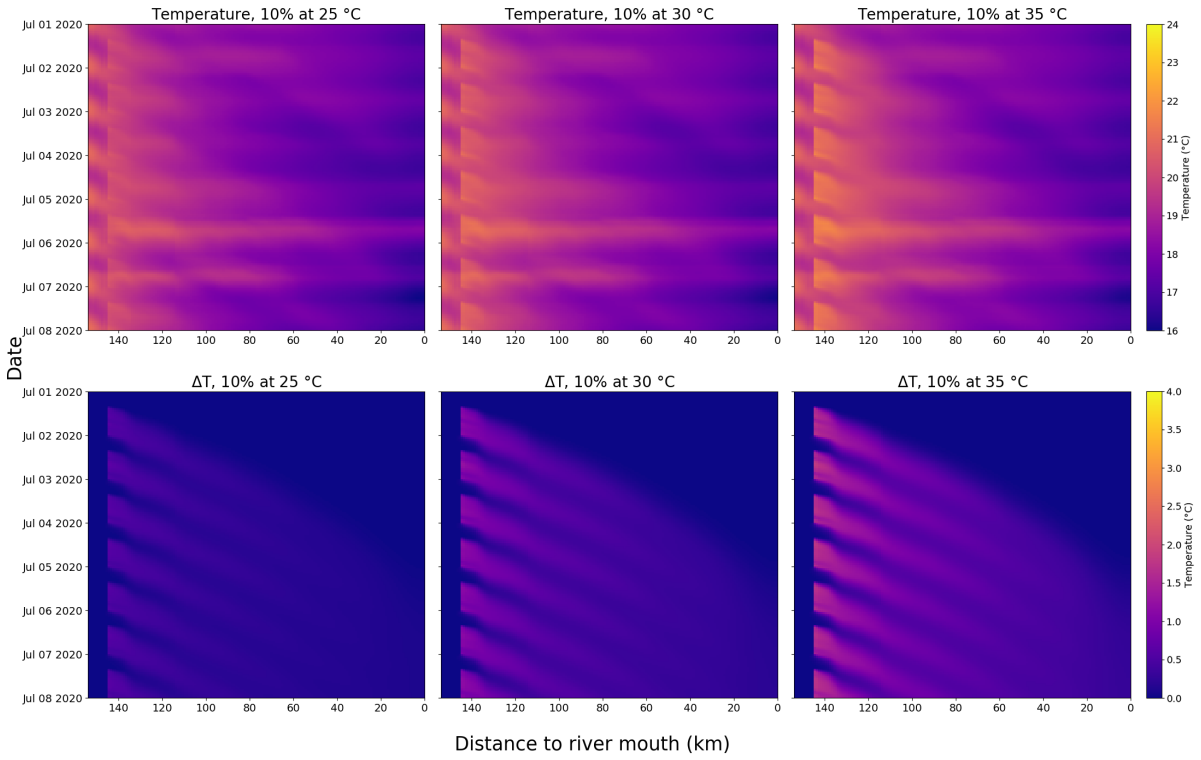

Figure 4.10. Temperatures and temperature increments as a result of the 10% discharge from a peaking power plant.

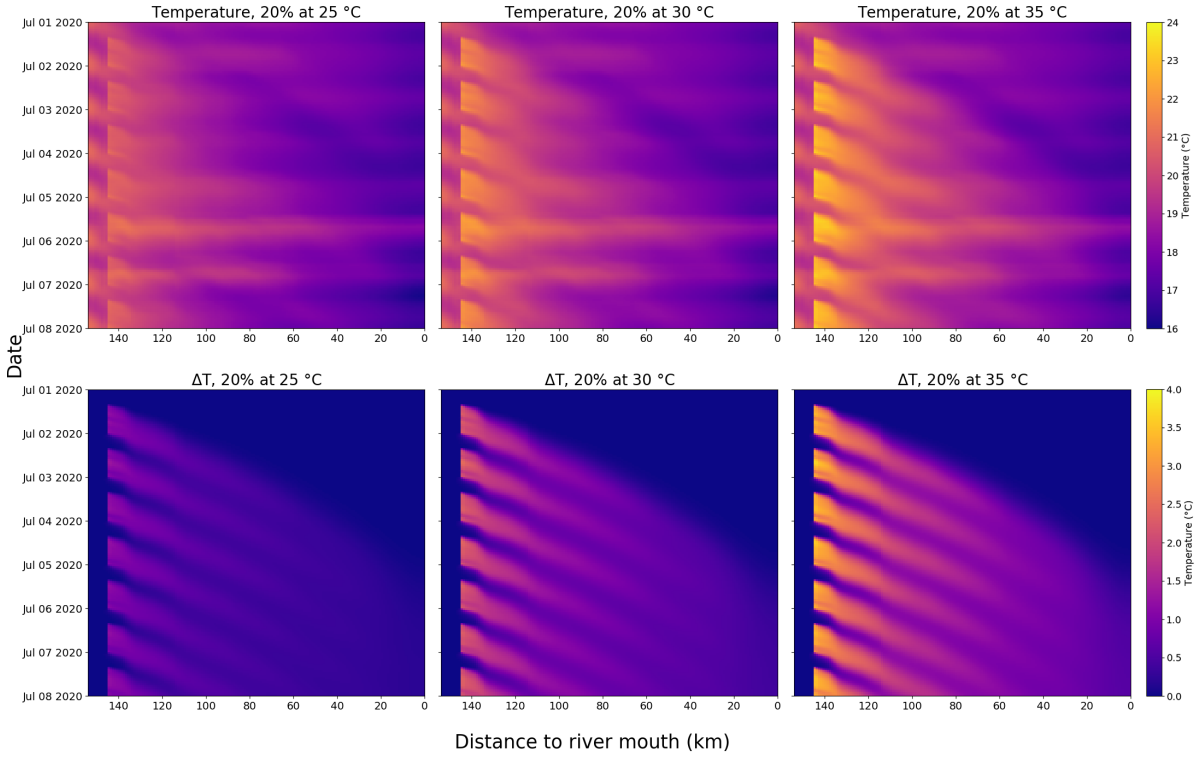

Figure 4.11. Temperatures and temperature increments as a result of the 20% discharge from a peaking power plant.

4.3.5. Climate change scenarios

The 'two power plants' scenarios of the smallest (SD2; 2% discharge at 25 °C, 40 km apart) and the largest thermal disturbances (LD2; 20% discharge at 35 °C, 15 km apart) were selected to explore how thermal pollution from multiple power plants on the same river can be further exacerbated by climate change (see section *4.3.3.1*). For both scenarios, temperature increments resulting from power plant effluents were, unsurprisingly, larger if a more severe climate scenario was applied, and further increased as the flow propagated downstream (Fig. 4.12). Despite the contrasting temperatures and temperature increments in the SD2 and LD2 scenarios, ΔT_{week_PP1}, ΔT_{week_mouth} and M_{7d} showed consistent additional increases as a result of the same climate scenarios (Table 4.7). The additional increase in ΔT_{week_PP2} was not considered due to different locations of the downstream power plant on the river (134 km vs. 109 km).

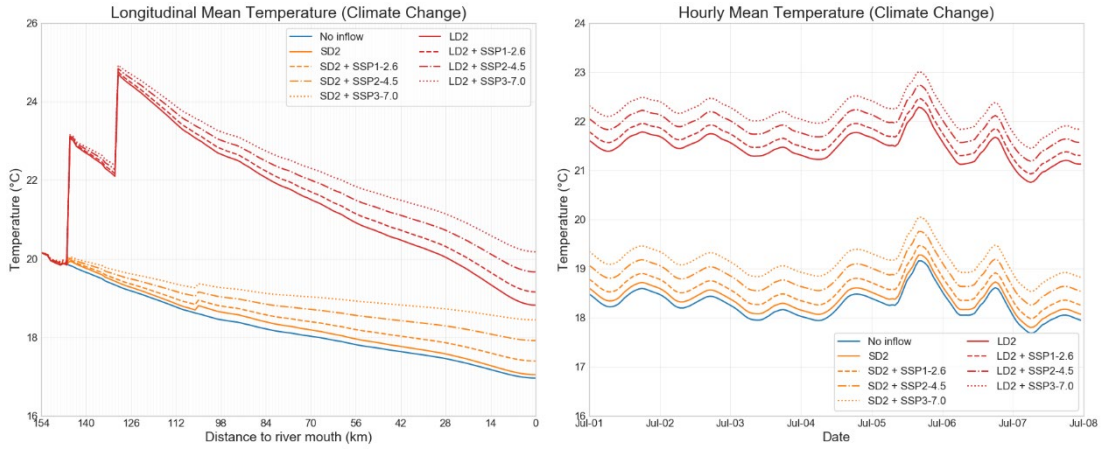

Figure 4.12. Longitudinal and hourly variations of water temperatures for the 'two power plants' scenarios with the smallest (*SD2*) and the largest thermal disturbances (*LD2*) and their combinations with climate scenarios in the modelled river.

Table 4.7. Weekly mean temperatures and temperature increments relative to the baseline 'no inflow' scenario at the first (T_{week_PP1} & ΔT_{week_PP1}) and the second power plant (T_{week_PP2} & ΔT_{week_PP2}) and the mouth of the river (T_{week_mouth} & ΔT_{week_mouth}) as well as the 7-day average increments of hourly mean temperatures of the modelled river (M_{7d}) for the 'two power plants' scenarios with the smallest (*SD2*) and the largest thermal disturbances (*LD2*)

and their combinations with the IPCC climate scenarios.

Scenario	T_{week_PP1}	ΔT_{week_PP1}	T_{week_PP2}	ΔT_{week_PP2}	T_{week_mouth}	ΔT_{week_mouth}	M_{7d}
SD2	19.94	0.11	18.80	0.21	17.05	0.09	0.12
SD2 + SSP1-2.6	19.96	0.14	18.94	0.35	17.39	0.43	0.31
SD2 + SSP2-4.5	20.01	0.18	19.15	0.55	17.92	0.95	0.60
SD2 + SSP3-7.0	20.05	0.22	19.36	0.77	18.44	1.48	0.88
LD2	23.06	3.24	24.70	5.40	18.82	1.86	3.20
LD2 + SSP1-2.6	23.09	3.26	24.76	5.46	19.15	2.19	3.38
LD2 + SSP2-4.5	23.12	3.29	24.84	5.54	19.66	2.70	3.65
LD2 + SSP3-7.0	23.16	3.33	24.93	5.63	20.18	3.21	3.92

4.4. Discussion

4.4.1. Establishing a semi-conceptual model for river temperature simulation

In this study, we created a conceptual river model by using the River Trent as a template for implementation of the process-based Heat Source model. Process-based models are a preferred approach in predicting river temperature as they calculate energy fluxes and determine the temperature change on the basis of our pre-existing understanding of relevant physical processes and their interactions (MacDonald et al., 2014; van Vliet et al., 2016; Dugdale et al., 2017). Because of the inherent complexity, these models usually require substantial long-term data for model calibration and validation to provide accurate estimations. However, in-situ measured water temperature data are scarce and rarely available (particularly in certain jurisdictions such as England), often of low spatial and temporal resolution, and can be highly influenced by climate change and anthropogenic interventions (Caissie, 2006; Webb et al., 2007; Watts et al., 2015; Klaar et al., 2020). Instead of pursuing accurate estimations, we therefore ran Heat Source with a water temperature time-series including the major diurnal and seasonal variations generated by using a stochastic approach.

Importantly, it was not our goal to forecast future water temperatures of a specific river, but instead to use the model as a base template to examine how river temperature changes in response to thermal effluents from power plants via comparison of different scenarios. Similar applications of process-based models can be found in recent studies of predicting river temperature change in response to climate or land-use change scenarios, particularly those regarding the effects of riparian vegetation shading (Trimmel et al., 2018; Dugdale et al., 2019; Dugdale et al., 2020; Spanjer et al., 2022). In addition, it was noteworthy that our model was not calibrated to any site-specific data but directly implemented with a combination of stochastically acquired and short-term data. The benefit of this approach is that the outputs are more generalisable between rivers and therefore widely applicable to similar-sized rivers, globally.

4.4.2. Comparing the relative importance of effluent discharge vs. temperature in thermal pollution

In our single power plant scenarios, we explored the relative importance of effluent discharge and temperature in thermal pollution by comparing the temperature increase to the scenario of smallest heat input (2% discharge at 25 °C) in T_{week_PP1} and M_{7d} due to typical increases (to 20% and 35 °C) of the two intrinsically incomparable variables. The result suggests a greater importance on the effluent discharge than the temperature. This can be confirmed with the calculation of gained heat using the formula for specific heat capacity, showing approximately 4.65 times higher thermal energy increase by increasing the effluent discharge to 20% than by increasing the temperature to 35 °C (detailed calculation process in section *4.6*). In that case, the effluent discharge should be prioritised over the temperature in the management and regulation of power plant discharge. However, current studies and regulations on thermal effluents are primarily focused on the temperature (e.g. 35 °C at Keadby 1 & 2 Power Station, UK; 28 °C in EU Freshwater Fish Directive 2006/44/EC) rather than the discharge that accounts for the amount of the impact (European Community, 2006; Förster & Lilliestam, 2010; van Vliet et al., 2012; Madden et al., 2013; AECOM, 2021). The overlooked importance of

effluent discharge could cause fairly large thermal impacts at temperatures lower than those listed in regulatory guidance (e.g. the 20% discharge at 25 °C). These impacts are most likely to occur from small capacity power plants using once-through cooling (OTC) systems in upper river reaches that return a large but cooler discharge of thermal effluent to a relatively small stream or river. Hence, future research and policy decisions should take into account not only the effluent temperature but the discharge as well.

4.4.3. Exploring the propagation and interaction of power plant impacts along the river

As it is our aim to discover how far thermal effluents remain distinct and interact along the river, we examined the spatial patterns of water temperature change in response to the impacts of an individual power plant and multiple power plants. When there was only one power plant discharging effluent at the upstream site, it was noted that the differences in river temperature between scenarios were larger immediately at the power plant outfall but gradually reduced as the flow propagated downstream. As the thermal effluent just entered the river, the water temperature was raised higher by a larger heat input than a smaller input. Meanwhile, a higher water temperature led to a greater temperature gradient, promoting the heat dissipation via latent, sensible and longwave fluxes and thereby accelerating the decrease in water temperature downstream towards equilibrium with air temperature, heat losses and thus temperature differences between scenarios. This calls for an optimised plan for power generation in upstream areas so as to ensure adequate cooling for power plant operations, allowing river temperatures to drop to ambient in order to accommodate a second power plant downstream. High water temperatures associated with an excessively large heat input could easily overwhelm heat dissipation and persist further along the river, potentially extending the spatial ‘window’ of thermally stressful temperatures for sensitive biota (Gaudard et al., 2018), and reducing thermal efficiency in the downstream OTC-based power plant (Miara et al., 2018; Johnson et al., 2019). In contrast, only small temperature increases versus the baseline scenario were observed in the scenario with the smallest heat input, but these nevertheless did not drop to

zero at the end of the modelled reach. This is consistent with a previous study by Stewart et al. (2013) who found that minor thermal impacts from power plants can propagate considerable distances downstream as a result of the slower heat dissipation in summer. The small but persistent thermal impact over a long distance raises the concern of possible cumulative effects resulting from a range of additional thermal stressors, such as impoundments, deforestation, urban runoff, and domestic sewage.

When a second power plant producing the same heat input was introduced in the downstream, the river temperature was higher at the downstream plant (T_{week_PP2}) than at the upstream plant (T_{week_PP1}) as long as the heat inputs at the downstream plant were high enough to counteract heat losses between the two power plants. These power plant pairs showcase the importance of careful design for each individual power plant as the thermal impacts can be further aggravated by the same large heat input from the downstream power plant. On the other hand, the temperature rise relative to the baseline scenario (ΔT_{week}) was consistently higher at the downstream power plant. After the heat dissipation between two power plants, the remaining energy advected from the effluent of upstream power plant in combination with the heat input from the downstream power plant results in a larger ΔT_{week}, showing a cumulative 'relay' effect. This cumulative effect could be particularly problematic in rivers densely populated by thermoelectric power plants with large heat inputs (e.g. the Rhône in France, Gosse & Samie, 2020; the Tennessee and the Missouri in the USA, Miara et al., 2018). Furthermore, the remaining energy from the first power plant also raises the intake temperature of the condenser at the downstream power plant, which potentially results in a lower thermal efficiency. Consequently, a greater amount of cooling water will be abstracted to maintain optimal thermal efficiency of the downstream power plant and subsequently returned to the river. Given the relative importance of effluent discharge over temperature, the increased discharge is expected to impose amplified impacts on the downstream thermal regime.

These findings were consistent with earlier research by Miara et al. (2018) who investigated the impacts of thermal pollution on power supply at 128 OTC-based plants in the Mississippi River watershed using the coupled Water

Balance Model and Thermoelectric Power and Thermal Pollution Model (WBM-TP2M). By comparing the scenarios with and without power plant interactions along rivers in summer, they noted that the thermal effluents from 31–100 upstream power plants caused increased intake temperatures and reduced power outputs at 22–98 downstream plants between 1995–2015, and a total of 1076 such thermal interferences occurred between 1995–2005. In addition, owing to the highest thermal effluent to river discharge ratio (i.e. *I*/*Q*) and the power plant density, the Ohio-Tennessee basin had the longest thermally impacted reaches in which the temperature increments between 1–3 °C and exceeding 3 °C were 1641 km and 350 km, respectively. These results complement our study and jointly show that power plant effluent results in thermal impacts that propagate over long distances and interacts with downstream effluents to cause cumulative impacts that influence further downstream as a function of the effluent discharge and the number of power plants along the river.

4.4.4. Finding the optimal arrangement of multiple power plants along the same river

By using dissimilar heat inputs from the two power plants, we investigated how the location of power plant with larger input governed the thermal impacts. The longitudinal water temperature was highest at both up- and downstream power plants when the greater heat input (larger discharge at 30 °C or 35 °C / higher temperature for the 10% or 20% discharge) was located in the upstream, while the longitudinal water temperature at the downstream plant was much higher than at the upstream plant when the greater heat input was at the downstream site. Also, the maximum longitudinal temperature decreased when the larger heat input was at the downstream site though exceptions occurred when the two heat inputs were fairly large and close. The thermal impact from power plants inherently diminishes in a downstream direction due to heat dissipation from latent, sensible and longwave fluxes. This effect, however, is limited where there is insufficient distance for substantial heat dissipation to occur. When the larger heat input was located at the upstream site, the distance between power plants was insufficient for effective heat dissipation. In contrast, the heat

dissipation effect was maximised by positioning the larger heat input at the downstream site, which provided sufficient distance for evaporative cooling between power plants and took advantage of the greater cooling capacity in the downstream owing to the increased surface area. Hence, when implementing power plants in pairs (or more), it is preferable that the power plant(s) that creates the largest heat input (i.e. generally those with highest generation capacity) is in downstream locations, thus minimising thermal impacts in comparison to if it were located in upstream reaches. This is also in line with the real-world spatial configuration in which large-capacity power plants are mostly located near the river mouths for an ample supply of cooling water (Kenny et al., 2009). Furthermore, even when considering power plants with relatively small heat inputs, it is still critical to pay greater attention to regions with high densities of small power plants as these plants are expected to result in similar cumulative impacts to those by multiple or cascade small run-of-river hydropower plants (Kuriqi et al., 2021).

Given the attenuating effect of increasing the distance between power plants on the temperature increase in terms of longitudinal maximum, we explored the effect from other perspectives by using T_{week_PP2}, T_{week_mouth} and M_{7d} metrics. The increased distance resulted in a decline in T_{week_PP2} across all scenarios, which was more effective when the larger heat input (i.e. higher discharge or temperature) was at the upstream site. As the downstream power plant was moved further downstream, more thermal energy was dissipated via evaporative cooling due to the increased the surface area, thereby lowering the temperature increase caused by heated effluent. The heat dissipation from latent, sensible and longwave fluxes was also facilitated by the increased distance and thus particularly predominant for a larger heat input in the upstream. On the contrary, T_{week_mouth} was elevated by the increased distance, and this effect was more evident in scenarios when the larger heat input was downstream. As the distance between the power plants increased, the downstream power plant moved closer to the river mouth, shortening the distance for downstream heat dissipation and raising the T_{week_mouth}. In addition, the effect of heat dissipation was further undermined by a greater heat input from the downstream power plant, leading to a higher temperature increase that could be associated with severe environmental damage to the downstream

reach of the plant (Stewart et al., 2013). The two opposite effects of the increased distance deliver an important message to policy-makers that when evaluating the thermal impacts associated with multiple power plants, it is crucial to not only consider the relative position between power plants, but also pay attention to the position of power plants along the river.

In contrast to the other metrics, M_{7d}, as a summative metric for the overall impact in both space and time, showed two opposite responses to the increased distance between power plants, depending on the effluent temperature at the downstream site. The increased distance lowered M_{7d} when the temperature of downstream effluent was relatively high but raised M_{7d} when the downstream effluent was at the lowest temperature. When the larger heat input was at the downstream site, the decrease in M_{7d} was further facilitated by the increased distance because of the increasingly effective heat dissipation between power plants for a smaller heat input in the upstream as well as the shortened downstream section that experienced more severe thermal impacts from the downstream plant. However, when the smaller heat input (at a lower temperature in particular) was at the downstream site, M_{7d} was predominantly determined by the larger heat input in the upstream. Given that the water temperature raised by the larger heat input in the upstream gradually decreases downstream, the smaller input makes more impact in the lower reach than in the upper reach. In that case, it is expected that the thermal impact of power plant effluents can be largely alleviated at larger scales (e.g. catchment) by optimising the distance between power plants for heat dissipation, especially considering the real-world spatial configuration (i.e. large-capacity power plants in the downstream).

Stewart et al. (2013) explored the ecosystem services provided by river networks (described as ‘horizontal cooling towers’) which transport and dissipate waste heat from thermoelectric power plants along the river. By using a spatially distributed hydrology and water temperature model coupled with the TP2M, they calculated and compared the percentage of heat attenuated by the two services across eight river basins. The result was somewhat consistent with our findings that upstream placement of OTC-based power plants with large heat inputs fully utilised the long flow paths for greater heat attenuation but

increased the impacted distance, while downstream placement of the plants led to smaller impact on rivers but greater impact to coastal areas. Our study extends their findings by also investigating how the distance between power plants affects the cumulative impact of multiple power plants. Despite these useful initial investigations, there remains considerable uncertainty regarding the interaction of thermal effluent discharge and climate change impacts on rivers. It is therefore highly recommended that future research uses process-based models to simulate the water temperature change in response to effluents from multiple power plants in order to improve our understanding of multi-plant impact on river thermal regime for better controlling and reducing the thermal pollution.

4.4.5. Inspecting the effects of operation mode and climate change on power plant impacts

In thermopeaking scenarios, the operation of peaking power plant was replicated by adding periodic variability to the power generation regime. By visualising river temperatures across space and time (Figs. 4.9–4.11), we highlight the persistent thermal impact of single-day operation as well as the accumulated impacts of powerplant operation on two or more adjacent days, particularly in scenarios comprising larger heat input (i.e. higher discharge or temperature). Although the largest temperature increases were primarily associated with individual single-day operations, smaller increases were partly attributed to cumulative impacts that extended the period and distance over which the power plant acted. In the scenario of largest heat input, the minimum temperature increase is equivalent to the impact of 11- to 17-year global warming (based on estimated warming rates between 1980–2009 in Isaak et al., 2012). The interactions and the resulting cumulative impacts put an emphasis on the local power management which should consider the frequency of operation in case temperature limits are exceeded, leading to curtailed power generation or power plant shutdown (e.g. the Clean Water Act section 316a). Apart from water temperature increase, intermittent operations can also cause additional short-term temperature fluctuations (i.e. thermopeaking) and entail severe ecological implications, particularly on aquatic ectotherms (Kern et al.,

2015; Salinas et al., 2019; Verheyen & Stoks, 2019). Recent research indicated that the temperature fluctuations due to intermittent releases from hydropower plants promoted the drift and stranding of both fishes and invertebrates (Auer et al., 2022; Tonolla et al., 2022). Despite its ecological importance, research into powerplant-driven thermopeaking impacts is still rather scarce (Moreira et al., 2019; Reid et al., 2022). We therefore call for further rigorous monitoring and experimentation relating to thermopeaking from power plants in order to fill this pressing knowledge gap.

By applying the same mean air temperature increase from SSP-RCP climate scenarios, the river temperature in the 'two power plants' scenarios with the smallest and the largest thermal disturbances was further increased, both spatially and temporally, showing a similar pattern and magnitude. The additional temperature increase caused by climatic warming was very limited right after the thermal effluent entered the river but gradually enhanced as the flow propagated downstream. This process can be explained by the climate-induced rise in ambient temperature which minimises the temperature gradient between air and water and leads to reduced heat loss and temperature decline, thereby enabling the thermal impact to extend further downstream. In terms of the direct impact on river temperature, climate change makes a much smaller contribution compared to the power plant discharge to the river. However, its indirect impact by exacerbating other existing stresses can be of great significance. Besides, the similarity in the pattern and magnitude of temperature increases could be attributed to the application of uniformly increased air temperatures, which ignored more important consequences of climate change, including changes in daily temperature variability and high temperature extremes. Overlooking these changes can lead to an incomplete and inaccurate representation of climate change and thus unreliable model outputs. Bias-corrected data from global or regional climate models that is based on historical observations (Berg et al., 2012; Casanueva et al., 2020; Navarro-Racines et al., 2020) can better represent the climate conditions and thus be used as an alternative in order to refine the comparison of the impacts of climate change and power plant discharge via climate scenarios. It is also worth noting that we implemented these climate scenarios with the purpose of providing a conservative (and simplified) estimated range of thermal impact from power

plants compounded by climate change. In the real world, climate change may result in more severe and complex impacts on river thermal regimes, mainly via warming groundwater and surface water temperatures and altered flow patterns (e.g. warmer groundwater & flow reduction; Caissie, 2006; Papadaki et al., 2016). Hence, it is essential to allow for the exacerbating effect as well as the long-term impact of climate change when designing new power plants and setting standards for regulating thermal effluent.

4.5. Conclusion

This study demonstrated a successful application of a conceptual process-based model in simulating hypothetical river temperature changes in response to power plant discharge scenarios. We generated a series of power plant scenarios by using different combinations of effluent discharges and temperatures as well as distances between power plants. In the scenarios including only a single power plant, the results highlighted the relative importance of the discharge and temperature of thermal effluent and underlined that the thermal impact is ultimately determined by the thermal energy increase resulting from the combination of two variables.

When a second power plant was introduced in the downstream, the remaining energy advected from the effluent of upstream power plant is combined with the heat input from the downstream power plant to cause cumulative thermal impacts. Smaller heat inputs to rivers should therefore not be overlooked as they could be combined with other inputs along a river. To fully utilise the cooling capacity of a river, it was found preferable to position the power plant with the largest heat input at the downstream site, and as far from the upstream plant as possible. However, the attenuating effect of increasing spacing distance was invalid in terms of temperature change at the river mouth and inconsistent in mean temperature change over the entire river.

Additional variability was introduced to the thermal impact by adjusting the operation mode and climate variables. When the power plants were simulated as peaking plants, effluent resulting from individual single-day operations

caused additional short-term temperature fluctuations. With sufficiently large heat inputs, these effluents interacted in space and time to cause cumulative impacts that extended period and river length over which a temperature increase occurred. Climate change, as a gradual and long-term process, only led to small increases in river temperature but exacerbated the impact of thermal effluents.

Despite the minor impact on river temperature, effluents with small discharges at high temperatures (e.g. the 2% discharge at 35 °C) can be of much greater importance at the vicinity of the power plant (e.g. reach-scale), causing a localised impact on the river ecosystem (e.g. Kalinowska et al., 2012; El-Ghorab, 2013; Logan & Stillwell, 2018). In reality, the thermal regime of a river can be further complicated by other anthropogenic activities such as reservoir management, riparian deforestation and water abstraction. As a result of the complexity and diversity of these river modification activities, more comprehensive and in-depth research is required to investigate their interactions and cumulative impacts along the river from a thermal habitat perspective.

4.6. Supplementary materials

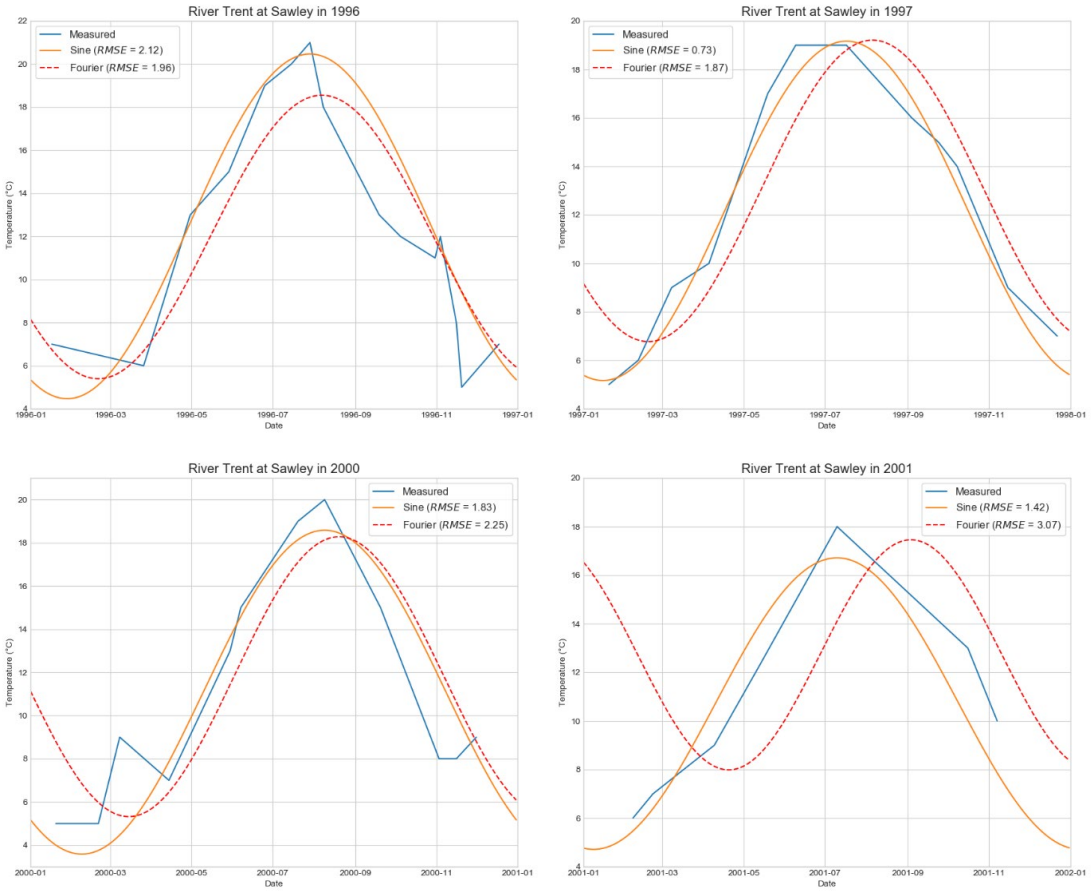

Figure 4.S1. Examples of performance comparison between sine function and Fourier series in regular years for monthly temperatures.

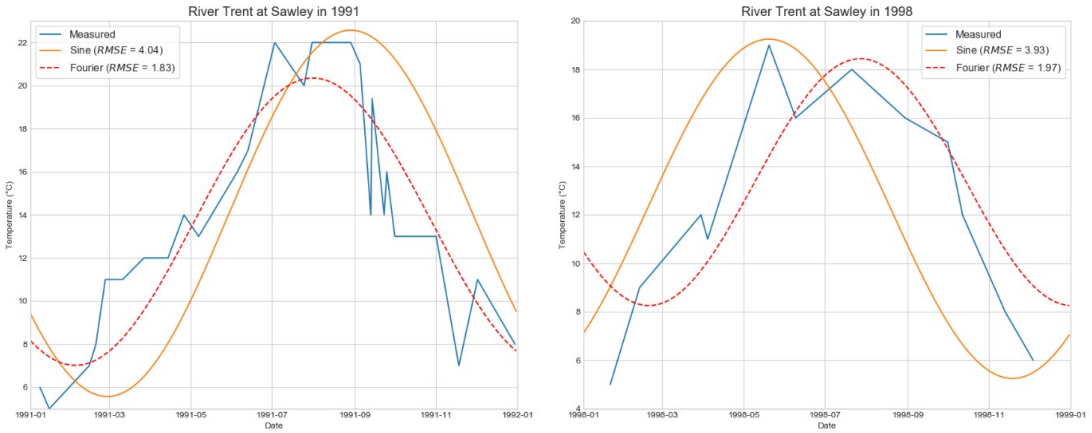

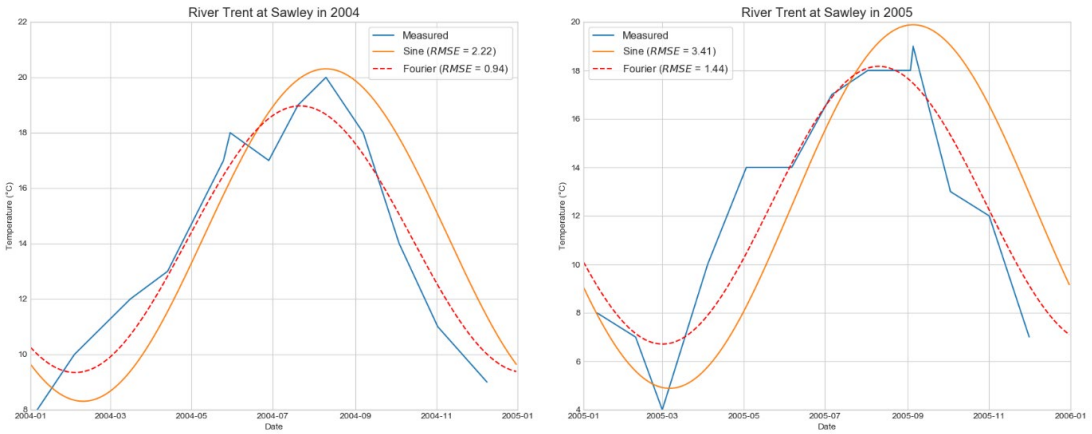

Figure 4.S2. Examples of performance comparison between sine function and Fourier series in unusual years for monthly temperatures.

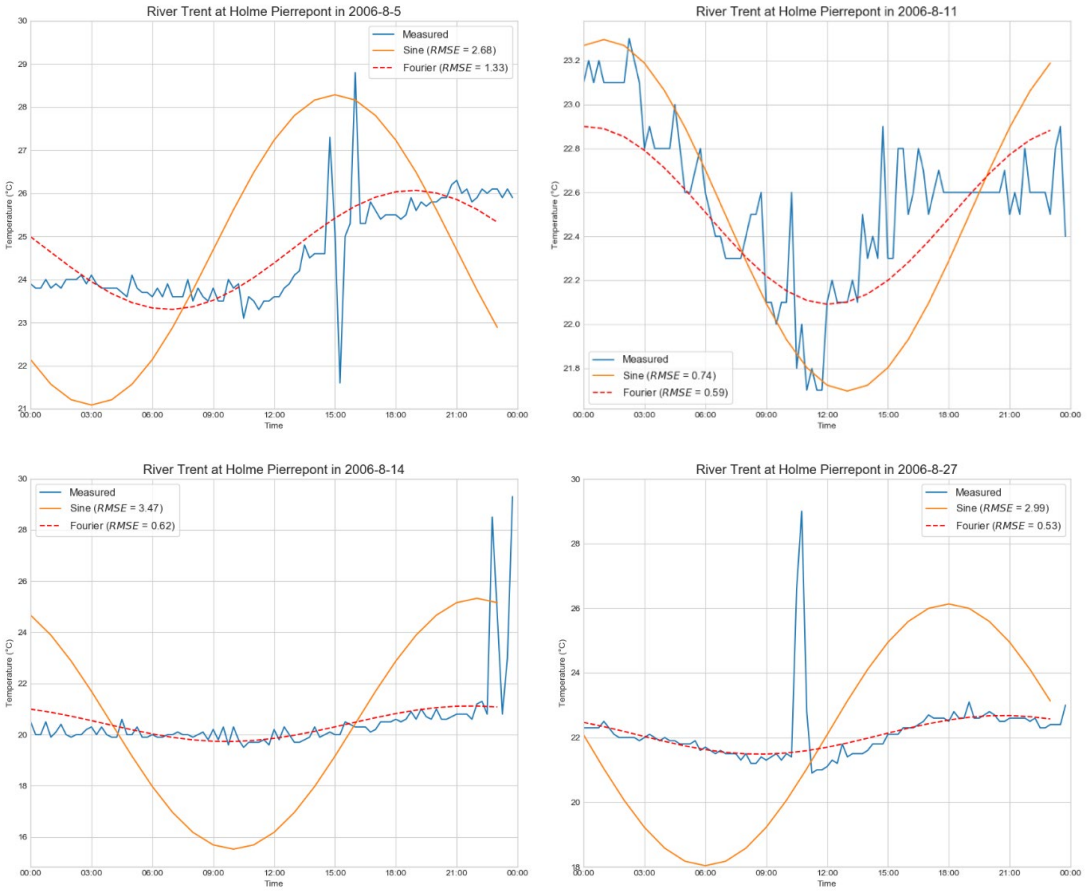

Figure 4.S3. Examples of performance comparison between sine function and Fourier series for hourly river temperatures in a day.

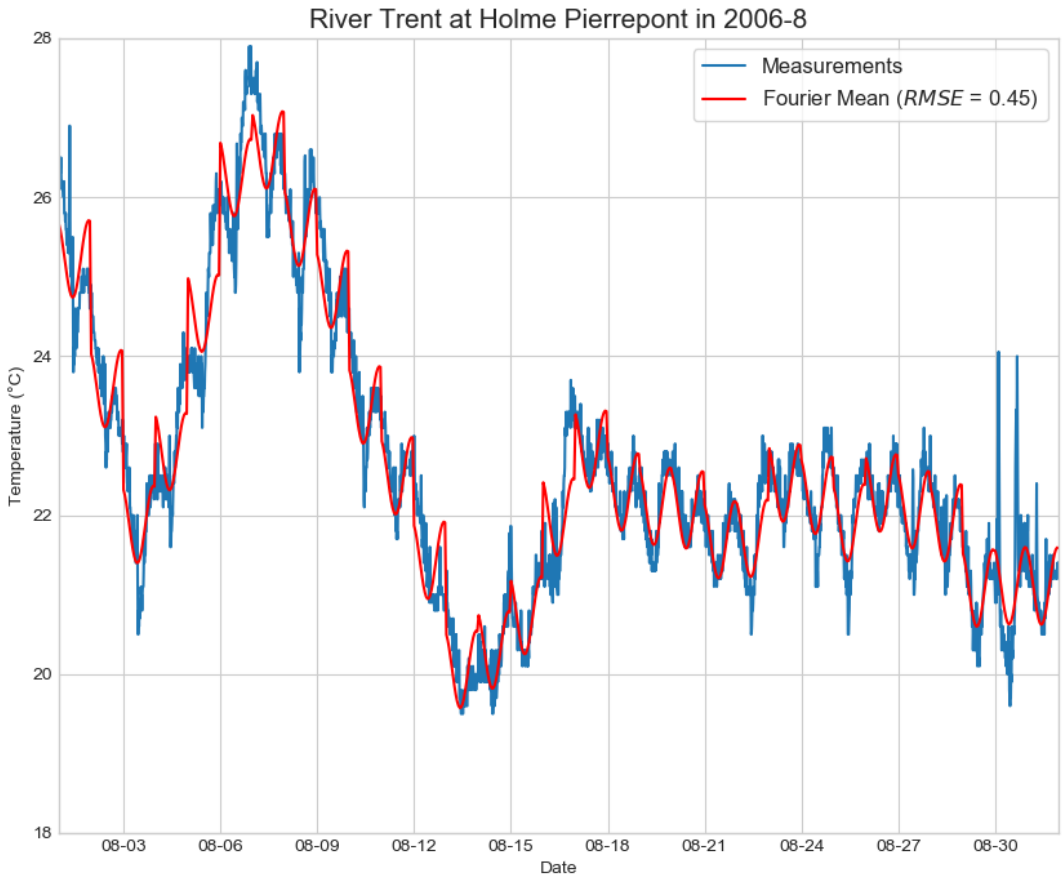

Figure 4.S4. Comparison between temperatures generated with Fourier series, and hourly measured data at Holme Pierrepont in August 2006.

In general, the Fourier series showed marginally lower root-mean-squared errors (RMSE) in monthly temperatures than the sine function in most regular years ($|\Delta RMSE| < 1$, 1993–2007). However, the sine function significantly outperformed the Fourier series in RMSE in some of the more recent years ($|\Delta RMSE| > 1$ in 1997, 2001 & 2007) and capturing more high temperatures throughout the year. Hence, the sine function was used for daily temperature generation. The Fourier series was less susceptible to abrupt increases or decreases which were very likely to be erroneous and thus used for generating hourly temperatures. By combining the two stochastic models, we obtained a reasonably representative hourly temperature data (e.g. RMSE = 0.45 in August).

S4.1: Calculation process for comparing the relative importance of the effluent discharge and temperature in raising water temperature

The formula for specific heat capacity of water is:

$$\Delta Q = m_w \cdot c_w \cdot \Delta T_w$$

where ΔQ is the change in thermal energy (J), m_w is the mass of water (kg), c_w is the specific heat capacity of water ($J \cdot kg^{-1} \cdot °C^{-1}$) and ΔT_w is the change of water temperature (°C).

Given the water temperature at the power plant T_w is:

$$T_w = 19.83\ ℃$$

For scenario of 2% at 25 °C to be increased to 35 °C, the increased thermal energy ΔQ_t is:

$$\Delta Q_T = m_w \cdot c_w \cdot (35\ ℃ - 25\ ℃) = 10 m_w c_w$$

For scenario of 2% at 25 °C to be increased to 20% (20% = 10·2%), the increased thermal energy ΔQ_D is:

$$\Delta Q_D = (10 \cdot m_w \cdot c_w) \cdot (25\ ℃ - T_w) - (m_w \cdot c_w) \cdot (25\ ℃ - T_w)$$

$$\Delta Q_D = (10 \cdot m_w \cdot c_w - m_w \cdot c_w) \cdot (25\ ℃ - 19.83\ ℃)$$

$$\Delta Q_D = 46.53 m_w c_w$$

Therefore,

$$\frac{\Delta Q_D}{\Delta Q_T} = \frac{46.53 m_w c_w}{10 m_w c_w} = 4.653$$

N.B. The calculation was a coarse estimation to understand the relative importance of the two cooling parameters in thermal pollution, performed under the assumption that the effluent discharge is minor relative to the river discharge. However, the effluent discharge increased to 20% are expected to cause more severe impacts as it accounts for a high percentage of the river flow. Therefore, 4.653 times was a conservative estimation.

Also, we can calculate when the impact by larger discharge will be more severe than that by higher temperature by:

$$\Delta Q_D - \Delta Q_T > 0$$

$$9 m_w c_w \cdot (25 - T_w) - 10 m_w c_w > 0$$

$$T_w < 23.88\ ℃$$

Therefore, 2% at 25 °C increased to 20% will have a higher thermal impact than that increased to 35 °C as long as the river temperature is lower than 23.88 °C.

Chapter 5: Investigating the effect of thermal history on the response of aquatic ectotherms to thermal stress

5.1. Introduction

Temperature is a critical environmental control on aquatic life, with extensive biological implications for all organisms (Angilletta, 2009). In particular, aquatic ectotherms are susceptible to temperature variations as their body temperatures are closely related to the temperature of surrounding water. Spatial and temporal variability of water temperature occur naturally in freshwater ecosystems due to diurnal and seasonal (in temperate regions) cycles in solar radiation. These variations influence chemical and biological processes (e.g. metabolism, growth and reproduction) and hence, the distribution, physiology and behaviour of life in rivers. However, the natural spatio-temporal variability can be disturbed by climate change and anthropogenic activities such as deforestation, urbanisation, and flow abstraction (Caissie, 2006; Hannah & Garner, 2015; Ficklin et al., 2023). When the temperature becomes unfavourable, aquatic ectotherms can either move to a more suitable habitat or adapt over multiple generations or acclimate to the new thermal regime in order to optimise their survival (Hofmann & Todgham, 2010; Narum et al., 2013; Chen et al., 2018a; Semsar-kazerouni & Verberk, 2018; Ahti et al., 2020; Andrews et al., 2023).

Thermal adaptation typically occurs too slowly to prevent the loss of performance in an organism in response to temperature changes (Buckley et al., 2015). Similarly, seeking thermally favourable habitats has an energy cost, as well as potentially increasing predation risk and reducing opportunities for foraging and mating (Sears et al., 2016; Sunday et al., 2016). Thermal acclimation can occur within a single generation and thus acts as a critical mechanism in improving performance in new thermal environments and improving the chances of survival against temperature change (Ferris & Wilson, 2012; Seebacher et al., 2015). A rise in water temperature enhances the

metabolic rate of an animal and, thus, the energy expenditure for respiration, growth and development (Brown et al., 2004). As a result, ectotherms have to make necessary physiological and behavioural adjustments (e.g. reduced locomotor activity and elevated feeding activity) to protect themselves from negative consequences of accelerated metabolism (e.g. reduction in body size). Therefore, although animals can acclimate to different thermal regimes, this comes at a cost to the organism.

Aquatic organisms inhabiting different thermal regimes can develop differing capacities for thermal acclimation, which determines the resilience of an individual, and species, to stressful temperatures (Maazouzi et al., 2011; Foucreau et al., 2014). Warm-acclimated animals typically have lower sensitivities to thermal stress and higher survival rates than cold-acclimated animals, particularly at prolonged higher temperatures (Whiteley & Faulkner, 2005; Foucreau et al., 2014; Semsar-kazerouni & Verberk, 2018). Aside from acclimation to lower or higher temperatures, ectotherms can also acclimate to temperature variations across different temporal scales (e.g. acute and chronic temperature exposure), which is of vital importance in determining the survival against climate change (Kern et al., 2015; Kefford et al., 2022). Organisms living in more thermally variable sites can benefit from the acclimation to a wider range of temperatures and exhibit a reduced response and enhanced tolerance to higher temperatures than those organisms in less thermally variable sites (Strange et al., 2002; Schaefer & Ryan, 2006; Blevins et al., 2013). However, acute thermal variation above thermal optima can be particularly detrimental to performance if it occurs too quickly for organisms to respond and acclimate to (Kefford et al., 2022).

Given the important role that thermal acclimation can play in buffering negative impacts of temperature change resulting from anthropogenic activities (e.g. power plant discharge) and climate change, increasing attention has been paid to the influence of thermal history (i.e. habitat temperature regime) experienced by the animal on the development of thermal acclimation capacity. Past research has been primarily focused on the thermal tolerance and performance of aquatic ectotherms at steady temperatures, with a relatively long period of settling (> 2d) before acclimation experiments begin (Maazouzi et al., 2011;

Foucreau et al., 2014; Semsar-kazerouni & Verberk, 2018). However, there remains a lack of research about how these aquatic ectotherms would respond and adjust to rapidly changing temperatures (such as those associated with powerplant thermal effluent) that offer different conditions for growth and survival. Moreover, studies that have explored differential acclimation rates of animals sourced from differing thermal regimes, have collected animals from sites that are distant from one another, likely having other environmental differences beyond just temperature (e.g. water chemistry, light levels, organic matter) (Cottin et al., 2012; Foucreau et al., 2013; Foucreau et al., 2014). In order to ensure water temperature is the only factor that affects the acclimation to new thermal regimes, the consistency of all environmental variables but water temperature needs to be confirmed across collection sites as well as across treatments. Therefore, this study aimed to address these aforementioned issues by investigating how aquatic ectotherms inhabiting sites in close proximity with markedly different thermal regimes would make physiological and behavioural adjustments to survive against both acute and chronic thermal stress under controlled laboratory conditions. To achieve this, we examined and compared the weekly changes in the survival, as well as locomotor and feeding activities, of freshwater shrimp *Gammarus pulex* from two close habitats with contrasting temperature variabilities exposed to different temperature treatments, including constantly high and intermittently high temperatures.

5.2. Methodology

5.2.1. Animal collection and experiment set-up

Freshwater shrimp (*Gammarus pulex*) were selected as target animals because of their widespread distribution in British streams as well as typically high abundance and trophic importance in freshwater ecosystems (e.g. organic matter decomposition and food sources for fish and invertebrate predators; Kelly et al., 2002; Väinölä et al., 2008). *Gammarus* are also a widely used model organism in toxicology studies (Agatz et al., 2014; Rosenfeldt et al., 2015; Lüderwald et al., 2019; Lebrun et al., 2020; Raths et al., 2023). They are

generally considered to be tolerant to organic pollution (Gerhardt et al., 2007; MacNeil et al., 2009; Gergs et al., 2013) but are known to be sensitive to other pressures including chemical pollution, microplastic ingestion and temperature (Zubrod et al., 2014; Redondo-Hasselerharm et al., 2018; Díaz-Morales et al., 2023).

Invertebrate samples were collected in October 2022 from two contrasting sites along the River Dove; upstream of significant groundwater spring inflows where annual water temperature ranges from 0–25 °C, and in spring inflows where the annual temperature ranges from 9.1–9.3 °C. Therefore, populations of shrimp living at these two sites have acclimated to markedly different thermal regimes (described further below). In order to collect invertebrates from habitats as similar as possible with the exception of water temperature, the river site was selected only about 300 m upstream of the spring site on the same river, with no tributaries situated between the sites (Fig. 5.1). The two sites shared similar riparian vegetation (grazed pasture with deciduous trees, mainly the Common Ash *Fraxinus excelsior*) and in-stream habitat conditions (e.g. aquatic vegetation, leaf and wood debris as well as gravel drift deposits underlain by mudstone, siltstone and sandstone the Millstone grit group).

a)

b)

Figure 5.1. The river (a) and the spring site (b) for invertebrate sampling.

Shrimp were caught using a kick-sampling methodology. As community composition was not of interest to this study, the operator targeted areas where shrimp were likely to be found (i.e. depositional areas with coarse organic materials) and continued sampling until sufficient animals for experiments had been caught. The kick-net was held immediately downstream of the operator and the riverbed was disturbed into the net, followed by hand search of larger organic materials, such as leaf packs, which were manually placed into the kick net. The kick net contents were then deposited in a white tray, and shrimp were manually removed from the tray into a bucket of river water and transported back to the laboratory.

All collected shrimp were individually identified before being transferred into microcosms to ensure that they were *G. pulex* as opposed to an invasive shrimp (e.g. *Crangonyx* sp. or *Dikerogammarus* sp.). They were then counted and photographed for subsequent size measurements using the image analyser software, ImageJ. The size was determined as the length (mm), measured dorsally along the body from the top of the cephalothorax to the base of the telson (Fig. 5.2). Since sex and body size have been found to have a limited effect on the temperature preference in *G. pulex* (Kenna et al., 2017), mature individuals with reasonable sizes (*body length* ≥ *6 mm*) were selected and transferred into microcosms. The microcosms were 100 ml beakers with a white

sand substrate (for higher contrast to detect shrimp in images and videos) and dechlorinated tap water. Each microcosm contained only one individual to avoid statistical dependence due to interactive activities between shrimp (e.g. cannibalism; Dick, 1995). In total, three thermal chambers that were able to house multiple microcosms were prepared for three temperature treatments, which were 1) control (constant 10 °C), 2) chronic (constant 15 °C) and 3) spiked (10 °C with 20 °C spikes for 2 hours per day; three spikes per week; Fig. 5.3). The spiked temperature treatment was designed to replicate the intermittent power plant operations when electricity use peaks for two hours (e.g. 7–9am and 5–7pm; Hiley, 2023), and implemented to investigate how aquatic organisms would respond to these abrupt, anthropogenically-controlled temperature changes. These treatments were performed for four weeks, with water temperature checked using a temperature probe before and during the experiment. However, the 20 °C experiment was carried out for only one week as most of the shrimp had perished by this point.

Figure 5.2. Example of size measurement in ImageJ. The approximate size of *G. pulex* was determined by measuring the length of the curve (*in red*).

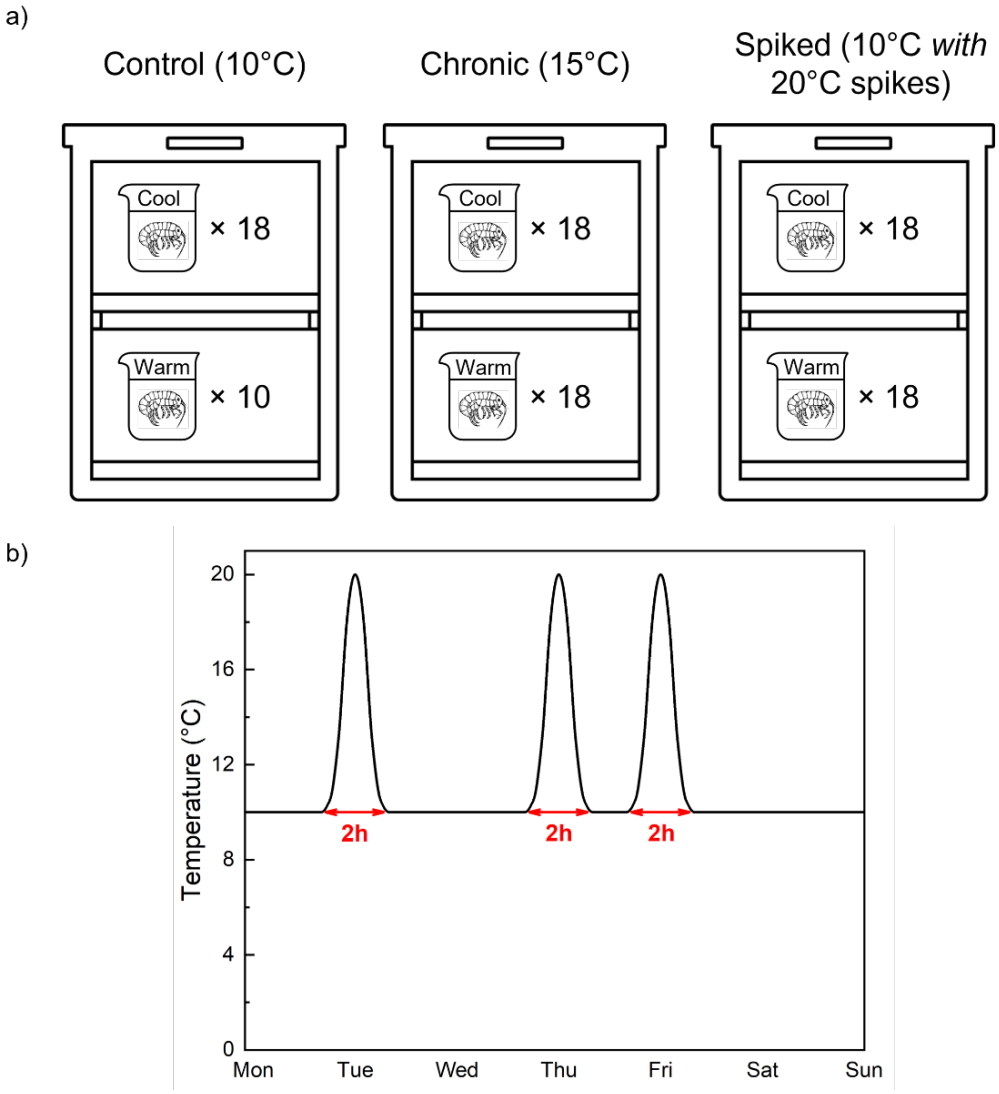

Figure 5.3. Schematic diagrams showing a) the arrangement of microcosms in temperature chambers and b) weekly temperature regime in the spiked 20 °C chamber.

Microcosms were placed in each chamber and connected to an aeration system to guarantee well-oxygenated water. Water level was regularly checked and refilled with dechlorinated tap water at the same temperature (from a reservoir in the same chamber) to offset any evaporative loss during experiments. Complete water changes were undertaken weekly, at the same time as experimental measurements were collected (described below). The chambers were kept in diffused daylight and away from direct sunlight as *Gammarus* usually shelter from sunlight (Sexton, 1928). Shrimp were fed once a week with a 5 mm-diameter circular leaf disc (*wt.* = 1.85 ± 0.42 mg, *n* = 50) which was made by cutting an oak leaf (easily fragmented) with a hole punch and softened

by conditioning in dechlorinated tap water, thereby ensuring that the same amount of palatable food was provided across all microcosms.

In order to ensure the consistency in the initial condition across chambers, all individuals were acclimated at a control temperature (10 °C) within chambers for 24 h before experiments commenced. After the acclimation period, the temperature in the chronic chamber was gradually increased from 10 °C to 15 °C over a one-hour period. The temperature regime of the spiked 20 °C chamber was designed by adjusting the temperature first from 10 °C to 20 °C and inversely from 20 °C to 10 °C at a rate of 5 °C per half hour (Fig. 5.3b). The chronic and spiked chambers each contained 36 microcosms, representing 18 animals (replications) from each of the two sites, whereas the control chamber had 18 animals from Dove spring but only 10 animals from the Dove river because of the limited number of shrimp available from the collected sample (Fig. 5.3a). As a result, the experiments consisted of a total of 100 microcosms across the three temperature chambers. All experiments were conducted and approved in accordance with the guidelines of the University of Nottingham's Code of Research Conduct and Research Ethics.

5.2.2. Responses to the temperature regimes

5.2.2.1. Locomotor activities

Immobility time and travel distance are two common locomotor variables that respectively relate to fatigue and energy consumption and can thus indicate stress-induced behaviours. Both were used here to indicate thermal stress (Tang et al., 2014; Valencia et al., 2019; Johnson et al., 2023). Each week, microcosms were temporarily removed in batches from chambers for photography and videography. The activity of the shrimp in each microcosms was recorded with digital videography to later calculate the immobility time and the total distance travelled by individuals within a 5-min observation period using an ImageJ-based tracking API, AnimalTracker (Everatt et al., 2013; Gulyás et al., 2016). Shrimp were allowed to settle for 5 min after being removed from chambers before video recording commenced. Given the short

duration of locomotion experiments, the temperature in the microcosms did not change significantly despite being outside of the thermal chambers for a short period (5 minutes). A threshold of 0.5 mm moved in 1 second was set to determine whether the shrimp was immobile.

5.2.2.2. Survival and feeding activity

The survival of amphipods was confirmed weekly by checking if an individual showed any movement after disturbance to the water (i.e. when removed for activity measurements). Dead individuals were removed from the chamber and transferred to small pots filled with methanol for preservation. Feeding rate is a measure of the quantity of food ingested by an animal over a given time period and is thus used to detect stress-induced changes in appetite and food intake. The leaf discs remaining after weekly consumption were photographed, with their areas subsequently measured in ImageJ to calculate a weekly feeding rate (Fig. 5.4). Photographs were also taken of leaf discs in microcosms without a shrimp in each chamber to serve as a control group to account for the potential microbial breakdown of leaf discs (e.g. decomposition).

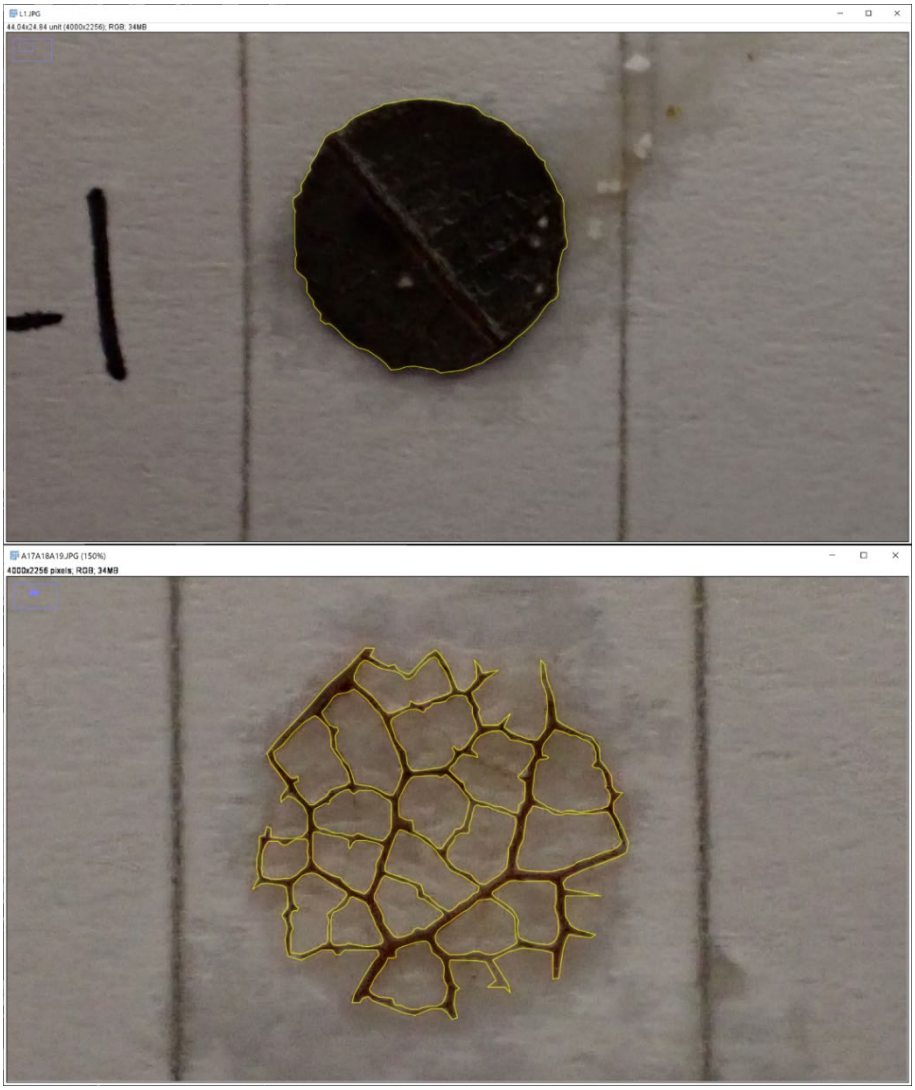

Figure 5.4. Examples of estimating the area of remaining leaf discs after weekly consumption in ImageJ. The pictures show the delineation of a rather intact (*top*) and a completely-consumed (*bottom*) leaf disc for area estimation.

5.2.3. Statistical analysis

Two statistical approaches, a) two-way analysis of variance (ANOVA) and b) one-way ANOVA with repeated measures, were applied to explore whether shrimp inhabiting sites with contrasting thermal regimes (spring vs. river) would exhibit different responses to a range of temperature treatments via comparing the performance of different experimental groups within the same week and the performance of each experimental group across four weeks, respectively.

With the purpose of testing whether there are differences in locomotor and

feeding activities due to the chamber temperature or the site, or whether there is a difference in locomotor and feeding activities by the combination or interaction of chamber temperature and site, two-way ANOVA tests with post-hoc Tukey HSD (Honestly Significant Difference) analyses were employed to examine the effects of chamber temperature and site as well as their interactions on immobility time, travel distance and leaf disc consumption. Follow-up simple effect analyses with Bonferroni corrections were performed when the effect of interaction between two variables was significant ($p < 0.05$).

In addition, to determine whether there is a difference in locomotor and feeding activities amongst spring or river shrimp after a 4-week exposure (i.e. the first, second, third and fourth experimental week) to each of the three distinct thermal treatments (10 °C, 15 °C and spiked 20 °C), one-way ANOVA with repeated measures with a Greenhouse-Geisser correction was used to assess the change in immobility time, travel distance and leaf disc consumption with respect to time, followed by Tukey HSD post-hoc tests. The analyses were only conducted for the shrimp that survived at the end of experiment. However, the analyses for spring shrimp in the spiked 20 °C chamber were only conducted for the first three weeks as a result of very few remaining individuals in the final week (< 3). Before the ANOVA tests were conducted, the Shapiro-Wilk test and Levene's test were performed to ensure the normality assumption and the homogeneity of variances, respectively. All data analyses were performed using GraphPad Prism 9 software.

5.3. Results

5.3.1. Survival rate

Under four contrasting temperature regimes, the weekly cumulative survival rates varied differently for shrimp inhabiting the thermally less variable Dove spring site and the thermally more variable Dove river site (Table 5.1 & Fig. 5.5). The experiment at a constant 20 °C ceased after the first week as there was a sharp decrease in the survival rate of shrimp from both spring and river sites (to 55.6% and 50.0%, respectively). At the lowest temperature (10 °C), shrimp

from the spring site had high survival for the first two weeks whereas the shrimp at the river site had an initial loss of animals. By week 4, the two shrimp populations were more similar, with mortality of spring shrimp increasing in week 3 and 4, compared to the decreased mortality of river shrimp in weeks 3 and 4. The highest survival rates were recorded in the 15 °C chamber, with 61.1% of the spring shrimp and 58.8% of the river shrimp still alive at the end of the experiment. A divergence in survival did occur between the spring and river shrimp for the spiked experiments. For spring shrimp, spiked temperatures caused the greatest mortality of all treatments, which in week 1 was equivalent to chronic 20 °C temperatures. By the end of the 4-week experiment, only 11.1% of the animals remained. In contrast, river shrimp had better survival in the spiked treatment, with 50% of animals surviving to the end of the experiment and being the second highest survival rate of the treatments.

Table 5.1. Weekly number of spring and river shrimp that survived in the 10 °C, 15 °C, spiked 20 °C (s20) and 20 °C chambers by the end of each experimental week.

	10 °C		15 °C		s20 °C		20 °C	
Week	*Spring*	*River*	*Spring*	*River*	*Spring*	*River*	*Spring*	*River*
0	18	10	18	17	18	18	18	10
1	16	8	16	13	9	16	10	5
2	14	5	14	11	7	11		
3	10	3	12	10	5	9		
4	7	3	11	10	2	9		

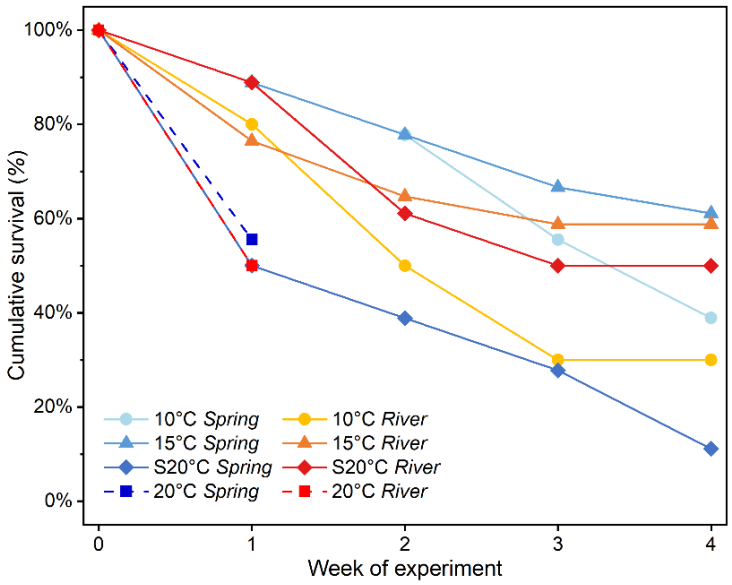

Figure 5.5. Weekly cumulative survival rates for shrimp inhabiting the thermally

less variable Dove spring site (*blue*) and the thermally more variable Dove river site (*orange & red*) in chambers with different temperature regimes.

In all cases, the survival rates of shrimp declined weekly, ranging from 11.1% to 61.1% at the end of the 4-week experiment. Given that dissolved oxygen levels remained high and feeding behaviour continued throughout the experiment, mortality is expected to be associated with thermal regimes. We attribute this association to the thermal acclimation achieved across all treatments. In all treatments, shrimp from the thermally more variable river site showed signs of acclimation after two weeks, with mortality being greatest in the first two weeks but slowing in week 3 and ceasing completely in the final week. In contrast, shrimp from the thermally less variable spring site showed no signs of acclimation and mortality occurred at a broadly consistent rate through time across all treatments, albeit with a steeper gradient in the warmer treatments. Additionally, a shrimp in the 15 °C chamber that was stuck and dead in the aeration hose during the experiment was removed from the analyses as its death was not attributed to the temperature.

5.3.2. Locomotor activity

5.3.2.1. Immobility time

For both spring and river shrimp, there was no significant change in immobility time over the experimental period in all treatments (all $p > 0.05$; Table 5.2 & 5.3). In the first and last week of experiment, there were no significant effects of chamber temperature (*wk1*: $F_{3,86} = 1.941$, $p = 0.13$; *wk4*: $F_{2,36} = 0.960$, $p = 0.39$), site (*wk1*: $F_{1,86} = 0.140$, $p = 0.71$; *wk4*: $F_{1,36} = 0.100$, $p = 0.75$) or interaction between chamber temperature and site (*wk1*: $F_{3,86} = 0.631$, $p = 0.60$; *wk4*: $F_{2,36} = 0.018$, $p = 0.98$) on immobility time (Figs. 5.6a & 5.6d & Table 5.4). In contrast, chamber temperature was the only factor that significantly affected the immobility time in the second week ($F_{2,57} = 3.801$, $p < 0.05$; Fig. 5.6b & Table 5.4). Neither the site ($F_{1,57} = 0.974$, $p = 0.33$) nor the interaction between chamber temperature and site ($F_{2,57} = 1.062$, $p = 0.35$) contributed to significant effects. Post-hoc analysis indicated that the immobility time of both spring and

river shrimp did not differ significantly at three temperature regimes ($p > 0.05$) but was significantly longer in the 10 °C chamber than in the 15 °C chamber ($p < 0.05$).

In the third week, there was a significant main effect of chamber temperature on immobility time ($F_{2,44} = 7.717$, $p < 0.01$; Fig. 5.6c & Table 5.4). However, this main effect was qualified by a significant interaction between chamber temperature and site ($F_{2,44} = 5.223$, $p < 0.01$). Simple effect analyses suggested that for spring shrimp, the immobility time was significantly longer in the spiked 20 °C chamber than in the 10 °C ($p < 0.05$) and 15 °C chambers ($p < 0.001$). River shrimp, on the other hand, did not differ significantly in immobility time between three treatments (all $p > 0.05$). Additionally, spring shrimp had significantly longer immobility time than river shrimp in the spiked 20 °C chamber ($p < 0.01$), compared to non-significant differences from river shrimp in immobility time in the 10 °C and 15 °C chambers ($p > 0.05$).

Table 5.2. Mean values (± standard deviations) of immobility time (sec), travel distance (mm), and disc consumption (%) of spring shrimp in the 10 °C, 15 °C and spiked 20 °C (s20) chambers. *p*-value < 0.05 from one-way ANOVA with repeated measures indicates significant changes over time.

10 °C chamber (n=7)					
	Week 1	Week 2	Week 3	Week 4	*p*
Immobility time (sec)	143.2 ± 84.3	90.0 ± 86.0	85.4 ± 73.4	99.6 ± 92.0	0.31
Travel distance (mm)	1519 ± 1189	2519 ± 1763	3126 ± 2290	2697 ± 2293	0.29
Disc consumption (%)	29.0 ± 14.9	17.1 ± 11.8	22.2 ± 11.6	26.6 ± 20.9	0.30
15 °C chamber (n=11)					
	Week 1	Week 2	Week 3	Week 4	*p*
Immobility time (sec)	96.8 ± 49.6	64.4 ± 61.4	37.9 ± 40.0	64.5 ± 74.2	0.06
Travel distance (mm)	1726 ± 1294	4701 ± 2828	4749 ± 1875	3688 ± 2399	< 0.01
Disc consumption (%)	25.3 ± 14.5	48.1 ± 27.5	44.7 ± 31.1	41.7 ± 28.7	0.18
s20 °C chamber (n=5)					
	Week 1	Week 2	Week 3		*p*
Immobility time (sec)	70.4 ± 52.8	159.1 ± 112.0	194.5 ± 39.4		0.08
Travel distance (mm)	2660 ± 1442	1232 ± 2033	220.5 ± 266.6		0.09
Disc consumption (%)	24.6 ± 4.2	18.6 ± 8.1	26.9 ± 16.1		0.33

Table 5.3. Mean values (± standard deviations) of immobility time (sec), travel distance (mm), and disc consumption (%) of river shrimp in the 10 °C, 15 °C and spiked 20 °C (s20) chambers. *p*-value < 0.05 from one-way ANOVA with repeated measures indicates significant changes over time.

10 °C chamber (n=3)					
	Week 1	Week 2	Week 3	Week 4	*p*
Immobility time (sec)	72.7 ± 88.0	81.0 ± 106.1	87.1 ± 45.8	112.7 ± 63.1	0.78
Travel distance (mm)	2947 ± 1424	1802 ± 1788	2638 ± 447.4	2163 ± 749	0.50
Disc consumption (%)	18.2 ± 7.1	25.2 ± 5.0	36.6 ± 27.3	45.6 ± 29.1	0.44
15 °C chamber (n=10)					
	Week 1	Week 2	Week 3	Week 4	*p*
Immobility time (sec)	65.5 ± 47.9	88.8 ± 69.1	82.8 ± 73.4	67.2 ± 44.1	0.68
Travel distance (mm)	2583 ± 1449	2444 ± 2011	2659 ± 2258	2852 ± 1856	0.92
Disc consumption (%)	25.5 ± 10.3	32.7 ± 18.9	33.7 ± 20.4	30.5 ± 17.6	0.57
s20 °C chamber (n=9)					
	Week 1	Week 2	Week 3	Week 4	*p*
Immobility time (sec)	100.8 ± 78.6	72.6 ± 63.1	93.2 ± 79.5	79.1 ± 80.6	0.80
Travel distance (mm)	2479 ± 2182	3427 ± 1759	2476 ± 2099	3127 ± 2525	0.54
Disc consumption (%)	16.1 ± 5.8	27.8 ± 24.0	19.6 ± 9.7	19.3 ± 11.0	0.39

Table 5.4. Two-way ANOVA analyses (*p < 0.05; **p < 0.01; ns: not significant) on the effects of chamber temperature ($T_{chamber}$) and site (T_{site}) as well as their interactions on immobility time, travel distance, and disc consumption.

	Immobility time				*Travel distance*				*Disc consumption*			
Week	I	II	III	IV	I	II	III	IV	I	II	III	IV
$T_{chamber}$	ns	*	**	ns	*	*	**	ns	ns	**	ns	ns
T_{site}	ns	ns	ns	ns	ns	ns	ns	ns	ns	ns	ns	ns
$T_{chamber}$* T_{site}	ns	ns	**	ns	ns	*	*	ns	*	ns	ns	ns

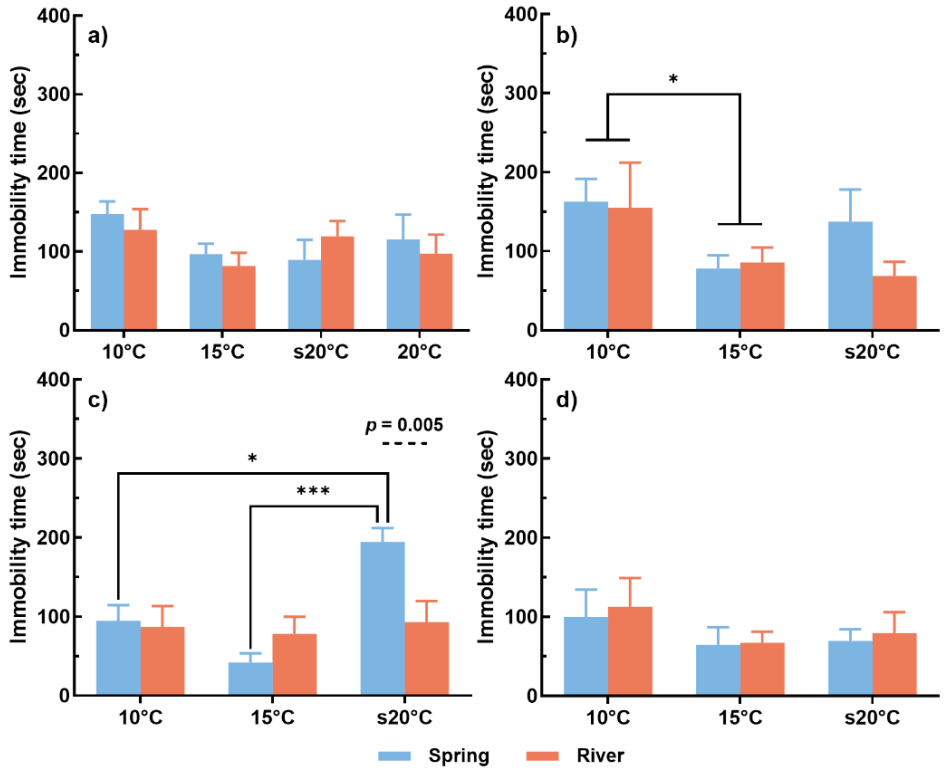

Figure 5.6. Mean (± s.e.m) of immobility time for shrimp from the spring and river sites in the 10 °C, 15 °C, spiked 20 °C (s20) and 20 °C chambers at the end of a) week 1, b) week 2, c) week 3 and d) week 4. Asterisks indicate overall significant differences between treatments or significant differences between treatments for shrimp from the same site: *$p < 0.05$ and ***$p < 0.001$ (two-way ANOVA). *p*-value above dashed line indicates significant differences between shrimp from the spring and river sites under the same treatment. Note that the 20 °C chamber only ran for week 1.

5.3.2.2. Travel distance

For river shrimp, there was no significant change in travel distance over the experimental period in all treatments (all $p > 0.05$; Table 5.2 & 5.3). Spring shrimp showed a significant increase in travel distance in the second and third weeks in the 15 °C chamber ($p < 0.05$ and $p < 0.01$) though they presented no significant change over the experimental period in the 10 °C and the spiked 20 °C chambers (all $p > 0.05$). In the first week, chamber temperature was the only factor that significantly affected the travel distance ($F_{3,86} = 2.911$, $p < 0.05$;

Fig. 5.7a & Table 5.4). Neither the site ($F_{1,86}$ = 0.394, p = 0.53) nor the interaction between chamber temperature and site ($F_{3,86}$ = 0.356, p = 0.79) contributed to significant effects. Post-hoc analysis indicated that the travel distance of both spring and river shrimp did not differ significantly at four temperature regimes (p > 0.05) but was significantly longer in the 20 °C chamber than in the 10 °C chamber (p < 0.05). In contrast, there were no significant effects of chamber temperature ($F_{2,36}$ = 0.443, p = 0.65), site ($F_{1,36}$ = 0.233, p = 0.63) or interaction between chamber temperature and site ($F_{2,36}$ = 0.135, p = 0.87) on travel distance in the last week of experiment (Figs. 5.7d & Table 5.4).

There was also a significant main effect of chamber temperature on travel distance in the following two weeks (*wk2*: $F_{2,57}$ = 4.801, p < 0.05; *wk3*: $F_{2,44}$ = 5.690, p < 0.01; Figs. 5.7b & 5.7c & Table 5.4). However, this main effect was qualified by a significant interaction between chamber temperature and site (*wk2*: $F_{2,57}$ = 4.535, p < 0.05; wk3: $F_{2,44}$ = 4.627, p < 0.05). Simple effect analyses suggested that for spring shrimp, the travel distance was significantly longer in the 15 °C chamber than in the 10 °C chamber in week 2 (p < 0.01) and the spiked 20 °C chamber in week 2 and 3 (p < 0.05 and p < 0.001). River shrimp, on the other hand, did not show significant differences in travel distance between three treatments in both weeks (p > 0.05). In the third week, spring shrimp had significantly longer travel distance than river shrimp in the 15 °C chamber (p < 0.05), while spring shrimp exhibited significantly shorter travel distance than river shrimp in the spiked 20 °C chamber (p < 0.05).

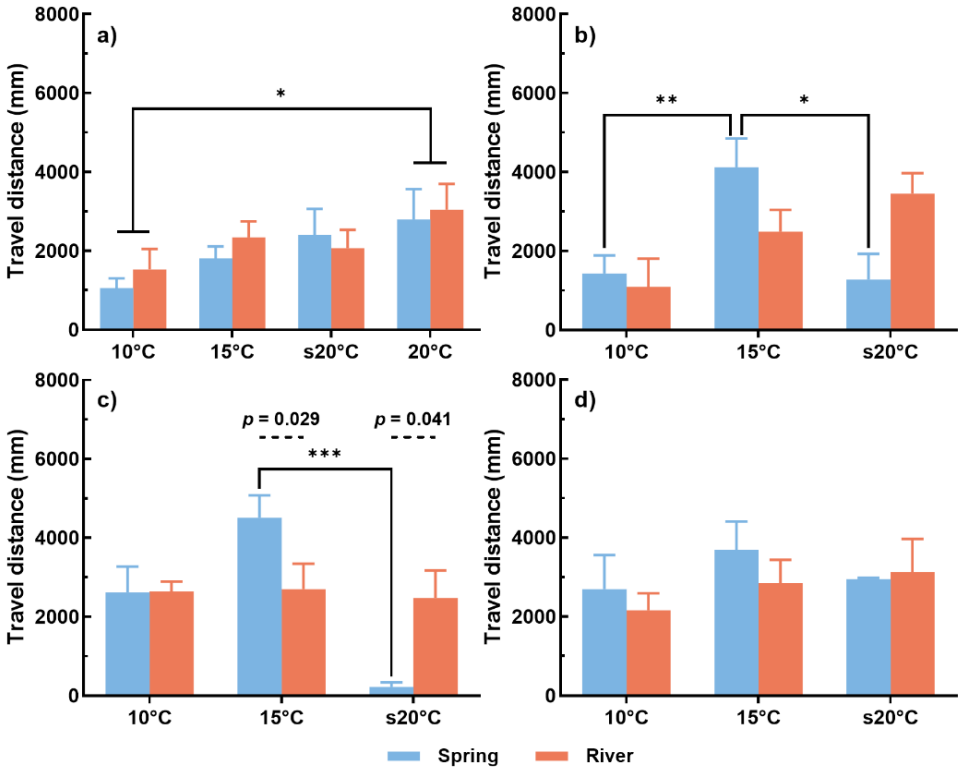

Figure 5.7. Mean (± s.e.m) of travel distance for shrimp from the spring and river sites in the 10 °C, 15 °C, spiked 20 °C (s20) and 20 °C chambers at the end of a) week 1, b) week 2, c) week 3 and d) week 4. Asterisks indicate overall significant differences between treatments or significant differences between treatments for shrimp from the same site: *$p < 0.05$, **$p < 0.01$ and ***$p < 0.001$ (two-way ANOVA). *p*-values above dashed lines indicate significant differences between shrimp from the spring and river sites under the same treatment. Note that the 20 °C chamber only ran for week 1.

5.3.3. Feeding activity

For both spring and river shrimp, there was no significant change in disc consumption over the experimental period in all treatments (all $p > 0.05$; Table 5.2 & 5.3). In the first week of experiment, neither the chamber temperature ($F_{3,86} = 2.528$, $p = 0.06$) nor the site ($F_{1,86} = 0.185$, $p = 0.67$) contributed to significant effects on disc consumption (Figs. 5.8a & Table 5.4). However, there was a significant effect of interaction between chamber temperature and site ($F_{3,86} = 2.819$, $p < 0.05$). Simple effect analyses suggested that river shrimp

showed significantly higher disc consumption in the 20 °C chamber than in the spiked 20 °C chamber ($p < 0.01$). Spring shrimp, on the other hand, did not differ significantly in disc consumption between the four treatments ($p > 0.05$). Additionally, spring shrimp had significantly lower disc consumption than river shrimp in the 20 °C chamber ($p < 0.05$), whereas shrimp from both sites showed no significant difference in disc consumption in the 10 °C, 15 °C and spiked 20 °C chambers (all $p > 0.05$).

In the second week, chamber temperature was the only factor that significantly affected the disc consumption ($F_{2,57} = 6.003$, $p < 0.01$; Fig. 5.8b & Table 5.4). Neither the site ($F_{1,57} = 0.436$, $p = 0.84$) nor the interaction between chamber temperature and site ($F_{2,57} = 1.998$, $p = 0.15$) contributed to significant effects. Post-hoc analysis indicated that the disc consumption of shrimp was significantly higher in the 15 °C chamber than in the 10 °C and spiked 20 °C chambers ($p < 0.01$ and $p < 0.05$). By contrast, there were no significant effects of chamber temperature (*wk3*: $F_{2,44} = 2.155$, $p = 0.13$; *wk4*: $F_{2,36} = 2.563$, $p = 0.09$), site (*wk3*: $F_{1,44} = 0.026$, $p = 0.87$; *wk4*: $F_{1,36} = 0.442$, $p = 0.51$) or interaction between chamber temperature and site (*wk3*: $F_{2,44} = 1.340$, $p = 0.27$; *wk4*: $F_{2,36} = 1.684$, $p = 0.20$) on disc consumption in the last two weeks (Figs. 5.8c & 5.8d & Table 5.4). Leaf discs in the control microcosms (no shrimp present) stayed intact over the experimental period (weekly loss < 1%), and hence the effect of microbial breakdown and leaching was negligible (MacNeil et al., 2011).

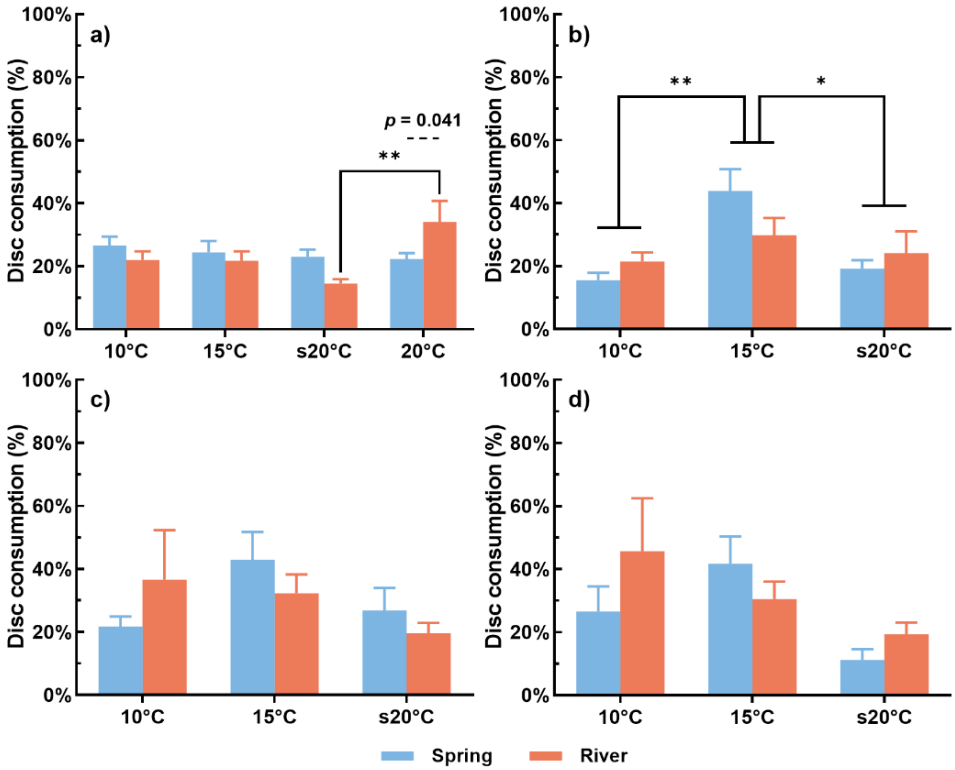

Figure 5.8. Mean (± s.e.m) in percentages of leaf disc consumed by shrimp from the spring and river sites in the 10 °C, 15 °C, spiked 20 °C (s20) and 20 °C chambers at the end of a) week 1, b) week 2, c) week 3 and d) week 4. Asterisks indicate overall significant differences between treatments or significant differences between treatments for shrimp from the same site: *$p < 0.05$ and **$p < 0.01$ (two-way ANOVA). p-values above dashed lines indicate significant differences between shrimp from the spring and river sites under the same treatment. Note that the 20 °C chamber only ran for week 1.

5.4. Discussion

5.4.1. Survival and performance after short exposure to treatments

Shrimp from two thermally contrasting sites of the River Dove exhibited dissimilarities in survival rates after a week's exposure to four distinct thermal treatments. As expected, the persistently high temperature (20 °C) was the most lethal for shrimp from both sites, which led to a considerable loss of

animals after the first experimental week. Shrimp from the constant temperature, relatively cool, spring site showed a similar mortality to shrimp from the diurnally and seasonally variable-temperature river site in the 20 °C chamber. A possible explanation for the high mortality is that organisms synthesise heat shock proteins (HSPs) in response to thermal stress in order to expand their tolerance to wider range of temperature and facilitate their survival (Kültz, 2003). However, a persistently high temperature can trigger a continuous expression of HSPs that is highly energy-consuming, which forces organisms to re-allocate energy away from important processes like growth and respiration to compensate for this energy demand (Slos & Stoks, 2008; Sokolova, 2013; Rossi et al., 2017; Morgan et al., 2018). Consequently, important processes and functions can be impaired by insufficiently allocated energy, which deteriorates animal health and makes it difficult to survive at a persistently high temperature. In particular, spring water shrimp suffered more from such impairment as they had similar survival rates and performance under both spiked and constant 20 °C regimes. A high temperature that is far beyond the narrow thermal range (i.e. 9.1–9.3 °C) experienced by shrimp from the spring site could exceed their capability of coping with temperature changes (i.e. acclimation), possibly accounting for the consistently high vulnerability to high temperatures with and without variabilities.

Despite the dissimilarities in survival rates, there were no significant differences between treatments in immobility time and disc consumption between the shrimp that survived after the first week, suggesting that the temperature change had no significant impact on these two performance indicators. However, shrimp from the river site in the 20 °C chamber had a higher disc consumption than those in other chambers (albeit only statistically significant in the spiked 20 °C chamber) and a significantly higher disc consumption than shrimp from the spring site in the same chamber. This implies that there could potentially exist a threshold of feeding activity for shrimp above which animal requires additional food intake for maintaining body weight and health. Although no studies have confirmed this threshold, there is evidence showing that increased feeding rate in *Gammarus sp.* is small from 5 °C to 15 °C (Pile et al., 2023) but large from 15 °C to 25 °C (Pellan et al., 2016), broadly corroborating the findings here. There was also a tendency for an increased travel distance with higher temperatures, although the differences in travel distance from 15 °C

to 10 °C and 20 °C were not statistically significant. This suggests that swimming activity can be promoted by short-term exposure to increased temperature, irrespective of thermal history (Vellinger et al., 2012).

5.4.2. Survival and performance after longer exposure to treatments

5.4.2.1. Constant temperatures

Significant differences in performance were mainly identified in the second and third weeks of experiment as the shrimp differentially acclimated to the new thermal conditions. During this period, shrimp from both sites exhibited higher survival rates in the 15 °C chamber than in the 10 °C chamber. Locomotor and feeding activities were also higher (i.e. shorter immobility time, longer travel distances and higher disc consumption) in the 15 °C chamber. The higher survival rates and performance collectively suggest a lower stress experienced by these shrimp under the temperature regime. This is consistent with other European studies where *G. pulex* presented a distinct preference for temperatures close to 15 °C at both individual and population levels (Sutcliffe et al., 1981; Maazouzi et al., 2011; Moenickes et al., 2011; Grabner et al., 2014; Kenna et al., 2017). However, caution should be taken when comparing optimal temperatures as thermal optima can be different depending on the performance traits used (e.g. locomotor vs. feeding activity; Iacarella et al., 2015) and geographic locations (Foucreau et al., 2014).

The exposure to a lower temperature than optimum can also cause an impact on survival. Despite the relatively high survival rates in the first week, both populations of shrimp in the 10 °C chamber experienced greater mortalities in the following weeks. Without having to maintain a high metabolic rate, shrimp exhibited low locomotor and feeding activities at a low temperature in the first two weeks. However, as the experiment proceeded, there was an increase in these activities (albeit not statistically significant), showing phenotypic adjustments for coping with temperature change and optimising fitness. Given that the increase in disc consumption was more pronounced in shrimp from the river site than the spring site, we speculate that the shrimp from the river site

had a higher energy demand for matching their thermal tolerance to cold and stable temperatures such as HSP synthesis. Therefore, sufficient energy supply for essential processes related to thermal tolerance is crucial to survival. However, the energy intake can be restricted by a low water temperature (Van der Velde et al., 2009; Maier et al., 2011), which inhibits energy-demanding physiological processes like metabolism, growth and development (e.g. failed moults observed during these experiments). As a result, only individuals that managed to optimise the energy allocation and maintain energy-demanding processes could acclimate to low-temperature stress and exhibit higher locomotor and feeding activities. In the 10 °C treatment, shrimp from the spring site presented a tendency towards a drop in survival rates, although they were reared under a similar temperature regime (constant 9 °C vs. constant 10 °C). This could be associated with discrepancies in other factors associated with survival (e.g. food, light and oxygen level) between laboratory and natural conditions; for example, in clear, shallow spring water, the thermal regime experienced by shrimp might be complicated by direct solar radiation on their body, in addition to the temperature of the water.

The documented changes in survival and behaviour are indicative of the different acclimation abilities of the shrimp populations from spring and river sites. Although shrimp from the spring site in the 10 °C chamber had a consistent performance over the four weeks, those in the 15 °C chamber showed a marked increase in locomotor and feeding activities from the second week onwards (although only the increase in travel distance was statistically significant). The contrasting response to the two temperature regimes indicates that the performance of cooler-adapted shrimp can be effectively enhanced by a higher water temperature as long as the optimum temperature is not exceeded. For ectothermic organisms like *G. pulex*, a higher temperature than the habitat temperature (from ~9 °C to 15 °C) considerably increases metabolic rates as well as energy intake (i.e. disc consumption) and expenditure (i.e. travel distance; Welton et al., 1983; Maazouzi et al., 2011; Kenna et al., 2017). Shrimp from the river site in the same thermal chamber exhibited a rather consistent performance through time after the first week, suggesting that their performance was less susceptible to temperature changes. When viewed in conjunction with the unchanged survival rates in the final two weeks of the

experiment, this suggests that shrimp from the river site acclimated to different temperatures faster than shrimp from the spring site, most likely because the shrimp population at the river site have experienced higher and more variable temperatures (0–25 °C) in contrast to the spring site, where temperatures are near-constant. Therefore, the thermal performance of aquatic ectotherms is not only determined by the current temperature regime, but also by the past thermal history prior to initiating new temperature acclimations (Lagerspetz & Vainio, 2006). The variability in temperatures experienced by animals could be an important control on their ability to acclimate to altered thermal regimes, as has been shown for cold-adapted organisms at high latitudes and altitudes (e.g. Lancaster et al., 2015; González-Tokman et al., 2020; Gilbert & Farrell, 2021).

5.4.2.2. Variable vs. constant temperatures

Under the spiked 20 °C temperature regime, shrimp from the spring and river sites showed a clear difference in responses to acute thermal stress. Weekly survival rates indicated that spring shrimp were extremely vulnerable to the acute changes in temperature, whereas river shrimp were tolerant to the same acute changes, and eventually acclimated to the spiked temperature regime. The different responses were also identified in behavioural indicators, with spring shrimp in the spiked 20 °C chamber having significantly lower locomotor activity compared to river shrimp under the same conditions, and spring shrimp in constant thermal conditions. River shrimp did not show significant differences in locomotor or feeding activities compared to those surviving at the optimum temperature, indicating a lower stress level. This is consistent with a previous study by Strange et al. (2002) who found that Orangethroat darters *Etheostoma spectabile* from the spring branch with smaller temperature variations showed a lower thermal tolerance than those from the stream reach with greater temperature variations. The discrepancies in survival and behaviour can be thus attributed to the past thermal history, which renders shrimp inhabiting the thermally less variable spring site more susceptible to intermittent temperature changes than shrimp inhabiting the thermally more variable river site. This is because aquatic ectotherms that have experienced a broad thermal range can synthesise HSPs over a wide range of temperatures to cope with an increase

in temperature and facilitate their survival, in contrast to ectotherms experiencing a very narrow (or stable) thermal range which are unable (or very limited in their ability) to activate the HSP synthesis in response to thermal stress (Hofmann et al., 2000; Tomanek, 2008; Tomanek, 2010). However, studies associated with climate change impact have shown that other biological processes such as growth and development have to be sacrificed for improved survival and behaviour as a consequence of the high energy expenditure on HSP synthesis, with profound implications for life-history traits such as reduction in body size and adult longevity (Belén Arias et al., 2011; Folguera et al., 2011).

Moreover, it is noteworthy that the survival rates of river shrimp in the spiked 20 °C chamber were much higher than in the constant 10 °C chamber, indicating an improved survival due to intermittent increases in water temperature. In this case, the survival of shrimp inhabiting the river site is more dependent on the cumulative energy inputs (i.e. high temperatures) that ensure sufficient feeding activities for essential physiological processes (e.g. growth and moulting). The survival rates of shrimp from the spring site, on the other hand, were much higher in the constant 10 °C chamber than in the spiked 20 °C chamber, suggesting that temperature stability is key to the survival, which makes sense given their long-term, population-level adaptation to near-constant water temperatures in spring inflows.

Given that water temperature can vary tremendously in space and time as a result of anthropogenic activities and climate change, greater attention should be given to the key species adapted to relatively low temperatures with small fluctuations (e.g. spring-fed streams) for their importance in maintaining local ecological stability. Whilst such areas may provide important refugia for mobile animals to exploit as rivers warm (Kurylyk et al., 2015; Fullerton et al., 2017; Hitt et al., 2017), it is less clear whether the populations that reside in these areas will be able to repopulate other areas of the river network after population declines (i.e. after a very hot summer), or whether such communities can survive even subtle increases in temperature of such areas, which is concerning given noted increases in groundwater temperatures, globally (Kurylyk et al., 2014; Menberg et al., 2014; Jyväsjärvi et al., 2015).

5.5. Conclusion

In this study, freshwater shrimp *Gammarus pulex* from two sites with contrasting thermal regimes were exposed to a range of temperature treatments and their response monitoring weekly for changes in their survival and behaviour. Shrimp from spring and river sites both exhibited high vulnerabilities to a persistently high temperature (20 °C) after the first week of experiments. This could be attributed to energy reallocation from important processes like growth and respiration to compensate for HSP synthesis. Spring shrimp also showed high vulnerabilities at intermittently high temperatures (spiked 20 °C), probably because the high temperature is beyond the narrow thermal range (i.e. 9.1–9.3 °C) experienced by these shrimp over multiple generations.

It was noted that the optimal temperature for survival and performance was 15 °C for longer exposure, irrespective of thermal history, which is consistent with other European studies on *G. pulex*. However, researchers need to be careful when comparing optimal temperatures as thermal optima can vary depending on the performance traits and geographic locations. A lower than optimum temperature can also cause an impact on survival by restricting the energy intake and inhibiting energy-demanding physiological processes. In addition to temperature, temperature variability is crucial to the survival of aquatic ectotherms inhabiting thermally stable environments. Hence, species adapted to relatively low temperatures with small fluctuations (e.g. spring-fed streams) should be given more attention as they are particularly vulnerable to thermal changes due to their reduced inability to acclimate to temperatures outside of the experienced thermal range.

In contrast, river shrimp displayed faster acclimation to both spiked and constant 20 °C temperatures than spring shrimp, owing to the wider thermal range and greater thermal variability of their habitat. However, the improved survival and behaviour of these shrimp was likely achieved at the expense of other important biological processes, such as growth and development. Therefore, future studies on thermal stress induced by climate change and anthropogenic thermal pollution should focus not only the survival and behavioural changes, but also changes in life-history traits such as longevity

and body size.

Chapter 6: Discussion

6.1. Achievement of aims

This thesis evaluated the potential impacts of thermal pollution from power plants on rivers by exploring where power plants are most likely to have serious thermal detriment, how multiple power plants may interact to create compound thermal impacts, and how chronic and acute raised temperatures may affect an aquatic ectotherm. Implications of powerplants were explored across different spatial (global, regional, and local) and temporal (river: hourly temperature variations; aquatic life: survival and behavioural changes within a week to a couple of weeks) scales, achieving the following aims:

1) To map and assess the relative significance of power plants as a source of thermal pollution on a national scale and develop an impact index for thermal pollution (Chapter 3).

2) To model the whole-river scale impacts of both individual and multiple power plants to observe how far downstream thermal effluents remain distinct and/or interact along a hypothetical river system (Chapter 4).

3) To investigate how aquatic ectotherms inhabiting sites with different temperature variabilities would differ in their survival and behaviours in response to acute and chronic thermal stress (Chapter 5).

Here, some key findings that address each aim are presented, below.

6.1.1. Aim 1: quantification and assessment of thermal pollution from power plants

Chapter 3 addressed Aim 1 by compiling a national power-plant dataset with information on cooling systems by integrating different datasets and inspecting uncertain plants via Google Earth, and then developing a novel index to quantify thermal pollution from power plants.

Raptis et al. (2017) performed a global assessment of thermal pollution from power plants with once-through cooling (OTC) systems by building on a series of papers that developed a model at smaller scales (Verones et al., 2010; Pfister & Suh, 2015; Raptis & Pfister, 2016). They identified pollution hotspots by using a characterisation factor in an environmental assessment model of freshwater thermal pollution from power plants, considering space, time and applied cooling technology. The thermal emissions were calculated by solving relevant thermodynamic cycles (e.g. Rankine cycle) for power generating units with relevant data from the World Electric Power Plants Database (WEPP). However, the calculations were computing- and data-intensive, and the proprietary database is relatively expensive, difficult to obtain and contains uncertain power generating units which cannot be found in other databases. In addition, the research only took into account sizable power plants with large capacities, which accounted for only 58% of total cooling system units. Therefore, Chapter 3 developed a computationally simple and low data-intensive index as a tool for quantifying thermal pollution from power plants with a wide range of generating capacities and power plant types.

As the index was developed to explore potential impacts of thermal effluent relative to river discharge, the calculation required data sets associated with both power plants and their receiving rivers. Despite considerable effort in compiling a high-quality dataset from multiple sources, the uncertainties from inspection, together with unclear and missing cooling information, dramatically reduced the number of power plants that could be used for index calculation. This highlights the scarcity and low quality of power plant data, which is highly problematic to assessing their potential impacts. The index was initially calculated for the only remaining 62 power plants in the USA, which indicated that five coal-fired power plants applying OTC systems were severely or highly vulnerable to thermal stress. These power plants were confirmed to be old plants using outdated generating units with deteriorating condition and low thermal efficiencies, resulting in large discharges of substantially warmed cooling water. Confidence in the index was increased by the success in assessing and locating these power plants that potentially generate a large amount of thermal pollution. Furthermore, a scenario-based analysis demonstrated that the index, in combination with background information (e.g.

technology used, lake or cooling pond nearby, and power plants used as peaking or base load power plants), provided accurate and informative assessments of thermal pollution, which was not confined to plants using OTC systems.

This chapter also examined the upstream catchment areas for thermal power plants. Global analyses showed that most thermal power plants were located in upstream catchment areas smaller than 500 km^2, consistent with the analyses across large countries and regions. These findings indicate that a surprisingly large number of thermal power plants are located in the upstream reaches of rivers, where thermal impacts are more likely to be severe relative to lower reaches, because of the relatively cool water in upland areas and reduced thermal buffering due to relatively low water volumes. The lack of assessment of thermal pollution in these areas underlines the importance of developing an efficient assessment approach, as well as a pressing need for readily accessible high-quality power plant data.

6.1.2. Aim 2: the whole-river scale impacts of individual and multiple power plants

In Chapter 4, power plant discharge scenarios generated using different combinations of related parameters (i.e. discharges, temperatures, operation mode and distances between power plants) were run in a conceptual water temperature model of a low-gradient, moderately-sized UK river to investigate how far downstream thermal effluents remain distinct and/or interact along a hypothetical river system.

This chapter demonstrated a method for leveraging modelling approaches to better utilise existing temperature monitoring data, which is of low spatial and temporal resolution, to explore the impacts of thermal effluents from power plants on river temperature. The water temperature model ran with a mix of real and simulated data and allowed the simulation of hypothetical power plant discharge scenarios. The simulation results with a single power plant suggested that the effluent discharge makes a greater contribution to temperature

increases than the effluent temperature. However, current studies and regulations on thermal effluents are mainly focused on the temperature rather than the discharge, which could potentially lead to overlooking large thermal impacts at temperatures lower than those listed in regulatory guidance (e.g. the 20% discharge at 25 °C).

The simulation results of scenarios with two power plants showed that the energy advected from the effluent of upstream power plant was combined with the heat input from the downstream power plant to cause cumulative thermal impacts. To alleviate these cumulative impacts by fully utilising the cooling capacity of a river, it was found preferable to position the power plant with the largest heat input at the downstream site, and as far from the upstream plant as possible. However, whilst minimising thermal impacts on rivers, such arrangements could lead to greater thermal impacts to coastal areas.

To better replicate real-world circumstances, additional variability was introduced to the thermal impact by adjusting the operation mode and climate variables. When the power plants operated as peaking plants, thermal effluent resulting from individual single-day operations caused additional short-term temperature fluctuations (i.e. thermopeaking). With sufficiently large heat inputs, these effluents interacted spatially and temporally to cause cumulative impacts that extended the period and river length over which a temperature increase occurred. Climate change, as a gradual and long-term process, only led to small increases in river temperature but indirectly exacerbated the impact of thermal effluents.

6.1.3. Aim 3: the response to thermal stress and association with thermal history

In Chapter 5, a series of laboratory experiments were performed to investigate the difference in the survival and behaviours of aquatic organisms inhabiting environments with different temperature variations, across a range of thermal conditions in order to predict the ecological consequences of climate change and anthropogenic thermal pollution.

This chapter found that freshwater shrimp (*Gammarus pulex*) from river and spring sites showed both similar and different responses to temperature regimes. As expected, river and spring shrimp were both vulnerable to a persistently high temperature (20 °C). This could be associated with the continuous expression of HSPs, which is highly energy-consuming and therefore leads to insufficient energy for other important processes like growth and respiration, ultimately deteriorating animal health and eventually leading to death. Intermittently high temperatures (spiked 20 °C) also caused substantial loss of spring shrimp; however, river shrimp that had acclimated to a variable thermal regime were less impacted, and showed no significant changes in survival rates and performance in week 3 and 4. Given the close proximity of spring and river sites (<1 km), this suggests that organisms inhabiting thermally more variable sites could be more tolerant to acute thermal stress than those inhabiting thermally less variable site. The improved thermal tolerance can be attributed to the wider thermal range and greater thermal variability of their habitat, which highlights the importance of thermal history in the response of aquatic ectotherms to thermal stress. This result corroborates the work of others looking at other organisms (Nyamukondiwa et al., 2018; Smith & Lancaster, 2020) and extends these findings by also considering behavioural changes in response to thermal stress, which is particularly important considering ongoing climate change and human interference (i.e. thermal discharge).

The results of the chapter showed that the exposure to a lower temperature than optimum can also impact survival of shrimp. The most likely explanation for this is that the low water temperature restricts the feeding activities and thus inhibits energy-demanding physiological processes like metabolism, growth and development (e.g. moulting failure). This finding could be of great importance for cold-water thermal pollution, such as that resulting from dam releases.

6.2. Data scarcity and its implications

This research has highlighted that thermal power plants are an important

source of thermal pollution, broadly distributed across river networks, including in upland areas (Chapter 3), and that their discharged effluents cause complex alterations to thermal regimes (Chapter 4) and have significant ecological implications (Chapter 5). Although a thermal pollution index was created and validated by using the best data available, data scarcity and uncertainty remains a challenge that requires greater attention and efforts. Government and local authorities could request that companies owning power plants monitor and report effluent discharge and temperature data, utilising equipment that can provide high resolution data (e.g. pressure transducers and temperature loggers). However, this is hard to realise in practice because confidential information on generators and cooling systems could be revealed and possibly extracted by competing companies, undermining corporate interests. There are proprietary databases (e.g. WEPP) that record some thermal effluent data from power plants, but access is charged at a high price, and data is still limited, effectively preventing these consequences. Therefore, for researchers, a more plausible route is to develop new approaches to improving data quality and accessibility. For example, a new python-based toolset, called 'powerplantmatching' (PPM) will clean, standardise and combine multiple power plant databases to acquire key data (e.g. generators, installed capacities) and is extended to include and process additional datasets such as OpenStreetMap to further improve the data quality (Gotzens et al., 2019; Jesse et al., 2020; Kumar et al., 2021; Morgenthaler et al., 2021; Parzen et al., 2023). In addition to merging and improving existing data sets, thermal-infrared remote (TIR) sensing can be used to monitor thermal pollution from power plants and obtain high-resolution data on its magnitude, location and development (Ma et al., 2017; Yavari & Qaderi, 2020; Nie et al., 2021). These efforts in obtaining higher-quality data are promising, and could allow the widespread application of our index to help decision-makers to quickly and accurately locate and assess the river segments or catchments that are susceptible to thermal pollution, and choose the most appropriate mitigation strategies.

6.3. Powerplant impacts: challenges and opportunities

The aforementioned efforts in improving power plant data also reflect a growing

recognition that there is a pressing need for better understanding of thermal pollution associated with power plants, especially given the ongoing impacts of climate change and power plant expansion (Pfister & Suh, 2015; Raptis et al., 2016; Raptis et al., 2017). By investigating the upstream catchment areas of power plants regionally and globally, it was found that most thermal power plants reside in upstream reaches of major rivers, which are typically characterised by high vulnerability to thermal changes. This is because of smaller water volumes and reduced exposure to solar radiation coupled with narrower channels being more readily shaded by topography and riparian vegetation and greater connectivity to cool groundwater inputs, creates cooler ambient water temperatures (e.g. Johnson et al., 2014). Ecological communities in upland rivers are also considered to be the most sensitive to change because they are likely to have genetically adapted to relatively stable, cool temperatures over long periods (1000s years), there is less potential to migrate upstream to cooler water and because they already reside relatively near the source of the river (Lancaster et al., 2015; González-Tokman et al., 2020; Gilbert & Farrell, 2021). There is also greater uncertainty in impacts in upstream river reaches because these are typically the most data sparse areas of river (e.g. see Birrell et al., 2020), resulting in less information to inform appropriate monitoring and management.

Both the individual and cumulative impacts of power plants remain poorly understood, particularly in upstream river regions, because of a lack of monitoring data. As such, a conceptual process-based model was used to simulate hypothetical river temperatures in this thesis, exploring responses to power plant discharge scenarios. The results demonstrate that thermal impacts from power plants can propagate considerable distances downstream, and combine with the thermal impacts of power plants located downstream, to cause cumulative impacts, irrespective of the size of those impacts. Although power plants in upstream reaches tended to have smaller generating capacities than those located downstream and, as such, were typically responsible for smaller absolute thermal impacts (Chapter 3), the relative significance of these was large (i.e. relative to the receiving water) and could persist over long distances (> 150 km). Therefore, there is great potential for smaller power plants located in upstream reaches to interact and cause complex, cumulative

impacts, especially if compounded with other potential causes of thermal stress such as impoundments, deforestation, urban runoff, and domestic sewage outflows. Due to the inherent complexity in catchment-scale hydrology, different catchments could respond very differently to power plant effluent and it is therefore challenging to monitor and/or assess the cumulative impacts of power plants along a specific river network. However, approaches to modelling such impacts could build on recent work that explores multiple, or “cascade”, run-of-river hydropower plants, which shift the thermal regime from a continuous to a “stepped” profile and exert ecological impacts, including alterations to community composition and structure (Kuriqi et al., 2021; Bonacina et al., 2023b; Chapter 2).

6.4. Ecological implications of thermal effluent

It was noted that the impacts of power plants on water temperature are complicated by both the operation mode and climate variables (Chapter 4). Climate change exacerbates existing thermal stresses by raising ambient temperatures within the receiving water body. Thermal effluents from power plants operated as peaking plants bring about additional short-term temperature fluctuations (i.e. thermopeaking) relative to constant discharging effluent, which could be responsible for significant ecological impacts, yet are critically understudied. Therefore, Chapter 5 investigated the changes in survival and behaviour of freshwater shrimp (*Gammarus pulex*) inhabiting two close sites with vastly different thermal regimes, particularly temperature variabilities, in response to acute and chronic thermal stress. To replicate the intermittent operations of a peaking power plant, shrimp were exposed to a thermal regime with spiked temperatures. Shrimp inhabiting thermally more variable river sites (annual temperature range 0–25 °C) exhibit greater thermal tolerance and faster acclimation to intermittently high temperatures than shrimp inhabiting a thermally less variable spring site (constant 9 °C). This implies that the capacity for thermal acclimation is dependent on the experienced thermal history of an organism, which consists not only of the average temperature, but also the range of temperatures experienced. This corroborates past research (Nyamukondiwa et al., 2018), but further extends over this work by exploring

the effect of thermal history on acclimation to intermittently high temperatures. From the results, it is expected that the ecological impacts of power plant discharge will be more pronounced at thermally less variable sites than those that are thermally variable. It also suggests that although warmer effluent is temporally limited in a thermopeaking scenario, the ecological impacts can be at least equally detrimental as a constant effluent of the same temperature where recipient organisms are adapted to relatively consistent and cool temperatures.

Despite the complexity in response to raised temperatures due to differential acclimation rates, it is important to note that shrimp from both sites displayed very low thermal tolerance to a persistently high (20 °C) temperature, suggesting that there could be a temperature threshold over which acclimation is not possible. Such a theory has been suggested by Morgan et al. (2020) who raised zebrafish (*Danio rerio*) over multiple generations with the aim of increasing thermal maxima in one population and decrease thermal minima in another. They found that the rate of change of increased thermal maxima decreased with each generation, with a total increase of 0.22 °C over the 6 generations, In contrast, the thermal minima was reduced by a similar margin with each generation, being lowered by 0.74 °C over the same period. Morgan et al. (2020) interpreted this as evidence of an upper thermal threshold, beyond which further acclimation is not possible. Consequently, it is strongly recommended that research on the thermal acclimation of organisms is carried out at both individual and community levels, providing key information for adjusting power plant operations and minimising / mitigating the potential ecological impacts of thermal pollution.

6.5. Limitations and future work

Although this research is novel and represents an important contribution that improves understanding of power plant thermal pollution and resulting ecological impacts, it is acknowledged that there are limitations that need to be overcome in future work. First, this research examined the largest possible impact of effluent discharge (i.e. maximum temperature at the outfall) in

summer, with the purpose of providing a conservative estimated upper limit of thermal impact from power plants. In real-world circumstances, new power plants are employed with advanced technologies to improve thermal efficiencies (e.g. combined cycle gas turbine) and to reduce thermal discharges (e.g recirculating cooling). As such, thermal impacts of some newer power plants may not be as large as reported here; however, without better data sets it is difficult to predict. In addition, it was found here that effluent discharge was the main determinate of thermal impact, as opposed to effluent temperature, and so mitigations to reduce effluent temperature may not be as impactful as those to reduce effluent volumes.

The focus on summer also offers only a snapshot of potential impacts. Changes in river temperature and ecological response in other seasons are rarely studied or reported (see Wilby & Johnson, 2014), but could be highly significant. Again, data limitation makes modelling and assessment problematic but increased autumn and winter temperatures will have important ecological impacts on organisms' phenology, behaviour and potentially, survival (Everall et al., 2014). For example, Firkus et al. (2018) found that warmed water temperatures promoted the spawning of two fish species (Johnny Darters, *Etheostoma nigrum*; Fathead Minnows, *Pimephales promelas*) in winter. In contrast, wild Yellow Perch (*Perca flavescens*) had reduced egg sizes and reproductive success as a result of warmer water temperatures in winter (Farmer et al., 2015). Therefore, the modelling work presented should be considered as a precautionary approach to decision making, offering initial guidance on scenarios that are likely (or unlikely) to be problematic, and the actual impacts will need to be assessed and interpreted according to site- and context-specific conditions of both the receiving freshwater system and of the power plant operation (e.g. geographical location, time of discharge).

Furthermore, the model for investigating water temperature change was one-dimensional, which did not allow for the horizontal and vertical mixing of thermal pollution to be assessed, and thus some potentially significant impacts were not incorporated. Chapter 4 showed that effluents with small discharges at high temperatures (e.g. the 2% discharge at 35 °C) contributed to a relatively minor impact on river temperature. However, it could be of much greater importance

at the vicinity of the power plant (e.g. reach-scale), causing highly localised impacts on the river ecosystem (e.g. Kalinowska et al., 2012; El-Ghorab, 2013; Logan & Stillwell, 2018). Localised impacts exemplify the importance of scale in assessing thermal pollution. Novel approaches, including the use of drone-based thermal imagery are opening up this area to rapid study, presenting high spatial resolution data for analysis of localised thermal impacts and potential thermal barriers along river networks (Dugdale et al., 2017). Powerplant discharges are yet to be studied in this way, but such approaches will be important in future studies in this area.

Besides, the approach to developing climate scenarios in Chapter 4 was simplistic and did not allow for the changes in temperature variability (e.g. daily temperature variability and high temperature extremes), resulting in inaccurate representations of climate change. Climate change intensifies the hydrological cycle, which alters the precipitation pattern in intensity, extremes, and seasonality, and thus exacerbates extreme hydrological events such as floods and droughts (Feng et al., 2013; Kumar, 2013; Wu et al., 2013; Trenberth et al., 2014; Deng et al., 2018). It is therefore essential to account for these climate-induced variabilities in our river temperature model to better describe temperature-related processes (e.g. evaporation and flow reduction), ultimately providing a more reliable estimation of the combined impacts of power plant discharge and climate change on thermal regime. Given that the climate-induced variability in temperature increases over time, bias correction is an indispensable post-processing procedure for minimising discrepancies between the outputs directly from climate models (e.g. global or regional climate models) and historical observations (Berg et al., 2012; Casanueva et al., 2020; Navarro-Racines et al., 2020). Hence, bias-corrected climate data is recommended to be used in future studies related to the impact of climate change as well as its combined impact with other sources of thermal pollution.

Another limitation lies in the lack of size measurements for shrimp for confirming the negative consequence of HSP synthesis. The photos of shrimp were taken weekly, but were of low quality and could not be used for growth analyses because the errors relative to measurements were unacceptably large. Hence, a high-performance camera is essential for future studies on short-term growth,

given the size of the experiment animal.

We suggest priority should be given to the following research foci:

- Work to address the poor accessibility, quality and resolution of global datasets, utilising modelling approaches where necessary to produce and infill missing information.

- Utilise opportunities for synthesising thermal data sets to explore future power plant placement, particularly including interactions between multiple plants and with other sources of thermal impacts, such as dams, deforestation and urban areas.

- The design and implementation of national and regional monitoring networks utilising novel methodologies for monitoring thermal regimes and optimising the benefit / minimising the impact of power plant infrastructure.

- Thermal modelling research should usefully focus not only on chronic, gradual temperature changes, but also on regular and irregular sudden jumps in temperature associated with hydropeaking activities, which could have disproportionately problematic ecological impacts.

- Further investigation into the differential acclimation of organisms to changing temperature regimes, based on the thermal regimes experienced over their life cycle, with implications for predictions of future biodiversity loss due to climate change.

- Research on the sub-lethal impacts of temperature changes, and the costs of acclimation, which could indicate impacts before species are lost from the community and allow assessment of the resilience of communities to thermal change (i.e. those already pressured by temperature are less likely to survive further increases).

List of references

Adams, C. M., Winkelman, D. L. and Fitzpatrick, R. M. (2023) Impact of wastewater treatment plant effluent on the winter thermal regime of two urban Colorado South Platte tributaries. *Frontiers in Environmental Science*, 11.

AECOM (2021) Keadby 3 Low Carbon CCGT Generating Station Project, Environmental Permit Variation Application: Appendix D3 - Assessment of Best Available Techniques for Cooling.

Agatz, A., Ashauer, R. and Brown, C. D. (2014) Imidacloprid perturbs feeding of Gammarus pulex at environmentally relevant concentrations. *Environmental Toxicology and Chemistry*, 33(3), 648-653.

Ahti, P. A., Kuparinen, A. and Uusi-Heikkilä, S. (2020) Size does matter — the eco-evolutionary effects of changing body size in fish. *Environmental Reviews*, 28(3), 311-324.

Akbarzadeh, A. and Leder, E. H. (2016) Acclimation of killifish to thermal extremes of hot spring: Transcription of gonadal and liver heat shock genes. *Comparative Biochemistry and Physiology Part A: Molecular & Integrative Physiology*, 191, 89-97.

Al-Ghussain, L. (2019) Global warming: review on driving forces and mitigation. *Environmental Progress & Sustainable Energy*, 38(1), 13-21.

Andrews, R., Hayes, D. and Zorn, T. (2021) Multi-model evaluation of longitudinal temperature fluctuations and the dominant influencing factors among Michigan streams. *Authorea Preprints*.

Andrews, K. R., Seaborn, T., Egan, J. P., Fagnan, M. W., New, D. D., Chen, Z., Hohenlohe, P. A., Waits, L. P., Caudill, C. C. and Narum, S. R. (2023) Whole genome resequencing identifies local adaptation associated with environmental variation for redband trout. *Molecular Ecology*, 32(4), 800-818.

Angel, S., Parent, J., Civco, D. L., Blei, A. & Potere, D. (2011) The dimensions of global urban expansion: Estimates and projections for all countries, 2000–2050. *Progress in Planning,* 75(2)**,** 53-107.

Angilletta, M. J. (2009) Thermal adaptation: a theoretical and empirical synthesis.

Anneli Korhonen, I. & Lagerspetz, K. Y. H. (1996) Heat shock response and thermal

acclimation in Asellus aquaticus. *Journal of Thermal Biology,* 21(1)**,** 49-56.

Asquith, W. H., Roussel, M. C., and Vrabel, J. (2006) Statewide analysis of the drainage-area ratio method for 34 streamflow percentile ranges in Texas. *U.S. Geological Survey Scientific Investigations Report 2006–5286*, 34p., 1 appendix.

Attia, S. I. (2015) The influence of condenser cooling water temperature on the thermal efficiency of a nuclear power plant. *Annals of Nuclear Energy*, 80, 371-378.

Auer, S., Hayes, D. S., Führer, S., Zeiringer, B. and Schmutz, S. (2022) Effects of cold and warm thermopeaking on drift and stranding of juvenile European grayling (Thymallus thymallus). *River Research and Applications*, 39(3), 401-411.

Auer, S. K., Salin, K., Rudolf, A. M., Anderson, G. J. & Metcalfe, N. B. (2015) Flexibility in metabolic rate confers a growth advantage under changing food availability. *J Anim Ecol,* 84(5)**,** 1405-11.

Averyt, K., Huber-Lee, A., Macknick, J., Madden, N., Rogers, J. and Tellinghuisen, S. (2011) Freshwater Use by US Power Plants: A Report of the Energy and Water in a Warming World Initiative.

BEEMS (2011) Thermal standards for cooling water from new build nuclear power stations. *Scientific Advisory Report Series 2011.*

Belén Arias, M., Josefina Poupin, M. and Lardies, M. A. (2011) Plasticity of life-cycle, physiological thermal traits and Hsp70 gene expression in an insect along the ontogeny: Effect of temperature variability. *Journal of Thermal Biology*, 36(6), 355-362.

Bellgraph, B. J., McMichael, G. A., Mueller, R. P. and Monroe, J. L. (2010) Behavioural response of juvenile Chinook salmon Oncorhynchus tshawytscha during a sudden temperature increase and implications for survival. *Journal of Thermal Biology*, 35(1), 6-10.

Benyahya, L., Caissie, D., St-Hilaire, A., Ouarda, T. B. M. J. and Bobée, B. (2007) A Review of Statistical Water Temperature Models. *Canadian Water Resources Journal*, 32(3), 179-192.

Bilous, M. and Dunmall, K. (2020) Atlantic salmon in the Canadian Arctic: potential dispersal, establishment, and interaction with Arctic char. *Reviews in Fish Biology and Fisheries*, 30(3), 463-483.

Birrell, J. H., Shah, A. A., Hotaling, S., Giersch, J. J., Williamson, C. E., Jacobsen, D. and Woods, H. A. (2020) Insects in high-elevation streams: Life in extreme environments imperiled by climate change. *Global Change Biology*, 26(12), 6667-6684.

Blevins, Z. W., Effert, E. L., Wahl, D. H. and Suski, C. D. (2013) Land use drives the physiological properties of a stream fish. *Ecological Indicators*, 24, 224-235.

Bonacina, L., Fasano, F., Mezzanotte, V. and Fornaroli, R. (2023a) Effects of water temperature on freshwater macroinvertebrates: a systematic review. *Biological Reviews*, 98(1), 191-221.

Bonacina, L., Mezzanotte, V. and Fornaroli, R. (2023b) From a continuous thermal profile to a stepped one: The effect of run of river hydropower plants on the river thermal regime. *River Research and Applications*, 1-14.

Boyd, M. and Kasper, B. (2003) Analytical methods for dynamic open channel heat and mass transfer: methodology for the Heat Source Model Version 7.0, Watershed Sciences Inc., Portland, Oregon.

Brittain, J. E. (1990) Life History Strategies in Ephemeroptera and Plecoptera. *In:* Campbell, I. C. (ed.) *Mayflies and Stoneflies: Life Histories and Biology.* Dordrecht: Springer Netherlands. 1-12.

Brown, J. H., Gillooly, J. F., Allen, A. P., Savage, V. M. and West, G. B. (2004) TOWARD A METABOLIC THEORY OF ECOLOGY. *Ecology*, 85(7), 1771-1789.

Buckley, L. B., Ehrenberger, J. C. and Angilletta Jr, M. J. (2015) Thermoregulatory behaviour limits local adaptation of thermal niches and confers sensitivity to climate change. *Functional Ecology*, 29(8), 1038-1047.

Burdon, F. J., Munz, N. A., Reyes, M., Focks, A., Joss, A., Räsänen, K., Altermatt, F., Eggen, R. I. L. and Stamm, C. (2019) Agriculture versus wastewater pollution as drivers of macroinvertebrate community structure in streams. *Science of The Total Environment*, 659, 1256-1265.

Burt, B. & Ramey, B. (2020) U.S. Power Industry Outlook 2021. *Turbomachinery Magazine, Handbook 2021*. [Online]. Available at: https://www.turbomachinerymag.com/view/u-s-power-industry-outlook-2021. [Accessed 27th May 2021].

Byers, E. A., Hall, J. W. & Amezaga, J. M. (2014) Electricity generation and cooling water use: UK pathways to 2050. *Global Environmental Change,* 25**,** 16-30.

Caissie, D. (2006) The thermal regime of rivers: a review. *Freshwater Biology*, 51(8), 1389-1406.

Caissie, D., El-Jabi, N. & Satish, M. G. (2001) Modelling of maximum daily water temperatures in a small stream using air temperatures. *Journal of Hydrology,* 251(1)**,** 14-28.

Caissie, D., El-Jabi, N. and St-Hilaire, A. (1998) Stochastic modelling of water temperatures in a small stream using air to water relations. *Canadian Journal of Civil Engineering*, 25(2), 250-260.

Caissie, D., Satish, M. G. and El-Jabi, N. (2007) Predicting water temperatures using a deterministic model: Application on Miramichi River catchments (New Brunswick, Canada). *Journal of Hydrology*, 336(3), 303-315.

Calosi, P., Bilton, D. T. and Spicer, J. I. (2008) Thermal tolerance, acclimatory capacity and vulnerability to global climate change. *Biology Letters*, 4(1), 99-102.

CARMA – Carbon Monitoring for Action. (2021) *Carbon Monitoring for Action*. Available at: https://www.cgdev.org/topics/carbon-monitoring-action. [Accessed 27th May 2021].

Chang, C.-W., Wangm, Y. T. and Tzeng, W.-N. (2010) Morphological study on vertebral deformity of the thornfish Terapon jarbua in the thermal effluent outlet of a nuclear power plant in Taiwan. *J Fish Soc Taiwan*, 37, 1-11.

Chen, Z., Farrell, A. P., Matala, A., Hoffman, N. and Narum, S. R. (2018a) Physiological and genomic signatures of evolutionary thermal adaptation in redband trout from extreme climates. *Evolutionary Applications*, 11(9), 1686-1699.

Chen, X., Wang, Y.-h., Ye, C., Zhou, W., Cai, Z.-c., Yang, H. and Han, X. (2018b) Atmospheric Nitrogen Deposition Associated with the Eutrophication of Taihu Lake. *Journal of Chemistry*, 2018, 1-10.

Claireaux, G., Webber, D. M., Lagardère, J. P. and Kerr, S. R. (2000) Influence of water temperature and oxygenation on the aerobic metabolic scope of Atlantic cod (Gadus morhua). *Journal of Sea Research*, 44(3), 257-265.

Clusella-Trullas, S., Garcia, R. A., Terblanche, J. S. and Hoffmann, A. A. (2021) How useful are thermal vulnerability indices? *Trends Ecol Evol*, 36(11), 1000-1010.

Cobas, M., Danko, A. S., Pazos, M. and Sanromán, M. A. (2016) Removal of metal and organic pollutants from wastewater by a sequential selective technique. *Bioresource*

Technology, 213, 2-10.

Cook, M. A., King, C. W., Davidson, F. T. and Webber, M. E. (2015) Assessing the impacts of droughts and heat waves at thermoelectric power plants in the United States using integrated regression, thermodynamic, and climate models. *Energy Reports*, 1, 193-203.

Cottin, D., Roussel, D., Foucreau, N., Hervant, F. and Piscart, C. (2012) Disentangling the effects of local and regional factors on the thermal tolerance of freshwater crustaceans. *Naturwissenschaften*, 99(4), 259-264.

Cox, M. M. and Bolte, J. P. (2007) A spatially explicit network-based model for estimating stream temperature distribution. *Environmental Modelling & Software*, 22(4), 502-514.

Dallas, H. F. and Ketley, Z. A. (2011) Upper thermal limits of aquatic macroinvertebrates: Comparing critical thermal maxima with 96-LT50 values. *Journal of Thermal Biology*, 36(6), 322-327.

Dallas, H. F. and Rivers-Moore, N. A. (2012) Critical Thermal Maxima of aquatic macroinvertebrates: towards identifying bioindicators of thermal alteration. *Hydrobiologia*, 679(1), 61-76.

Delnat, V., Tran, T. T., Janssens, L. and Stoks, R. (2019) Daily temperature variation magnifies the toxicity of a mixture consisting of a chemical pesticide and a biopesticide in a vector mosquito. *Science of The Total Environment*, 659, 33-40.

de Paul Obade, V. and Moore, R. (2018) Synthesizing water quality indicators from standardized geospatial information to remedy water security challenges: A review. Environment International, 119, 220-231.

Deng, S., Chen, T., Yang, N., Qu, L., Li, M. and Chen, D. (2018) Spatial and temporal distribution of rainfall and drought characteristics across the Pearl River basin. *Science of The Total Environment*, 619-620, 28-41.

Díaz-Morales, D. M., Khosravi, M., Grabner, D. S., Nahar, N., Bommarito, C., Wahl, M. and Sures, B. (2023) The trematode Podocotyle atomon modulates biochemical responses of Gammarus locusta to thermal stress but not its feeding rate or survival. *Science of The Total Environment*, 858, 159946.

Dick, J. T. A. (1995) The cannibalistic behaviour of two Gammarus species (Crustacea: Amphipoda). *Journal of Zoology*, 236(4), 697-706.

Dittmar, M. (2012) Nuclear energy: Status and future limitations. *Energy*, 37(1), 35-40.

Dugdale, S. J., Bergeron, N. E. and St-Hilaire, A. (2015) Spatial distribution of thermal refuges analysed in relation to riverscape hydromorphology using airborne thermal infrared imagery. *Remote Sensing of Environment*, 160, 43-55.

Dugdale, S. J., Franssen, J., Corey, E., Bergeron, N. E., Lapointe, M. and Cunjak, R. A. (2016) Main stem movement of Atlantic salmon parr in response to high river temperature. *Ecology of Freshwater Fish*, 25(3), 429-445.

Dugdale, S. J., Hannah, D. M. and Malcolm, I. A. (2017) River temperature modelling: A review of process-based approaches and future directions. *Earth-Science Reviews*, 175, 97-113.

Dugdale, S. J., Hannah, D. M. and Malcolm, I. A. (2020) An evaluation of different forest cover geospatial data for riparian shading and river temperature modelling. *River Research and Applications*, 36(5), 709-723.

Dugdale, S. J., Malcolm, I. A. and Hannah, D. M. (2019) Drone-based Structure-from-Motion provides accurate forest canopy data to assess shading effects in river temperature models. *Science of The Total Environment*, 678, 326-340.

Dugdale, S. J., Malcolm, I. A., Kantola, K. and Hannah, D. M. (2018) Stream temperature under contrasting riparian forest cover: Understanding thermal dynamics and heat exchange processes. *Science of The Total Environment*, 610-611, 1375-1389.

Durance, I. & Ormerod, S. J. (2009) Trends in water quality and discharge confound long-term warming effects on river macroinvertebrates. *Freshwater Biology,* 54(2)**,** 388-405.

Environment Agency (2016) Standard rules SR2010No2 – discharge to surface water: cooling water and heat exchangers.

EEA – European Environment Agency (2009) *Water resources across Europe — confronting water scarcity and drought.* Copenhagen: European Environment Agency.

EIA – U.S. Energy Information Administration (2008) *Form EIA-923 detailed data with previous form data (EIA-906/920).* Available at: https://www.eia.gov/electricity/data/eia923/archive/xls/f923_2008.zip. [Accessed 27th May 2021].

EIA – U.S. Energy Information Administration (2014) *Many newer power plants have cooling systems that reuse water.* Available at: https://www.eia.gov/todayinenergy/detail.php?id=14971 [Accessed 27th May 2021].

EIA – U.S. Energy Information Administration (2019) *Natural gas-fired reciprocating engines are being deployed more to balance renewables*. Available at: https://www.eia.gov/todayinenergy/detail.php?id=37972. [Accessed 27th May 2021].

El-Ghorab, E. A. S. (2013) Physical model to investigate the effect of the thermal discharge on the mixing zone (Case Study: North Giza Power Plant, Egypt). *Alexandria Engineering Journal*, 52(2), 175-185.

Energy Justice Network (2021) *Basic Facility Search*. Available at: http://www.energyjustice.net/map/searchfacility-basic.php. [Accessed 27th May 2021].

ENTSO-E - European Network of Transmission System Operators for Electricity (2017) *ENTSO-E Mission Statement*. Available at: https://www.entsoe.eu/about/inside-entsoe/objectives/. [Accessed 27th May 2021].

Environment Agency (2022) *Surface Water Temperature Archive up to 2007*. Available at: https://www.data.gov.uk/dataset/d1f77818-9cc4-430e-a970-f386c5d835eb/surface-water-temperature-archive-up-to-2007 [Accessed 7th March 2023].

European Community (2006) Directive 2006/44/EC of the European Parliament and of the Council of 6 September 2006 on the quality of fresh waters needing protection or improvement in order to support fish life.

Everall, N., Johnson, M., Wilby, R. and Bennett, C. (2014) Detecting phenology change in the mayfly Ephemera danica: Responses to spatial and temporal water temperature variations. *Ecological Entomology*, 40.

Everatt, M. J., Bale, J. S., Convey, P., Worland, M. R. and Hayward, S. A. L. (2013) The effect of acclimation temperature on thermal activity thresholds in polar terrestrial invertebrates. *Journal of Insect Physiology*, 59(10), 1057-1064.

Farmer, T. M., Marschall, E. A., Dabrowski, K. and Ludsin, S. A. (2015) Short winters threaten temperate fish populations. *Nature Communications*, 6(1), 7724.

Feigl, M., Lebiedzinski, K., Herrnegger, M. and Schulz, K. (2021) Machine-learning methods for stream water temperature prediction. *Hydrology and Earth System Sciences*,

25(5), 2951-2977.

Feller, M. C. (1981) Effects of clearcutting and slashburning on stream temperature in southwestern British Columbia. *JAWRA Journal of the American Water Resources Association,* 17(5)**,** 863-867.

Feng, M., Zolezzi, G. and Pusch, M. (2018) Effects of thermopeaking on the thermal response of alpine river systems to heatwaves. *Science of The Total Environment*, 612, 1266-1275.

Feng, X., Porporato, A. and Rodriguez-Iturbe, I. (2013) Changes in rainfall seasonality in the tropics. *Nature Climate Change*, 3(9), 811-815.

Ferchichi, H. and St-Hilaire, A. (2023) Are temperature time series measured at hydrometric stations representative of the river's thermal regime? *Canadian Water Resources Journal / Revue canadienne des ressources hydriques*, 48(2), 149-166.

Ferguson, B., Fisher, K., Golden, J., Hair, L., Haselbach, L., Hitchcock, D., Kaloush, K., Pomerantz, M., Tran, N. & Waye, D. (2008) Reducing Urban Heat Islands: Compendium of Strategies - Cool Pavements.

Ferris, R. and Wilson, R. S. (2012) The physiological arms race: Exploring thermal acclimation among interacting species. *Journal of Thermal Biology*, 37(3), 236-242.

Ficke, A. D., Myrick, C. A. and Hansen, L. J. (2007) Potential impacts of global climate change on freshwater fisheries. *Reviews in Fish Biology and Fisheries*, 17(4), 581-613.

Ficklin, D. L., Hannah, D. M., Wanders, N., Dugdale, S. J., England, J., Klaus, J., Kelleher, C., Khamis, K. and Charlton, M. B. (2023) Rethinking river water temperature in a changing, human-dominated world. *Nature Water*, 1(2), 125-128.

Firkus, T., Rahel, F. J., Bergman, H. L. and Cherrington, B. D. (2018) Warmed Winter Water Temperatures Alter Reproduction in Two Fish Species. *Environmental Management*, 61(2), 291-303.

Folguera, G., Bastías, D. A., Caers, J., Rojas, J. M., Piulachs, M.-D., Bellés, X. and Bozinovic, F. (2011) An experimental test of the role of environmental temperature variability on ectotherm molecular, physiological and life-history traits: Implications for global warming. *Comparative Biochemistry and Physiology Part A: Molecular & Integrative Physiology*, 159(3), 242-246.

Forster, J., Hirst, A. G. and Atkinson, D. (2012) Warming-induced reductions in body size are

greater in aquatic than terrestrial species. *Proceedings of the National Academy of Sciences*, 109(47), 19310-19314.

Förster, H. and Lilliestam, J. (2010) Modeling thermoelectric power generation in view of climate change. *Regional Environmental Change*, 10(4), 327-338.

Foucreau, N., Cottin, D., Piscart, C. and Hervant, F. (2014) Physiological and metabolic responses to rising temperature in Gammarus pulex (Crustacea) populations living under continental or Mediterranean climates. *Comparative Biochemistry and Physiology Part A: Molecular & Integrative Physiology*, 168, 69-75.

Foucreau, N., Piscart, C., Puijalon, S. and Hervant, F. (2013) Effect of Climate-Related Change in Vegetation on Leaf Litter Consumption and Energy Storage by Gammarus pulex from Continental or Mediterranean Populations. *PLOS ONE*, 8(10), e77242.

Frechette, D. M., Dugdale, S. J., Dodson, J. J. and Bergeron, N. E. (2018) Understanding summertime thermal refuge use by adult Atlantic salmon using remote sensing, river temperature monitoring, and acoustic telemetry. *Canadian Journal of Fisheries and Aquatic Sciences*, 75(11), 1999-2010.

Fullerton, A. H., Torgersen, C. E., Lawler, J. J., Faux, R. N., Steel, E. A., Beechie, T. J., Ebersole, J. L. and Leibowitz, S. G. (2015) Rethinking the longitudinal stream temperature paradigm: region-wide comparison of thermal infrared imagery reveals unexpected complexity of river temperatures. *Hydrological Processes*, 29(22), 4719-4737.

Fullerton, A. H., Torgersen, C. E., Lawler, J. J., Steel, E. A., Ebersole, J. L. and Lee, S. Y. (2017) Longitudinal thermal heterogeneity in rivers and refugia for coldwater species: effects of scale and climate change. *Aquatic Sciences*, 80(1), 3.

Garner, G., Malcolm, I. A., Sadler, J. P. and Hannah, D. M. (2017) The role of riparian vegetation density, channel orientation and water velocity in determining river temperature dynamics. *Journal of Hydrology*, 553, 471-485.

Gaudard, A., Weber, C., Alexander, T. J., Hunziker, S. and Schmid, M. (2018) Impacts of using lakes and rivers for extraction and disposal of heat. *WIREs Water*, 5(5), e1295.

GEO - Global Energy Observatory (2017) *Help File for Navigating Power Plants Data, Global Energy Observatory*. Available at: http://globalenergyobservatory.org/docs/HelpGeoPower.php. [Accessed 27th May 2021].

Gergs, R., Schlag, L. and Rothhaupt, K.-O. (2013) Different ammonia tolerances may facilitate spatial coexistence of Gammarus roeselii and the strong invader Dikerogammarus villosus. *Biological Invasions*, 15(8), 1783-1793.

Gerhardt, A., Kienle, C., Allan, I. J., Greenwood, R., Guigues, N., Fouillac, A.-M., Mills, G. A. and Gonzalez, C. (2007) Biomonitoring with Gammarus pulex at the Meuse (NL), Aller (GER) and Rhine (F) rivers with the online Multispecies Freshwater Biomonitor®. *Journal of Environmental Monitoring*, 9(9), 979-985.

Gilbert, M. J. H. and Farrell, A. P. (2021) The thermal acclimation potential of maximum heart rate and cardiac heat tolerance in Arctic char (Salvelinus alpinus), a northern cold-water specialist. *Journal of Thermal Biology*, 95, 102816.

Gilbert, H. E., Rosado, P. J., Ban-Weiss, G., Harvey, J. T., Li, H., Mandel, B. H., Millstein, D., Mohegh, A., Saboori, A. & Levinson, R. M. (2017) Energy and environmental consequences of a cool pavement campaign. *Energy and Buildings,* 157**,** 53-77.

Global Energy Monitor (2022a) *Joliet 9 Generating Station.* Available at: https://www.gem.wiki/Joliet_9_Generating_Station [Accessed 13th May 2023].

Global Energy Monitor (2022b) *Joliet 29 Generating Station.* Available at: https://www.gem.wiki/Joliet_29_Generating_Station [Accessed 13th May 2023].

Glose, A., Lautz, L. K. & Baker, E. A. (2017) Stream heat budget modeling with HFLUX: Model development, evaluation, and applications across contrasting sites and seasons. *Environmental Modelling & Software,* 92**,** 213-228.

González-Tokman, D., Córdoba-Aguilar, A., Dáttilo, W., Lira-Noriega, A., Sánchez-Guillén, R. A. and Villalobos, F. (2020) Insect responses to heat: physiological mechanisms, evolution and ecological implications in a warming world. *Biological Reviews*, 95(3), 802-821.

Gosse, P. and Samie, R. (2020) Water evaporation at wet-cooled nuclear power plants on river banks: Application to the French Rhône river. *Water-Energy Nexus*, 3, 155-169.

Gotzens, F., Heinrichs, H., Hörsch, J. and Hofmann, F. (2019) Performing energy modelling exercises in a transparent way - The issue of data quality in power plant databases. *Energy Strategy Reviews*, 23, 1-12.

Grabner, D. S., Schertzinger, G. and Sures, B. (2014) Effect of multiple microsporidian infections and temperature stress on the heat shock protein 70 (hsp70) response of

the amphipod Gammarus pulex. *Parasit Vectors*, 7, 170.

Graf, R. and Aghelpour, P. (2021) Daily River Water Temperature Prediction: A Comparison between Neural Network and Stochastic Techniques. *Atmosphere*, 12(9), 1154.

Grill, G., Lehner, B., Lumsdon, A. E., MacDonald, G. K., Zarfl, C. & Reidy Liermann, C. (2015) An index-based framework for assessing patterns and trends in river fragmentation and flow regulation by global dams at multiple scales. *Environmental Research Letters,* 10(1)**,** 015001.

Gulyás, M., Bencsik, N., Pusztai, S., Liliom, H. and Schlett, K. (2016) AnimalTracker: An ImageJ-Based Tracking API to Create a Customized Behaviour Analyser Program. *Neuroinformatics*, 14(4), 479-481.

Hahn, T. (2005) Respiration rates in bithynia tentaculata (l.) (gastropoda: bithyniidae) in response to acclimation temperature and acute temperature change. *Journal of Molluscan Studies,* 71(2)**,** 127-131.

Hannah, D. M. and Garner, G. (2015) River water temperature in the United Kingdom: Changes over the 20th century and possible changes over the 21st century. *Progress in Physical Geography: Earth and Environment*, 39(1), 68-92.

Hebert, C., Caissie, D., Satish, M. G. and El-Jabi, N. (2011) Study of stream temperature dynamics and corresponding heat fluxes within Miramichi River catchments (New Brunswick, Canada). *Hydrological Processes*, 25(15), 2439-2455.

Henry, C. L. and Pratson, L. F. (2019) Differentiating the Effects of Climate Change-Induced Temperature and Streamflow Changes on the Vulnerability of Once-Through Thermoelectric Power Plants. *Environmental Science & Technology*, 53(7), 3969-3976.

Herb, W. R., Janke, B., Mohseni, O. & Stefan, H. G. (2008) Thermal pollution of streams by runoff from paved surfaces. *Hydrological Processes,* 22(7)**,** 987-999.

Herb, W. R., Mohseni, O. & Stefan, H. G. (2009) Simulation of Temperature Mitigation by a Stormwater Detention Pond. *JAWRA Journal of the American Water Resources Association,* 45(5)**,** 1164-1178.

Hester, E. T. and Doyle, M. W. (2011) Human Impacts to River Temperature and Their Effects on Biological Processes: A Quantitative Synthesis1. *JAWRA Journal of the American Water Resources Association*, 47(3), 571-587.

Higashino, M. & Stefan, H. G. (2016) Water temperature dynamics and heat transport in a typical Japanese river. *Environmental Earth Sciences,* 75(7)**,** 618.

Hiley, C. (2023) *Peak and off-peak electricity times: why is electricity cheaper at night?* Available at: https://lookaftermybills.com/energy/peak-off-peak-energy-times/ [Accessed 27th March 2024].

Hitt, N. P., Snook, E. L. and Massie, D. L. (2017) Brook trout use of thermal refugia and foraging habitat influenced by brown trout. *Canadian Journal of Fisheries and Aquatic Sciences*, 74(3), 406-418.

Hoang, H., Recknagel, F., Marshall, J. & Choy, S. (2006) Elucidation of Hypothetical Relationships between Habitat Conditions and Macroinvertebrate Assemblages in Freshwater Streams by Artificial Neural Networks. *In:* Recknagel, F. (ed.) *Ecological Informatics: Scope, Techniques and Applications.* Berlin: Springer. 239-251.

Hofmann, G. E., Buckley, B. A., Airaksinen, S., Keen, J. E. and Somero, G. N. (2000) Heat-shock protein expression is absent in the antarctic fish Trematomus bernacchii (family Nototheniidae). *J Exp Biol*, 203(Pt 15), 2331-2339.

Hofmann, G. E. and Todgham, A. E. (2010) Living in the Now: Physiological Mechanisms to Tolerate a Rapidly Changing Environment. *Annual Review of Physiology*, 72(1), 127-145.

Hogg, I. D. & Williams, D. D. (1996) Response of Stream Invertebrates to a Global-Warming Thermal Regime: An Ecosystem-Level Manipulation. *Ecology,* 77(2)**,** 395-407.

Huang, X. P., Huang, L. M. and Yue, W. Z. (2003) The characteristics of nutrients and eutrophication in the Pearl River estuary, South China. *Mar Pollut Bull*, 47(1-6), 30-36.

Iacarella, J. C., Dick, J. T. A., Alexander, M. E. and Ricciardi, A. (2015) Ecological impacts of invasive alien species along temperature gradients: testing the role of environmental matching. *Ecological Applications*, 25(3), 706-716.

Ifran, U. (2021) *What's the worst that could happen? These five climate scenarios show us what the future of the planet could look like.* [Online]. Available at: https://www.vox.com/22620706/climate-change-ipcc-report-2021-ssp-scenario-future-warming [Accessed 5th June 2022].

International Energy Agency (IEA) (2013) *World Energy Outlook 2013.*

IPBES (2017) *Media Release: Nature's Dangerous Decline 'Unprecedented'; Species Extinction Rates 'Accelerating'* [Online]. Available at: https://ipbes.net/news/Media-Release-Global-Assessment [Accessed 11th June 2020].

Isaak, D. J., Wollrab, S., Horan, D. and Chandler, G. (2012) Climate change effects on stream and river temperatures across the northwest U.S. from 1980–2009 and implications for salmonid fishes. *Climatic Change*, 113(2), 499-524.

Issakhov, A. and Zhandaulet, Y. (2021) Thermal pollution zones on the aquatic environment from the coastal power plant: Numerical study. *Case Studies in Thermal Engineering*, 25, 100901.

Ibrahim, S. M. A., Ibrahim, M. M. A. and Attia, S. I. (2014) The Impact of Climate Changes on the Thermal Performance of a Proposed Pressurized Water Reactor: Nuclear-Power Plant. *International Journal of Nuclear Energy*, 2014, 793908.

Jackson, C. R., Sturm, C. A. & Ward, J. M. (2001) Timber Harvest Impacts On Small Headwater Stream Channels In The Coast Ranges Of Washington. *JAWRA Journal of the American Water Resources Association,* 37(6)**,** 1533-1549.

Jackson, F. L., Hannah, D. M., Ouellet, V. and Malcolm, I. A. (2021) A deterministic river temperature model to prioritize management of riparian woodlands to reduce summer maximum river temperatures. *Hydrological Processes*, 35(8).

Janke, B. D., Herb, W. R., Mohseni, O. & Stefan, H. G. (2013) Case Study of Simulation of Heat Export by Rainfall Runoff from a Small Urban Watershed Using MINUHET. *Journal of Hydrologic Engineering,* 18(8)**,** 995-1006.

Jeong, D. I., Daigle, A. and St-Hilaire, A. (2013) Development of a stochastic water temperature model and projection of future water temperature and extreme events in the Ouelle River basin in Québec, Canada. *River Research and Applications*, 29(7), 805-821.

Jesse, B.-J., Morgenthaler, S., Gillessen, B., Burges, S. and Kuckshinrichs, W. (2020) Potential for Optimization in European Power Plant Fleet Operation. *Energies*, 13(3), 718.

Jiang, B., Wang, F. S. & Ni, G. H. (2018) Heating Impact of a Tropical Reservoir on Downstream Water Temperature: A Case Study of the Jinghong Dam on the Lancang River. *Water,* 10(7)**,** 24.

Johnson, A., Loh, E., Verbitsky, R., Slessor, J., Franczak, B. C., Schalomon, M. and Hamilton, T. J. (2023) Examining behavioural test sensitivity and locomotor proxies of anxiety-like behaviour in zebrafish. *Scientific Reports*, 13(1), 3768.

Johnson, M. F. and Wilby, R. L. (2015) Seeing the landscape for the trees: Metrics to guide riparian shade management in river catchments. *Water Resources Research*, 51(5), 3754-3769.

Johnson, M. F., Wilby, R. L. and Toone, J. A. (2014) Inferring air–water temperature relationships from river and catchment properties. *Hydrological Processes*, 28(6), 2912-2928.

Johnson, M. P., Rybalov, L., Zhao, L. and Bald, S. (2019) Maximizing power production in path and tree riverine networks. *Sustainable Computing: Informatics and Systems*, 22, 300-310.

Johnson, S. L. & Jones, J. A. (2000) Stream temperature responses to forest harvest and debris flows in western Cascades, Oregon. *Canadian Journal of Fisheries and Aquatic Sciences,* 57(S2)**,** 30-39.

Jyväsjärvi, J., Marttila, H., Rossi, P. M., Ala-Aho, P., Olofsson, B., Nisell, J., Backman, B., Ilmonen, J., Virtanen, R., Paasivirta, L., Britschgi, R., Kløve, B. and Muotka, T. (2015) Climate-induced warming imposes a threat to north European spring ecosystems. *Global Change Biology*, 21(12), 4561-4569.

Kaka, H., Opute, P. A. and Maboeta, M. S. (2021) Potential Impacts of Climate Change on the Toxicity of Pesticides towards Earthworms. *Journal of Toxicology*, 2021, 8527991.

Kalinowska, M. B., Rowiński, P. M., Kubrak, J. and Mirosław-Świątek, D. (2012) Scenarios of the spread of a waste heat discharge in a river — Vistula River case study. *Acta Geophysica*, 60(1), 214-231.

Kanno, Y., Kim, S. and Pregler, K. C. (2023) Sub-seasonal correlation between growth and survival in three sympatric aquatic ectotherms. *Oikos*, 2023(3), e09685.

Kazmi, S. S. U. H., Wang, Y. Y. L., Cai, Y.-E. and Wang, Z. (2022) Temperature effects in single or combined with chemicals to the aquatic organisms: An overview of thermo-chemical stress. *Ecological Indicators*, 143, 109354.

Kefford, B. J., Ghalambor, C. K., Dewenter, B., Poff, N. L., Hughes, J., Reich, J. and Thompson, R. (2022) Acute, diel, and annual temperature variability and the thermal

biology of ectotherms. *Glob Chang Biol*, 28(23), 6872-6888.

Kelly, D. W., Dick, J. T. A. and Montgomery, W. I. (2002) The functional role of Gammarus(Crustacea, Amphipoda): shredders, predators, or both? *Hydrobiologia*, 485(1), 199-203.

Kenna, D., Fincham, W. N. W., Dunn, A. M., Brown, L. E. and Hassall, C. (2017) Antagonistic effects of biological invasion and environmental warming on detritus processing in freshwater ecosystems. *Oecologia*, 183(3), 875-886.

Kenny, J. F., Barber, N. L., Hutson, S. S., Linsey, K. S., Lovelace, J. K. and Maupin, M. A. (2005) *Estimated Use of Water in the United States in 2005.* U.S. Geological Survey Circular 1344. 52p.

Kenny, J. F., Barber, N. L., Hutson, S. S., Linsey, K. S., Lovelace, J. K. and Maupin, M. A. (2009) Estimated use of water in the United States in 2005. Circular. Reston, VA**:** 60.

Kern, P., Cramp, R. L. and Franklin, C. E. (2015) Physiological responses of ectotherms to daily temperature variation. *Journal of Experimental Biology*, 218(19), 3068-3076.

Ketabchy, M., Sample, D. J., Wynn-Thompson, T. & Yazdi, M. N. (2019) Simulation of watershed-scale practices for mitigating stream thermal pollution due to urbanization. *Science of The Total Environment,* 671**,** 215-231.

Kinouchi, T. (2007) Impact of long-term water and energy consumption in Tokyo on wastewater effluent: implications for the thermal degradation of urban streams. *Hydrological Processes*, 21(9), 1207-1216.

Kinouchi, T., Yagi, H. & Miyamoto, M. (2007) Increase in stream temperature related to anthropogenic heat input from urban wastewater. *Journal of Hydrology,* 335(1)**,** 78-88.

Kirillin, G., Shatwell, T. and Kasprzak, P. (2013) Consequences of thermal pollution from a nuclear plant on lake temperature and mixing regime. *Journal of Hydrology*, 496, 47-56.

Klaar, M. J., Shelley, F. S., Hannah, D. M. and Krause, S. (2020) Instream wood increases riverbed temperature variability in a lowland sandy stream. *River Research and Applications*, 36(8), 1529-1542.

Kosaka, Y. and Xie, S.-P. (2013) Recent global-warming hiatus tied to equatorial Pacific surface cooling. *Nature*, 501(7467), 403-407.

Kültz, D. (2003) Evolution of the cellular stress proteome: from monophyletic origin to

ubiquitous function. *J Exp Biol*, 206(Pt 18), 3119-3124.

Kumar, P. (2013) Seasonal rain changes. *Nature Climate Change*, 3(9), 783-784.

Kumar, A. S., Kouveliotis-Lysikatos, I., Nycander, E., Olauson, J., Marin, M., Amelin, M. and Söder, L. (2021). Open Nodal Power Flow Model of the Nordic Power System. 2021 IEEE Madrid PowerTech.

Kuriqi, A., Pinheiro, A. N., Sordo-Ward, A., Bejarano, M. D. and Garrote, L. (2021) Ecological impacts of run-of-river hydropower plants—Current status and future prospects on the brink of energy transition. *Renewable and Sustainable Energy Reviews*, 142, 110833.

Kurylyk, B. L., MacQuarrie, K. T. B., Linnansaari, T., Cunjak, R. A. and Curry, R. A. (2015) Preserving, augmenting, and creating cold-water thermal refugia in rivers: concepts derived from research on the Miramichi River, New Brunswick (Canada). *Ecohydrology*, 8(6), 1095-1108.

Kurylyk, B. L., MacQuarrie, K. T. B. and Voss, C. I. (2014) Climate change impacts on the temperature and magnitude of groundwater discharge from shallow, unconfined aquifers. *Water Resources Research*, 50(4), 3253-3274.

Lagerspetz, K. Y. H. and Vainio, L. A. (2006) Thermal behaviour of crustaceans. *Biological Reviews*, 81(2), 237-258.

Lancaster, L. T., Dudaniec, R. Y., Hansson, B. and Svensson, E. I. (2015) Latitudinal shift in thermal niche breadth results from thermal release during a climate-mediated range expansion. *Journal of Biogeography*, 42(10), 1953-1963.

Langford, T. E. (1971) The distribution, abundance and life-histories of stoneflies (Plecoptera) and mayflies (Ephemeroptera) in a British River, warmed by cooling-water from a power station. *Hydrobiologia,* 38(2)**,** 339-377.

Langford, T. E. L. (1990) Ecological effects of thermal discharges.

Langford, T. E. & Aston, R. J. (1972) The ecology of some British rivers in relation to warm water discharges from power stations. *Proceedings of the Royal Society of London. Series B. Biological Sciences,* 180(1061)**,** 407-419.

Langford, T. E. & Daffern, J. R. (1975) The emergence of insects from a British River warmed by power station cooling-water. *Hydrobiologia,* 46(1)**,** 71-114.

Lebrun, J. D., De Jesus, K., Rouillac, L., Ravelli, M., Guenne, A. and Tournebize, J. (2020) Single and combined effects of insecticides on multi-level biomarkers in the non-

target amphipod Gammarus fossarum exposed to environmentally realistic levels. *Aquatic Toxicology*, 218, 105357.

Lehner, B. and Grill, G. (2013) Global river hydrography and network routing: baseline data and new approaches to study the world's large river systems. *Hydrological Processes*, 27(15): 2171–2186. Data is available at www.hydrosheds.org.

Lehner, B., Liermann, C. R., Revenga, C., Vörösmarty, C., Fekete, B., Crouzet, P., Döll, P., Endejan, M., Frenken, K., Magome, J., Nilsson, C., Robertson, J. C., Rödel, R., Sindorf, N. & Wisser, D. (2011) High-resolution mapping of the world's reservoirs and dams for sustainable river-flow management. *Frontiers in Ecology and the Environment,* 9(9)**,** 494-502.

Lessard, J. L. & Hayes, D. B. (2003) Effects of elevated water temperature on fish and macroinvertebrate communities below small dams. *River Research and Applications,* 19(7)**,** 721-732.

Levin, A. A., Birch, T. J., Hillman, R. E. & Raines, G. E. (1972) Thermal Discharges: Ecological Effects. *Environmental Science & Technology,* 6(3)**,** 224-230.

Lewandowski, J., Arnon, S., Banks, E., Batelaan, O., Betterle, A., Broecker, T., Coll, C., Drummond, J. D., Gaona Garcia, J., Galloway, J., Gomez-Velez, J., Grabowski, R. C., Herzog, S. P., Hinkelmann, R., Höhne, A., Hollender, J., Horn, M. A., Jaeger, A., Krause, S., Löchner Prats, A., Magliozzi, C., Meinikmann, K., Mojarrad, B. B., Mueller, B. M., Peralta-Maraver, I., Popp, A. L., Posselt, M., Putschew, A., Radke, M., Raza, M., Riml, J., Robertson, A., Rutere, C., Schaper, J. L., Schirmer, M., Schulz, H., Shanafield, M., Singh, T., Ward, A. S., Wolke, P., Wörman, A. and Wu, L. (2019) Is the Hyporheic Zone Relevant beyond the Scientific Community? *Water*, 11(11), 2230.

Li, D. & Wang, J. (2018) Study of supercritical power plant integration with high temperature thermal energy storage for flexible operation. *Journal of Energy Storage,* 20**,** 140-152.

Li, Z. (2014) Watershed modeling using arc hydro based on DEMs: a case study in Jackpine watershed. *Environmental Systems Research*, 3(11), 12pp.

Liliana, T. (2012) Data on influence of cooling water discharge from Cernavodă Nuclear Power Plant on Danube River phytoplankton development. *Scientific Annals of the Danube Delta Institute*, 18, 249-260.

Lin, W. T., Chou, W. C., Lin, C. Y., Huang, P. H. & Tsai, J. S. (2008) WinBasin: using improved algorithms and the GIS technique for automated watershed modelling analysis from

digital elevation models. *International Journal of Geographical Information Science,* 22(1/2). 47–69.

Ling, F., Foody, G. M., Du, H., Ban, X., Li, X. D., Zhang, Y. H. & Du, Y. (2017) Monitoring Thermal Pollution in Rivers Downstream of Dams with Landsat ETM plus Thermal Infrared Images. *Remote Sensing,* 9(11)**,** 16.

Liu, W. and Qiu, R. (2007) Water eutrophication in China and the combating strategies. *Journal of Chemical Technology & Biotechnology*, 82(9), 781-786.

Logan, L. H. and Stillwell, A. S. (2018) Probabilistic assessment of aquatic species risk from thermoelectric power plant effluent: Incorporating biology into the energy-water nexus. *Applied Energy*, 210, 434-450.

Lüderwald, S., Schell, T., Newton, K., Salau, R., Seitz, F., Rosenfeldt, R. R., Dackermann, V., Metreveli, G., Schulz, R. and Bundschuh, M. (2019) Exposure pathway dependent effects of titanium dioxide and silver nanoparticles on the benthic amphipod Gammarus fossarum. *Aquatic Toxicology*, 212, 47-53.

Lynch, A. J., Myers, B. J. E., Chu, C., Eby, L. A., Falke, J. A., Kovach, R. P., Krabbenhoft, T. J., Kwak, T. J., Lyons, J., Paukert, C. P. and Whitney, J. E. (2016) Climate Change Effects on North American Inland Fish Populations and Assemblages. *Fisheries*, 41(7), 346-361.

Ma, P., Dai, X., Guo, Z., Wei, C. and Ma, W. (2017) Detection of thermal pollution from power plants on China's eastern coast using remote sensing data. *Stochastic Environmental Research and Risk Assessment*, 31(8), 1957-1975.

Maazouzi, C., Piscart, C., Legier, F. and Hervant, F. (2011) Ecophysiological responses to temperature of the "killer shrimp" Dikerogammarus villosus: Is the invader really stronger than the native Gammarus pulex? *Comparative Biochemistry and Physiology Part A: Molecular & Integrative Physiology*, 159(3), 268-274.

MacDonald, R. J., Boon, S. and Byrne, J. M. (2014) A process-based stream temperature modelling approach for mountain regions. *Journal of Hydrology*, 511, 920-931.

MacNeil, C., Dick, J. T. A., Gell, F. R., Selman, R., Lenartowicz, P. and Hynes, H. B. N. (2009) A long-term study (1949–2005) of experimental introductions to an island; freshwater amphipods (Crustacea) in the Isle of Man (British Isles). *Diversity and Distributions*, 15(2), 232-241.

Madden, N., Lewis, A. and Davis, M. (2013) Thermal effluent from the power sector: an analysis of once-through cooling system impacts on surface water temperature. *Environmental Research Letters*, 8(3), 035006.

Magurran, A. E. & Henderson, P. A. (2003) Explaining the excess of rare species in natural species abundance distributions. *Nature,* 422(6933)**,** 714-716.

Maier, G., Kley, A., Schank, Y., Maier, M., Mayer, G. and Waloszek, D. (2011) Density and temperature dependent feeding rates in an established and an alien freshwater gammarid fed on chironomid larvae. *Journal of Limnology*, 70(1), 123-128.

Malison, R. L., Frakes, J. I., Andreas, A. L., Keller, P. R., Hamant, E., Shah, A. A. and Woods, H. A. (2022) Plasticity of salmonfly (Pteronarcys californica) respiratory phenotypes in response to changes in temperature and oxygen. *J Exp Biol*, 225(18).

Mameri, D., Hayes, D. S., Führer, S., Fauchery, E., Schmutz, S., Monserat, A., Hasler, T., Graf, D. R. M., Santos, J. M., Ferreira, M. T. and Auer, S. (2023) Cold thermopeaking-induced drift of nase Chondrostoma nasus larvae. *Aquatic Sciences*, 85(2), 56.

MAPSearch (2021) *Electric Power GIS Data*. Available at: https://www.mapsearch.com/gis-asset-data/electric-power-gis-data/. [Accessed 27th May 2021].

Marcos-López, M., Gale, P., Oidtmann, B. C. and Peeler, E. J. (2010) Assessing the Impact of Climate Change on Disease Emergence in Freshwater Fish in the United Kingdom. *Transboundary and Emerging Diseases*, 57(5), 293-304.

Maria, V. D., Rahman, M., Collins, P., Dondi, G. & Sangiorgi, C. (2013) Urban Heat Island Effect: thermal response from different types of exposed paved surfaces. *International Journal of Pavement Research and Technology,* 6(4)**,** 414-422.

McCall, J., Macknick, J. and Hillman, D. (2016) Water-Related Power Plant Curtailments: An Overview of Incidents and Contributing Actors, National Renewable Energy Laboratory (NREL).

McGrane, S. J. (2016) Impacts of urbanisation on hydrological and water quality dynamics, and urban water management: a review. *Hydrological Sciences Journal,* 61(13)**,** 2295-2311.

Menberg, K., Blum, P., Kurylyk, B. L. and Bayer, P. (2014) Observed groundwater temperature response to recent climate change. *Hydrol. Earth Syst. Sci.*, 18(11), 4453-4466.

Mesa, M. G., Weiland, L. K. & Wagner, P. (2002) Effects of acute thermal stress on the survival, predator avoidance, and physiology of juvenile fall chinook salmon. *Northwest Science,* 76(2)**,** 118-128.

Met Office (2019) *Met Office MIDAS Open: UK Land Surface Stations Data (1853-current)*. Centre for Environmental Data Analysis, Available at: http://catalogue.ceda.ac.uk/uuid/dbd451271eb04662beade68da43546e1 [Accessed 16th February 2022].

Miara, A., Vörösmarty, C. J., Macknick, J. E., Tidwell, V. C., Fekete, B., Corsi, F. and Newmark, R. (2018) Thermal pollution impacts on rivers and power supply in the Mississippi River watershed. *Environmental Research Letters*, 13(3), 034033.

Miara, A., Vörösmarty, C. J., Stewart, R. J., Wollheim, W. M. and Rosenzweig, B. (2013) Riverine ecosystem services and the thermoelectric sector: strategic issues facing the Northeastern United States. *Environmental Research Letters*, 8(2), 025017.

Michel, A., Schaefli, B., Wever, N., Zekollari, H., Lehning, M. and Huwald, H. (2022) Future water temperature of rivers in Switzerland under climate change investigated with physics-based models. *Hydrol. Earth Syst. Sci.*, 26(4), 1063-1087.

Mielke, E., Anadon, L. D. & Narayanamurti, V. (2010) *Water Consumption of Energy Resource Extraction, Processing, and Conversion.* Harvard Kennedy School, Belfer Center for Science and International Affairs. 33.

Mint (2021) *Coal-fired power plant development to remain growth driver in India: Fitch.* [Online]. Available at: https://www.livemint.com/industry/energy/coalfired-power-plant-development-to-remain-growth-driver-in-india-fitch-11618312799083.html. [Accessed 27th May 2021].

Moenickes, S., Schneider, A. K., Mühle, L., Rohe, L., Richter, O. and Suhling, F. (2011) From population-level effects to individual response: modelling temperature dependence in Gammarus pulex. *J Exp Biol*, 214(Pt 21), 3678-3687.

Mohseni, O., Erickson, T. R. & Stefan, H. G. (2002) Upper Bounds for Stream Temperatures in the Contiguous United States. *Journal of Environmental Engineering,* 128(1)**,** 4-11.

Mohseni, O., Stefan, H. G. and Erickson, T. R. (1998) A nonlinear regression model for weekly stream temperatures. *Water Resources Research*, 34(10), 2685-2692.

Montzka, S. A., Dlugokencky, E. J. and Butler, J. H. (2011) Non-CO2 greenhouse gases and

climate change. *Nature*, 476(7358), 43-50.

Moore, R. D., Spittlehouse, D. L. & Story, A. (2005) Riparian microclimate and stream temperature response to forest harvesting: a review. *JAWRA Journal of the American Water Resources Association,* 41(4)**,** 813-834.

Moore, R. D., Sutherland, P., Gomi, T. and Dhakal, A. (2005) Thermal regime of a headwater stream within a clear-cut, coastal British Columbia, Canada. *Hydrological Processes*, 19(13), 2591-2608.

Moreira, M., Hayes, D. S., Boavida, I., Schletterer, M., Schmutz, S. and Pinheiro, A. (2019) Ecologically-based criteria for hydropeaking mitigation: A review. *Sci Total Environ*, 657, 1508-1522.

Morgan, R., Finnøen, M. H., Jensen, H., Pélabon, C. and Jutfelt, F. (2020) Low potential for evolutionary rescue from climate change in a tropical fish. *Proceedings of the National Academy of Sciences*, 117(52), 33365-33372.

Morgan, R., Finnøen, M. H. and Jutfelt, F. (2018) CTmax is repeatable and doesn't reduce growth in zebrafish. *Scientific Reports*, 8(1), 7099.

Morgenthaler, S., Dünzen, J., Stadler, I. and Witthaut, D. (2021) Three stages in the co-transformation of the energy and mobility sectors. *Renewable and Sustainable Energy Reviews*, 150, 111494.

Morrison, B. R. S. (1989) The growth of juvenile Atlantic salmon, Salmo salar L., and brown trout, Salmo trutta L., in a Scottish river system subject to cooling-water discharge. *Journal of Fish Biology,* 35(4)**,** 539-556.

Muftin, F. S., Nashaat, M. R. and Farhan, R. K. (2020) The Epipelic Algal Community in Tigris River and the Effect of Rasheed Power Plant Effluents on its Biodiversity. *Journal of Physics: Conference Series*, 1664(1), 012132.

Muschinski, T. and Katz, J. I. (2013) Trends in hourly rainfall statistics in the United States under a warming climate. *Nature Climate Change*, 3(6), 577-580.

Naresh, A. & Rehana, S. (2017) Modeling Stream Water Temperature using Regression Analysis with Air Temperature and Streamflow over Krishna River. *International Journal of Engineering Technology Science and Research,* 4(11)**,** 1292-1302.

Narum, S. R., Campbell, N. R., Meyer, K. A., Miller, M. R. and Hardy, R. W. (2013) Thermal adaptation and acclimation of ectotherms from differing aquatic climates. *Molecular*

Ecology, 22(11), 3090-3097.

NCRWQCB – North Coast Regional Water Quality Control Board (2014) Staff report supporting the policy for the implementation of the water quality objectives for temperature and action plan to address temperature impairment in the Mattole River watershed, action plan to address temperature impairment in the Navarro River watershed, and action plan to address temperature impairment in the Eel River watershed, Santa Rosa, California, USA.

NRDC (2014) Power Plant Cooling and Associated Impacts: The Need to Modernize U.S. Power Plants and Protect Our Water Resources and Aquatic Ecosystems. *NRDC Issue Brief.*

NRFA – UK National River Flow Archive (2022) *Gauged Daily Flows*. Available at: https://nrfa.ceh.ac.uk/data [Accessed 9th April 2022].

Nie, P., Wu, H., Xu, J., Wei, L., Zhu, H. and Ni, L. (2021) Thermal Pollution Monitoring of Tianwan Nuclear Power Plant for the Past 20 Years Based on Landsat Remote Sensed Data. *IEEE Journal of Selected Topics in Applied Earth Observations and Remote Sensing*, 14, 6146-6155.

Nordli, Ø., Przybylak, R., Ogilvie, A. E. J. and Isaksen, K. (2014) Long-term temperature trends and variability on Spitsbergen: the extended Svalbard Airport temperature series, 1898-2012. *Polar Research*, 33(0).

Nyamukondiwa, C., Chidawanyika, F., Machekano, H., Mutamiswa, R., Sands, B., Mgidiswa, N. and Wall, R. (2018) Climate variability differentially impacts thermal fitness traits in three coprophagic beetle species. *PLOS ONE*, 13(6), e0198610.

O'Driscoll, M. A. and DeWalle, D. R. (2006) Stream–air temperature relations to classify stream–ground water interactions in a karst setting, central Pennsylvania, USA. *Journal of Hydrology*, 329(1-2), 140-153.

ODEQ – Oregon Department of Environmental Quality (2008) Rogue River Basin temperature TMDL. In Appendix A: Temperature model calibration report, Portland, Oregon, USA.

ODEQ – Oregon Department of Environmental Quality (2012) Upper Deschutes and Little Deschutes Subbasins TMDLs, Bend, Oregon, USA.

Oksala, N. K. J., Ekmekçi, F. G., Özsoy, E., Kirankaya, Ş., Kokkola, T., Emecen, G., Lappalainen, J., Kaarniranta, K. & Atalay, M. (2014) Natural thermal adaptation

increases heat shock protein levels and decreases oxidative stress. *Redox Biology,* 3**,** 25-28.

Olden, J. D. & Naiman, R. J. (2010) Incorporating thermal regimes into environmental flows assessments: modifying dam operations to restore freshwater ecosystem integrity. *Freshwater Biology,* 55(1)**,** 86-107.

OPSD – Open Power System Data (2020) *A Free and Open Data Platform for Power System Modelling*. Available at: http://open-power-system-data.org. [Accessed 27th May 2021].

Ordnance Survey (2021a) OS MasterMap® Topography Layer [FileGeoDatabase geospatial data], Scale 1:1250, Tiles: GB, Updated: 18 November 2021, Ordnance Survey (GB), Using: EDINA Digimap Ordnance Survey Service, <https://digimap.edina.ac.uk>, Downloaded: 9th February 2022.

Ordnance Survey (2021b) OS Terrain 5 [ASC geospatial data], Scale 1:10000, Tiles: se80ne,se80nw,se80se,se80sw,se81ne,se81nw,se81se,se81sw,se82se,se82sw,sk01ne,sk01se,sk11ne,sk11nw,sk11se,sk11sw,sk12se,sk21ne,sk21nw,sk21sw,sk22ne,sk22nw,sk22se,sk22sw,sk23se,sk32ne,sk32nw,sk32se,sk32sw,sk33se,sk33sw,sk42ne,sk42nw,sk42sw,sk43ne,sk43se,sk43sw,sk52nw,sk53ne,sk53nw,sk53se,sk53sw,sk54se,sk63ne,sk63nw,sk64ne,sk64nw,sk64se,sk64sw,sk65se,sk74ne,sk74nw,sk74sw,sk75ne,sk75se,sk75sw,sk76ne,sk76se,sk77se,sk78ne,sk78se,sk79ne,sk79se,sk85nw,sk85sw,sk86nw,sk86sw,sk87nw,sk87sw,sk88nw,sk88sw,sk89ne,sk89nw,sk89sw, Updated: 13 November 2021, Ordnance Survey (GB), Using: EDINA Digimap Ordnance Survey Service, <https://digimap.edina.ac.uk>, Downloaded: 10th February 2022.

Ouellet, V., St-Hilaire, A., Dugdale, S. J., Hannah, D. M., Krause, S. and Proulx-Ouellet, S. (2020) River temperature research and practice: Recent challenges and emerging opportunities for managing thermal habitat conditions in stream ecosystems. *Science of The Total Environment*, 736, 139679.

Pan, S.-Y., Snyder, S. W., Packman, A. I., Lin, Y. J. and Chiang, P.-C. (2018) Cooling water use in thermoelectric power generation and its associated challenges for addressing water-energy nexus. *Water-Energy Nexus*, 1(1), 26-41.

Panizza, M. and Cerisola, G. (2001) Removal of organic pollutants from industrial wastewater by electrogenerated Fenton's reagent. *Water Research*, 35(16), 3987-3992.

Pankhurst, N. W. and King, H. R. (2010) Temperature and salmonid reproduction: implications for aquaculture. *Journal of Fish Biology*, 76(1), 69-85.

Papadaki, C., Soulis, K., Muñoz-Mas, R., Martinez-Capel, F., Zogaris, S., Ntoanidis, L. and Dimitriou, E. (2016) Potential impacts of climate change on flow regime and fish habitat in mountain rivers of the south-western Balkans. *Science of The Total Environment*, 540, 418-428.

Parzen, M., Abdel-Khalek, H., Fedotova, E., Mahmood, M., Frysztacki, M. M., Hampp, J., Franken, L., Schumm, L., Neumann, F., Poli, D., Kiprakis, A. and Fioriti, D. (2023) PyPSA-Earth. A new global open energy system optimization model demonstrated in Africa. *Applied Energy*, 341, 121096.

Peer, R. A. M. & Sanders, K. T. (2016) Characterizing cooling water source and usage patterns across US thermoelectric power plants: a comprehensive assessment of self-reported cooling water data. *Environmental Research Letters,* 11(12)**,** 124030.

Pellan, L., Médoc, V., Renault, D., Spataro, T. and Piscart, C. (2016) Feeding choice and predation pressure of two invasive gammarids, Gammarus tigrinus and Dikerogammarus villosus, under increasing temperature. *Hydrobiologia*, 781(1), 43-54.

Pfister, S. and Suh, S. (2015) Environmental impacts of thermal emissions to freshwater: spatially explicit fate and effect modeling for life cycle assessment and water footprinting. *The International Journal of Life Cycle Assessment*, 20(7), 927-936.

Pile, B., Warren, D., Hassall, C., Brown, L. E. and Dunn, A. M. (2023) Biological Invasions Affect Resource Processing in Aquatic Ecosystems: The Invasive Amphipod Dikerogammarus villosus Impacts Detritus Processing through High Abundance Rather than Differential Response to Temperature. *Biology*, 12(6), 830.

Pimm, A. J., Cockerill, T. T. and Taylor, P. G. (2018) The potential for peak shaving on low voltage distribution networks using electricity storage. *Journal of Energy Storage*, 16, 231-242.

Pörtner, H. O., Bock, C. and Mark, F. C. (2017) Oxygen- and capacity-limited thermal tolerance: bridging ecology and physiology. *J Exp Biol*, 220(Pt 15), 2685-2696.

Prats, J., Val, R., Armengol, J. and Dolz, J. (2010) Temporal variability in the thermal regime of the lower Ebro River (Spain) and alteration due to anthropogenic factors. *Journal of Hydrology*, 387(1-2), 105-118.

Preece, R. M. & Jones, H. A. (2002) The effect of Keepit Dam on the temperature regime of the Namoi River, Australia. *River Research and Applications,* 18(4)**,** 397-414.

Priya, A. K., Muruganandam, M., Rajamanickam, S., Sivarethinamohan, S., Gaddam, M. K. R., Velusamy, P., R, G., Ravindiran, G., Gurugubelli, T. R. and Muniasamy, S. K. (2023) Impact of climate change and anthropogenic activities on aquatic ecosystem – A review. *Environmental Research*, 238, 117233.

Qin, Y., Curmi, E., Kopec, G. M., Allwood, J. M. & Richards, K. S. (2015) China's energy-water nexus – assessment of the energy sector's compliance with the “3 Red Lines” industrial water policy. *Energy Policy,* 82**,** 131-143.

Rahel, F. J. and Olden, J. D. (2008) Assessing the Effects of Climate Change on Aquatic Invasive Species. *Conservation Biology*, 22(3), 521-533.

Rajesh, M. and Rehana, S. (2022) Impact of climate change on river water temperature and dissolved oxygen: Indian riverine thermal regimes. *Scientific Reports*, 12(1), 9222.

Ramaker, T. A. B., Meuleman, A. F. M., Bernhardi, L. and Cirkel, G. (2005) Climate change and drinking water production in The Netherlands: a flexible approach. *Water Science and Technology*, 51(5), 37-44.

Råman Vinnå, L., Wüest, A. and Bouffard, D. (2017) Physical effects of thermal pollution in lakes. *Water Resources Research*, 53(5), 3968-3987.

Raptis, C. E., Boucher, J. M. and Pfister, S. (2017) Assessing the environmental impacts of freshwater thermal pollution from global power generation in LCA. *Science of The Total Environment*, 580, 1014-1026.

Raptis, C. E. and Pfister, S. (2016) Global freshwater thermal emissions from steam-electric power plants with once-through cooling systems. *Energy*, 97(C), 46-57.

Raptis, C. E., van Vliet, M. T. H. and Pfister, S. (2016) Global thermal pollution of rivers from thermoelectric power plants. *Environmental Research Letters*, 11(10), 104011.

Raths, J., Schnurr, J., Bundschuh, M., Pinto, F. E., Janfelt, C. and Hollender, J. (2023) Importance of Dietary Uptake for in Situ Bioaccumulation of Systemic Fungicides Using Gammarus pulex as a Model Organism. *Environmental Toxicology and Chemistry*, n/a(n/a).

Redondo-Hasselerharm, P. E., Falahudin, D., Peeters, E. T. H. M. and Koelmans, A. A. (2018) Microplastic Effect Thresholds for Freshwater Benthic Macroinvertebrates.

Environmental Science & Technology, 52(4), 2278-2286.

Reid, C. H., Patrick, P. H., Rytwinski, T., Taylor, J. J., Willmore, W. G., Reesor, B. and Cooke, S. J. (2022) An updated review of cold shock and cold stress in fish. *Journal of Fish Biology*, 100(5), 1102-1137.

Ren, J., Shen, Z.-Z., Yang, J., Zhao, J. and Yin, J.-N. (2014) Effects of Temperature and Dry Density on Hydraulic Conductivity of Silty Clay under Infiltration of Low-Temperature Water. *Arabian Journal for Science and Engineering*, 39(1), 461-466.

Riahi, K., Rao, S., Krey, V., Cho, C., Chirkov, V., Fischer, G., Kindermann, G., Nakicenovic, N. and Rafaj, P. (2011) RCP 8.5—A scenario of comparatively high greenhouse gas emissions. *Climatic Change*, 109(1), 33.

Rivers-Moore, N. A., Ramulifho, P. A. and Foord, S. H. (2021) Baetid abundances are a rapid indicator of thermal stress and riparian zone intactness. *Journal of Thermal Biology*, 102, 103125.

Roberts, J. J., Fausch, K. D., Schmidt, T. S. and Walters, D. M. (2017) Thermal regimes of Rocky Mountain lakes warm with climate change. *PLOS ONE*, 12(7), e0179498.

Rosencranz, J., Cuddington, K., Brook, M., Koops, M. A. and Drake, D. A. (2021) Data-limited models to predict river temperatures for aquatic species at risk1. *Canadian Journal of Fisheries and Aquatic Sciences*, 78(9), 1268-1277.

Rosenfeldt, R. R., Seitz, F., Zubrod, J. P., Feckler, A., Merkel, T., Lüderwald, S., Bundschuh, R., Schulz, R. and Bundschuh, M. (2015) Does the presence of titanium dioxide nanoparticles reduce copper toxicity? A factorial approach with the benthic amphipod Gammarus fossarum. *Aquatic Toxicology*, 165, 154-159.

Rossi, A., Bacchetta, C. and Cazenave, J. (2017) Effect of thermal stress on metabolic and oxidative stress biomarkers of Hoplosternum littorale (Teleostei, Callichthyidae). *Ecological Indicators*, 79, 361-370.

Salinas, S., Irvine, S. E., Schertzing, C. L., Golden, S. Q. and Munch, S. B. (2019) Trait variation in extreme thermal environments under constant and fluctuating temperatures. *Philosophical Transactions of the Royal Society B: Biological Sciences*, 374(1768), 20180177.

Schaefer, J. and Ryan, A. (2006) Developmental plasticity in the thermal tolerance of zebrafish Danio rerio. *Journal of Fish Biology*, 69(3), 722-734.

Scranton, K. and Amarasekare, P. (2017) Predicting phenological shifts in a changing climate. *Proc Natl Acad Sci U S A*, 114(50), 13212-13217.

Scrine, J., Jochum, M., Ólafsson, J. S. & O'Gorman, E. J. (2017) Interactive effects of temperature and habitat complexity on freshwater communities. *Ecology and evolution,* 7(22)**,** 9333-9346.

Sears, M. W., Angilletta, M. J., Schuler, M. S., Borchert, J., Dilliplane, K. F., Stegman, M., Rusch, T. W. and Mitchell, W. A. (2016) Configuration of the thermal landscape determines thermoregulatory performance of ectotherms. *Proceedings of the National Academy of Sciences*, 113(38), 10595-10600.

Seebacher, F., White, C. R. and Franklin, C. E. (2015) Physiological plasticity increases resilience of ectothermic animals to climate change. *Nature Climate Change*, 5(1), 61-66.

Semsar-kazerouni, M. and Verberk, W. C. E. P. (2018) It's about time: Linkages between heat tolerance, thermal acclimation and metabolic rate at different temporal scales in the freshwater amphipod Gammarus fossarum Koch, 1836. *Journal of Thermal Biology*, 75, 31-37.

Sexton, E. W. (1928) On the Rearing and Breeding of Gammarus in Laboratory Conditions. *Journal of the Marine Biological Association of the United Kingdom*, 15(1), 33-55.

Shao, Y. T., Chuang, S.-Y., Chang, H.-Y., Tseng, Y.-C. and Shao, K.-T. (2018) Largescale mullet (Planiliza macrolepis) can recover from thermal pollution-induced malformations. *PLOS ONE*, 13(11), e0208005.

Smith, A. L. and Lancaster, T. L. (2020) Increased duration of extreme thermal events negatively affects cold acclimation ability in a high-latitude, freshwater ectotherm (Ischnura elegans; Odonata: Coenagrionidae). *EJE*, 117(1), 93-100.

Slos, S. and Stoks, R. (2008) Predation risk induces stress proteins and reduces antioxidant defense. *Functional Ecology*, 22(4), 637-642.

Sokolova, I. M. (2013) Energy-Limited Tolerance to Stress as a Conceptual Framework to Integrate the Effects of Multiple Stressors. *Integrative and Comparative Biology*, 53(4), 597-608.

Somero, G. N. (2010) The physiology of climate change: how potentials for acclimatization and genetic adaptation will determine ‘winners’ and ‘losers’. *The Journal of*

Experimental Biology, 213(6)**,** 912-920.

Spanjer, A. R., Gendaszek, A. S., Wulfkuhle, E. J., Black, R. W. and Jaeger, K. L. (2022) Assessing climate change impacts on Pacific salmon and trout using bioenergetics and spatiotemporal explicit river temperature predictions under varying riparian conditions. *PLOS ONE*, 17(5), e0266871.

Squires, L. E., Rushforth, S. R. & Brotherson, J. D. (1979) Algal response to a thermal effluent: study of a power station on the provo river, Utah, USA. *Hydrobiologia,* 63(1)**,** 17-32.

Stachowicz, J. J., Terwin, J. R., Whitlatch, R. B. and Osman, R. W. (2002) Linking climate change and biological invasions: Ocean warming facilitates nonindigenous species invasions. *Proceedings of the National Academy of Sciences*, 99(24), 15497-15500.

Stefan, H., Fang, X. & Eaton, J. (2001) Simulated Fish Habitat Changes in North American Lakes in Response to Projected Climate Warming. *Transactions of the American Fisheries Society,* 130**,** 459-477.

Stevens, L. E., Shannon, J. P. & Blinn, D. W. (1997) Colorado River benthic ecology in Grand Canyon, Arizona, USA: Dam, tributary and geomorphological influences. *Regulated Rivers-Research & Management,* 13(2)**,** 129-149.

Stewart, R. J., Wollheim, W. M., Miara, A., Vörösmarty, C. J., Fekete, B., Lammers, R. B. and Rosenzweig, B. (2013) Horizontal cooling towers: riverine ecosystem services and the fate of thermoelectric heat in the contemporary Northeast US. *Environmental Research Letters*, 8(2), 025010.

Strange, K. T., Vokoun, J. C. and Noltie, D. B. (2002) Thermal Tolerance and Growth Differences in Orangethroat Darter (Etheostoma spectabile) from Thermally Contrasting Adjoining Streams. *The American Midland Naturalist*, 148(1), 120-128, 129.

Sunday, J. M., Bates, A. E., Kearney, M. R., Colwell, R. K., Dulvy, N. K., Longino, J. T. and Huey, R. B. (2014) Thermal-safety margins and the necessity of thermoregulatory behavior across latitude and elevation. *Proceedings of the National Academy of Sciences*, 111(15), 5610-5615.

Sutcliffe, D. W., Carrick, T. R. and Willoughby, L. G. (1981) Effects of diet, body size, age and temperature on growth rates in the amphipod Gammarus pulex. *Freshwater Biology*, 11(2), 183-214.

Tang, M., He, T., Meng, Q.-y., Broussard, J. I., Yao, L., Diao, Y., Sang, X.-b., Liu, Q.-p., Liao, Y.-j., Li, Y. and Zhao, S. (2014) Immobility responses between mouse strains correlate with distinct hippocampal serotonin transporter protein expression and function. *International Journal of Neuropsychopharmacology*, 17(11), 1737-1750.

Tomanek, L. (2008) The Importance of Physiological Limits in Determining Biogeographical Range Shifts due to Global Climate Change: The Heat‐Shock Response. *Physiological and Biochemical Zoology*, 81(6), 709-717.

Tomanek, L. (2010) Variation in the heat shock response and its implication for predicting the effect of global climate change on species' biogeographical distribution ranges and metabolic costs. *Journal of Experimental Biology*, 213(6), 971-979.

Tonolla, D., Dossi, F., Kastenhofer, O., Doering, M., Hauer, C., Graf, W. and Schülting, L. (2022) Effects of hydropeaking on drift, stranding and community composition of macroinvertebrates: A field experimental approach in three regulated Swiss rivers. *River Research and Applications*, 39(3), 427-443.

Trenberth, K. E., Dai, A., van der Schrier, G., Jones, P. D., Barichivich, J., Briffa, K. R. and Sheffield, J. (2014) Global warming and changes in drought. *Nature Climate Change*, 4(1), 17-22.

Tress, S. (2010) *Struggle to Keep Fish, People & Power Companies Happy* [Online]. Available at: https://blogs.ei.columbia.edu/2010/08/18/struggle-to-keep-fish-people-power-companies-happy/ [Accessed 11th June 2020].

Trimmel, H., Weihs, P., Leidinger, D., Formayer, H., Kalny, G. and Melcher, A. (2018) Can riparian vegetation shade mitigate the expected rise in stream temperatures due to climate change during heat waves in a human-impacted pre-alpine river? *Hydrol. Earth Syst. Sci.*, 22(1), 437-461.

UNEP – United Nations Environment Programme (2020) *Emissions Gap Report 2020*. United Nations: New York, NY, USA, 128p.

Union of Concerned Scientists (2012) *UCS EW3 Energy-Water Database V.1.3*. Available at: www.ucsusa.org/ew3database. [Accessed 27th May 2021].

Union of Concerned Scientists (2013) *How it Works: Water for Power Plant Cooling* [Online]. Available at: https://www.ucsusa.org/resources/water-power-plant-cooling#:~:targetText=Most%20commonly%2C%20wet%2Drecirculating%20systems, condenser%20in%20the%20power%20plant.&targetText=Dry%2Dcooling%20system

s%20use%20air,the%20steam%20exiting%20a%20turbine. [Accessed 11th June 2020].

United Nation Population Division (2018) *World Urbanization Prospects: The 2018 Revision, Online Edition.* [Online]. Available at: https://population.un.org/wup/DataQuery/ [Accessed 11th June 2020].

U.S. EPA – United States Environmental Protection Agency (2012) *NHDPlus National Data*. Available at: https://www.epa.gov/waterdata/nhdplus-national-data. [Accessed 27th May 2021].

USGS – U.S. Geological Survey (2008) *USGS Surface-Water Data for the Nation*. Available at: https://waterdata.usgs.gov/nwis/sw. [Accessed 27th May 2021].

Väinölä, R., Witt, J. D. S., Grabowski, M., Bradbury, J. H., Jazdzewski, K. and Sket, B. (2008) Global diversity of amphipods (Amphipoda; Crustacea) in freshwater. *Hydrobiologia*, 595(1), 241-255.

Valencia, S., Gonzales, E. L., Adil, K. J., Jeon, S. J., Kwon, K. J., Cho, K. S. and Shin, C. Y. (2019) Comparative Behavioral Correlation of High and Low-Performing Mice in the Forced Swim Test. *Biomol Ther (Seoul)*, 27(4), 349-356.

van der Velde, G., Leuven, R. S. E. W., Platvoet, D., Bacela, K., Huijbregts, M. A. J., Hendriks, H. W. M. and Kruijt, D. (2009) Environmental and morphological factors influencing predatory behaviour by invasive non-indigenous gammaridean species. *Biological Invasions*, 11(9), 2043-2054.

Vannote, R. L. & Sweeney, B. W. (1980) Geographic Analysis of Thermal Equilibria: A Conceptual Model for Evaluating the Effect of Natural and Modified Thermal Regimes on Aquatic Insect Communities. *The American Naturalist,* 115(5)**,** 667-695.

van Vliet, M. T. H., Franssen, W. H. P., Yearsley, J. R., Ludwig, F., Haddeland, I., Lettenmaier, D. P. and Kabat, P. (2013) Global river discharge and water temperature under climate change. *Global Environmental Change*, 23(2), 450-464.

van Vliet, M. T. H., Ludwig, F., Zwolsman, J. J. G., Weedon, G. P. and Kabat, P. (2011) Global river temperatures and sensitivity to atmospheric warming and changes in river flow. *Water Resources Research*, 47(2).

van Vliet, M. T. H., van Beek, L. P. H., Eisner, S., Flörke, M., Wada, Y. and Bierkens, M. F. P. (2016) Multi-model assessment of global hydropower and cooling water discharge

potential under climate change. *Global Environmental Change*, 40, 156-170.

van Vliet, M. T. H., Yearsley, J. R., Ludwig, F., Vögele, S., Lettenmaier, D. P. and Kabat, P. (2012) Vulnerability of US and European electricity supply to climate change. *Nature Climate Change*, 2(9), 676-681.

Vellinger, C., Felten, V., Sornom, P., Rousselle, P., Beisel, J.-N. and Usseglio-Polatera, P. (2012) Behavioural and Physiological Responses of Gammarus pulex Exposed to Cadmium and Arsenate at Three Temperatures: Individual and Combined Effects. *PLOS ONE*, 7(6), e39153.

Verheyen, J. and Stoks, R. (2019) Temperature variation makes an ectotherm more sensitive to global warming unless thermal evolution occurs. *Journal of Animal Ecology*, 88(4), 624-636.

Verhille, C., MacDonald, M., Frazier, K., Demorest, G., Roche, A., & Albertson, L. (Accepted). Thermal tolerance of giant salmonfly nymphs (*Pteronarcys californica*) varies across populations in a regulated river. *Conservation Physiology*.

Verones, F., Hanafiah, M. M., Pfister, S., Huijbregts, M. A. J., Pelletier, G. J. & Koehler, A. (2010) Characterization Factors for Thermal Pollution in Freshwater Aquatic Environments. *Environmental Science & Technology,* 44(24)**,** 9364-9369.

Vyas, K. (2019) *Everything You Need to Know About Nuclear Power Plants* [Online]. Available at: https://interestingengineering.com/everything-you-need-to-know-about-nuclear-power-plants [Accessed 11th June 2020].

Walther, G.-R., Roques, A., Hulme, P. E., Sykes, M. T., Pyšek, P., Kühn, I., Zobel, M., Bacher, S., Botta-Dukát, Z., Bugmann, H., Czúcz, B., Dauber, J., Hickler, T., Jarošík, V., Kenis, M., Klotz, S., Minchin, D., Moora, M., Nentwig, W., Ott, J., Panov, V. E., Reineking, B., Robinet, C., Semenchenko, V., Solarz, W., Thuiller, W., Vilà, M., Vohland, K. & Settele, J. (2009) Alien species in a warmer world: risks and opportunities. *Trends in Ecology & Evolution,* 24(12)**,** 686-693.

Wanders, N., van Vliet, M. T. H., Wada, Y., Bierkens, M. F. P. and van Beek, L. P. H. (2019) High-Resolution Global Water Temperature Modeling. *Water Resources Research*, 55(4), 2760-2778.

Wang, X., Sun, X., Tang, J. & Yang, X. (2015) Urbanization-induced regional warming in Yangtze River Delta: potential role of anthropogenic heat release. *International*

Journal of Climatology, 35(15)**,** 4417-4430.

WATCO Group (no date) *RANKINE CYCLE*. Available at: https://www.watco-group.co/surface-condenser-in-thermal-power-plant/ [Accessed 11th June 2020].

Watts, G., Battarbee, R. W., Bloomfield, J. P., Crossman, J., Daccache, A., Durance, I., Elliott, J. A., Garner, G., Hannaford, J., Hannah, D. M., Hess, T., Jackson, C. R., Kay, A. L., Kernan, M., Knox, J., Mackay, J., Monteith, D. T., Ormerod, S. J., Rance, J., Stuart, M. E., Wade, A. J., Wade, S. D., Weatherhead, K., Whitehead, P. G. and Wilby, R. L. (2015) Climate change and water in the UK – past changes and future prospects. *Progress in Physical Geography: Earth and Environment*, 39(1), 6-28.

Wawrzyniak, V., Piégay, H. and Poirel, A. (2012) Longitudinal and temporal thermal patterns of the French Rhône River using Landsat ETM+ thermal infrared images. *Aquatic Sciences*, 74(3), 405-414.

Webb, B. W., Hannah, D. M., Moore, R. D., Brown, L. E. and Nobilis, F. (2008) Recent advances in stream and river temperature research. *Hydrological Processes*, 22(7), 902-918.

Weber, M., Rinke, K., Hipsey, M. R. and Boehrer, B. (2017) Optimizing withdrawal from drinking water reservoirs to reduce downstream temperature pollution and reservoir hypoxia. *Journal of Environmental Management*, 197, 96-105.

Welton, J. S., Ladle, M., Bass, J. A. B. and John, I. R. (1983) Estimation of Gut Throughput Time in Gammarus Pulex under Laboratory and Field Conditions with a Note on the Feeding of Young in the Brood Pouch. *Oikos*, 41(1), 133-138.

WEPP – World Electric Power Plants Database (2016) S*&P Global Platts, World Electric Power Plants Database, September 2016*. Available at: https://www.spglobal.com/platts/pt/products-services/electric-power/world-electric-power-plants-database. [Accessed 27th May 2021].

Whiteley, N. and Faulkner, L. S. (2005) Temperature Influences Whole‐Animal Rates of Metabolism but Not Protein Synthesis in a Temperate Intertidal Isopod. *Physiological and Biochemical Zoology*, 78(2), 227-238.

Wilby, R. L., Johnson, M. F. and Toone, J. A. (2014) Nocturnal river water temperatures: Spatial and temporal variations. *Science of The Total Environment*, 482-483, 157-173.

World Meteorological Organization (2021) *2020 was one of three warmest years on record.* [Online]. Available at: https://public.wmo.int/en/media/press-release/2020-was-one-of-three-warmest-years-record [Accessed 11th May 2023].

World Nuclear Association (2019) *Cooling Power Plants* [Online]. Available at: https://www.world-nuclear.org/information-library/current-and-future-generation/cooling-power-plants.aspx [Accessed 11th June 2020].

Worthington, T. A., Shaw, P. J., Daffern, J. R. and Langford, T. E. L. (2015) The effects of a thermal discharge on the macroinvertebrate community of a large British river: implications for climate change. *Hydrobiologia*, 753(1), 81-95.

WRI – World Resources Institute (2019) *Data Sets: Global Power Plant Database*. Available at: https://datasets.wri.org/dataset/globalpowerplantdatabase. [Accessed 27th May 2021].

Wright, S. A., Jr, F. M. H., Bradley, A. A. & Krajewski, W. (1999) Long-Term Simulation of Thermal Regime of Missouri River. *Journal of Hydraulic Engineering,* 125(3)**,** 242-252.

Wu, P., Christidis, N. and Stott, P. (2013) Anthropogenic impact on Earth's hydrological cycle. *Nature Climate Change*, 3(9), 807-810.

Yavari, S. M. and Qaderi, F. (2020) Determination of thermal pollution of water resources caused by Neka power plant through processing satellite imagery. *Environment, Development and Sustainability*, 22(3), 1953-1975.

Zhu, S., Nyarko, E. K. and Hadzima-Nyarko, M. (2018) Modelling daily water temperature from air temperature for the Missouri River. *PeerJ*, 6, e4894.

Zolezzi, G., Siviglia, A., Toffolon, M. and Maiolini, B. (2011) Thermopeaking in Alpine streams: event characterization and time scales. *Ecohydrology*, 4(4), 564-576.

Zubrod, J. P., Baudy, P., Schulz, R. and Bundschuh, M. (2014) Effects of current-use fungicides and their mixtures on the feeding and survival of the key shredder Gammarus fossarum. *Aquatic Toxicology*, 150, 133-143.